Quantifying Transport of Aquaculture Particulate Wastes

by

Brent A. Law

Submitted in partial fulfilment of the requirements
for the degree of Doctor of Philosophy

at

Dalhousie University
Halifax, Nova Scotia
March 2019

TABLE OF CONTENTS

LIST OF TABLES

LIST OF FIGURES

Abstract

Scientific understanding of aquaculture interactions with the environment is limited, especially with regard to the far-field transport and possible impacts of particulate wastes. Both modelling and field studies have focused on near-field effects from organic enrichment, while the far field has received far less attention. In chapter 2, a pilot study was carried out to determine the size, settling velocity, and density of suspended particles at an active salmon aquaculture cage site. Flocs had a larger fractal dimension and smaller component-particle density than in other studies, suggesting that particles from the aquaculture operation may be incorporated into suspended flocs with average settling velocities of 1 mm s^{-1}. In chapter 3, a laboratory study was carried out to examine the effect of bed sediment texture on the erodibility of salmon aquaculture waste fecal material and salmon feed pellets. Results show that cumulative mass eroded (CME) can vary by up to an order of magnitude depending on substrate composition, with a mud substrate having higher values than that of substrates composed of sand, gravel and cobble. In chapter 4, cores collected with an intact sediment-water interface were coupled to a Gust erosion chamber to examine the effect of increasing shear stress on bottom sediments in areas of salmon aquaculture. Cores were collected along transects of stations at a cohesive and a non-cohesive seabed site. Results show that as the amount of organics in bottom sediments increased the erodibility of the bed sediments decreased. In chapter 5, dispersal from a fin-fish aquaculture facility was simulated using the Benthic Boundary Layer Transport model (BBLT). Four waste classes were considered: fines, flocs, fecal waste and feed pellets, each with distinct settling velocities and critical erosion shear stresses. The resulting concentration of each class within the cage site varied by approximately 5 orders of magnitude with higher concentrations of fines and flocs in the far field as compared to fecal material and pellets.

Acknowledgements

This thesis is dedicated to my wonderful wife Jennifer and our two boys Zach and Alex. Thanks always for your support, I think I'm finally finished with school! I would also like to thank Paul Hill and Tim Milligan for all your help over the years for trying to make me wiser but more importantly for the stories and laughs. Here is to more years of working in the mud.

Chapter 1 - Introduction

As of 2007, over 75% of the world's natural fish stocks were over-exploited (FAO, 2007). To meet the demand of the world for fish and to lessen the pressure on over-exploited fish stocks, aquaculture has experienced rapid growth over the last quarter century. Aquaculture has doubled in Canada since 1996 and by 2007 generated close to one billion dollars annually in "landings" (Aquaculture Canada, 2007). By 2016, aquaculture in Canada annually produced about 200,000 tonnes, 75% of which was finfish, of that, 95% was farmed salmon (FAO, 2016).

With the expansion of the aquaculture industry, more specifically the salmon farming industry, environmental concerns have been raised over the fate of aquaculture waste material, primarily feed pellets and fecal matter. To date, research has focused primarily on the deposition of organic waste immediately under or adjacent to salmon net pens. Both modelling and field studies have focused on near-field effects from organic enrichment, while the far field has received far less attention. The near field is considered to be the area within a few hundred meters of the cage sites while the far field extends kilometers away from farming operations. Models to map the depositional footprint from salmon and other fin-fish farms using the settling characteristics of waste solids have become increasingly accurate (Panchang et al., 1997; Cromey et al., 2002a, Chamberlain and Stucchi, 2007). Models that map the subsequent resuspension and transport of waste material however are less accurate (Droppo et al., 2007; Chamberlain and Stucchi, 2007; Reid et al., 2009). A better understanding of the

cohesive nature of aquaculture waste material is required to produce accurate, far-field, coupled hydrodynamic-sediment transport models. In particular, cohesion affects the settling velocity and erosion rate of sediments, which are both fundamental parameters in sediment transport models.

The settling of fine grained particulate material in the ocean is governed by the process of flocculation, which is the aggregation of fine particles into larger, faster settling agglomerations known as "flocs" (Kranck, 1973, McCave, 1984, Kranck and Milligan, 1985, Milligan and Kranck, 1992; Milligan et al., 2007). Fine grained material has geometric mean diameters < 63 µm, and it is known as "mud". The controls on aggregation include particle encounter rate, which depends nonlinearly on concentration, particle contact efficiency and stickiness, and particle break-up due to turbulence (Hill, 1996, Milligan and Law, 2005). Effectively, an increase in particle encounter rate, increase in organic binding, or reduction in turbulent shear cause flocculation to increase, which in turn increases the settling of fine-grained material to the seabed.

The input of fecal material and feed from salmon aquaculture increases the amount of "sticky organic material" and hence cohesion in the water column and in the sediments surrounding aquaculture sites. Milligan and Law (2005) showed decadal changes in floc limit, which is a parameter derived from grain size distributions, from sediments collected in bays with intensive open-cage salmon aquaculture. The increased floc limit in bottom sediments was linked to increased organic loading which ultimately increased flocculation and the settling of fine-grained material to the seabed (Milligan and Law, 2005). These changes

were accompanied by increased sediment accumulation and an increase in organic matter in the seabed (Smith et al., 2005).

Increases in deposited organic matter can lead to the formation of microbial mats. These mats form when oxygen is depleted in the sediments and overlying water column and can become widespread in sulfide-rich waters (Grant and Gust, 1987). The formation of mats on the seabed is associated with a process known as "biostabilization" (Krumbein et al., 1994). This process occurs when organisms such as algae, fungi, microbes, combined with exo-polymeric substances (EPS) essentially "glue down' or stabilize the sediment bed (Droppo, 2001). This process occurs rapidly in the organic-enriched sediments around active aquaculture operations (Droppo et al., 2007). Changes in the seabed resulting from organic loading can also result in changes in organisms inhabiting an area from predominantly suspension and filter feeders to benthic organisms and bacteria that thrive in organic-rich, high sedimentation areas (Pohle et al., 2001, Wildish and Pohle, 2005).

Increased flocculation has potential consequences for the health of an ecosystem because contaminants are generally transported in the marine environment as part of flocs (Milligan and Loring, 1997). Flocculation packages contaminants into a form that is readily available for ingestion by filter-feeding organisms. Because flocs also contain large amounts of organic material, they are an attractive source of food for suspension-feeding organisms such as scallops, clams, and mussels (Cranford et al., 2005). Elevated levels of trace metals and organic matter have been documented in several studies around

salmon aquaculture operations (Schendel et al., 2004; Smith et al., 2005; Sutherland et al., 2006; Dean et al., 2007; Milligan and Law, 2013). In these studies, elevated concentrations of elements such as Zinc (Zn) and Phosphorus (P) have been linked to feed pellets and fecal material, while elevated concentrations of Copper (Cu) have been linked to increases in anthropogenic inputs such as anti-fouling paints. Metals in excess concentration above background such as Molybdenum (Mo) and Cadmium (Cd) have been linked to the precipitation of authigenic phases, usually in the presence of anoxia associated with the large organic loading to the sediments around fish farms (Smith et al., 2005). The relationships between flocculation, settling, sediment accumulation and biostabilization, and contaminant transport make understanding of floc size, settling velocity, and erodibility essential to accurate modeling of the far-field fate of aquaculture wastes.

Wave and current stress exerted on the seabed provide the work necessary to erode particles from the seabed, whereas particle size and mass, cohesion, porosity, consolidation, and biological activity define the erosion resistance of the seabed (Amos et al. 1992, 1997; Maa et al., 1998; Sanford and Maa, 2001, Wiberg et al., 2013). Overall understanding of cohesive sediment resuspension is incomplete because it is governed by not only hydrodynamic forces, the force of gravity, and friction, but also by cohesion, which depends on biological and electrochemical variables (Black et al., 2002, Droppo, 2007). Research on size sorting during the erosion of cores from the Gulf of Lions, France (Law et al, 2008) and in Seal Harbour, NS (Milligan and Law, 2013)

suggests that increases in clay (sediment particles <4 um in diameter) changes resuspension dynamics. In sediments that contain > 7.5% clay, a wide range of sizes are eroded at reduced but equal rates. Sediments with a smaller clay fraction exhibit greater erodibility and size-selective sorting over the entire particle size range. Sediment with a small clay fraction can be winnowed of its fine fraction during erosion, but sediments with a larger clay fraction cannot. When muddy sands are eroded, the smallest sediment sizes are winnowed from the bed, essentially cleaning the sands. In contrast, when muds are eroded, size sorting is reduced substantially. In short, after deposition, sands are "cleaned" by physical disturbance, but muds resist any further sorting. Even if muds are repeatedly resuspended and transported over great distances, they maintain their poorly sorted character and small mean grain size.   The addition of fine sediment to the seabed by aquaculture operations has the potential, then, to alter the erosion rate and texture of sediment near pens and possibly into the far field.

Quantifying the dispersal of finfish aquaculture waste through the use of modelling is necessary to predict the potential habitat impacts from farm systems and for siting criteria (Panchang et al., 1997; Cromey et al., 2002a; Reid et al., 2009). The accumulation of fecal material and feed pellets under cage sites and within a few hundred meters of farm sites is relatively well understood. The settling velocities of fecal material and pellets are large, 40 mm/s and 100 mm/s respectively, so the depositional footprint of these waste classes is relatively small and easily defined. In contrast, flocs have settling velocities on the order of 1 mm/s (Hill et al., 2001). Under stress, flocs can break up, resulting in settling

velocities nearing that of the component particles. Incorporation of floc-deposited sediment into the seabed will affect erosion rates. These important parameters around aquaculture sites are poorly constrained in present models, yet they have potential to impact the far field (Sutherland et al., 2006; Droppo et al., 2007).

The objectives of this study were to use a combination of field and laboratory measurements and modelling to understand and quantify the transport of aquaculture particulate matter, more specifically the erosion, horizontal flux, and settling of aquaculture waste products in the vicinity of salmon net pens. The field measurements were conducted at coastal locations with different physical forcing and sediment types, and the laboratory measurements similarly characterized a range of different bottom types. The scope of measurements was motivated by the changing farming practices in the industry.

Until recently, salmon farming in Atlantic Canada has been focused in the South-west region of New Brunswick and has been located in depositional areas where the seabed is predominantly mud. Over the last decade, however, expansion of the industry into other environments has occurred, including deeper water, hard bottom locations in Newfoundland and higher energy, wave dominated locations in Nova Scotia. In other parts of the world such as Norway, the largest producer of farmed Atlantic salmon, new sites are moving away from the deep fjords with muddy bottoms and towards coastal areas with sandy seabeds that are in shallower water and exposed to waves. The research undertaken here explicitly addresses the different energy regimes as well as

different bottom types into which salmon aquaculture operations are being extended around the globe.

The thesis has four primary chapters. Chapter 2 describes in-situ particle properties at an active salmon aquaculture site. This chapter has been published as a manuscript in *Aquaculture Environment Interactions* (Law et al., 2014). I was responsible for data collection, analysis and writing, Hill was responsible for manuscript editing and review, Maier helped with data analysis, Milligan with manuscript comments and editing and Page with field support and funding. Chapter 3 describes a set of lab experiments designed to characterize the erodibility of salmon waste products from different bottom substrates. This chapter has been published as a manuscript in *Aquaculture Environment Interactions* (Law et al., 2016). I was responsible for data collection, analysis and writing. Hill contributed with manuscript review and editing, Milligan with manuscript comments and Zions with lab and instrument support. Chapter 4 documents spatial and temporal variation in erodibility of surficial sediment at areas of active salmon aquaculture. This chapter has been submitted for publication in *Aquaculture and Environment Interaction*. I was responsible for data collection, analysis and writing. Hill was responsible for manuscript review and editing. Chapter 5 introduces a proof-of-concept modelling framework for improving the characterization of resuspension and dispersal of multiple size classes of salmon waste material. I was responsible for data collection, analysis, providing model parameters and writing. Drozdowski was responsible for model set-up and output and data analysis. Hill was responsible for manuscript review

and editing. Chapter 6 provides concluding remarks and recommends future

research directions.

Chapter 2

This chapter is a manuscript published in Aquaculture Environment Interactions. Citation is below:

Law, B.A, Hill, P.S., Maier, I., Milligan, T.G., Page, F., 2014. Size, settling velocity and density of small suspended particles at an active salmon aquaculture site. Aquaculture Environment Interactions, 6, 29-42, doi:10.3354/aei00116

Size, Settling Velocity and Density of Small Suspended Particles at an Active Salmon Aquaculture Site

Law, B.A.[1, 2,*], Hill, P.S. [2], Maier, I. [2], Milligan, T.G. [1], Page, F. [3]

[1] FISHERIES AND OCEANS CANADA, BEDFORD INSTITUTE OF OCEANOGRAPHY, DARTMOUTH, NOVA SCOTIA, CANADA, B2Y 4A2

[2] DEPARTMENT OF OCEANOGRAPHY, DALHOUSIE UNIVERSITY, HALIFAX, NOVA SCOTIA, CANADA, B3H 4J1

[3] FISHERIES AND OCEANS CANADA, ST. ANDREWS BIOLOGICAL STATION, ST. ANDREWS, NEW BRUNSWICK, CANADA, E5B 2L9

* Corresponding author
Brent Law
Habitat Sedimentologist
Fisheries and Oceans Canada
Bedford Institute of Oceanography
1 Challenger Drive, Dartmouth, Nova Scotia
Canada, B2Y 4A2
Brent.Law@mar.dfo-mpo.gc.ca
Telephone | Téléphone 902-426-8548
Facsimile | Télécopieur 902-426-6695
Government of Canada | Gouvernement du Canada

Abstract

Scientific understanding of aquaculture interactions with the environment is limited, especially with regard to the far-field transport and possible impacts of particulate wastes. A pilot study was carried out in southwest, New Brunswick, Canada in November 2008 to determine the size, settling velocity, and density of suspended particles at an active salmon aquaculture cage site. The model of Khelifa and Hill (2006) was fit to size versus settling velocity data to estimate the fractal dimension of flocs and the density of the component particles within flocs. Flocs had a larger fractal dimension and smaller component-particle density than in other studies, suggesting that particles from the aquaculture operation may be incorporated into suspended flocs with average settling velocities of 1 mm s^{-1}. Variability in particle size and packaging were interpreted in the context of near bed velocity, tidal stage, and wind speed and direction. This analysis indicated that advection dominated observed variations in particle size and packaging. Indicators of resuspension, aggregation, disaggregation, and deposition were not detected in the time series. Advection of flocs away from the study site provides a mechanism to transport wastes over distances greater than 1 km prior to deposition, so a settling class of 1 mm s^{-1} should be considered in depositional models of aquaculture wastes.

1. Introduction

As of 2007, over 75% of the world's natural fish stocks were over-exploited (FAO, 2007). To meet the demand of the world for fish and to lessen the pressure on over-exploited fish stocks, aquaculture has grown rapidly over the last quarter century. Aquaculture in Canada doubled from 1996 to 2007, and by 2007 it generated close to one billion dollars annually in "landings" (Aquaculture Canada, 2007). In 2009, aquaculture in Canada produced about 155,000 tonnes, 76% of which was finfish. Of that, 95% was farmed salmon.

With the expansion of salmon farming, environmental concerns have been raised over the fate of aquaculture waste material such as feed pellets and fecal material. To date, research has focused primarily on the deposition of organic waste immediately under or adjacent to salmon net pens, termed the "near-field". Increasingly accurate models use the settling characteristics of feed pellets and feces to map the areal extent of the near-field depositional footprint under net pens (Panchang et al., 1997; Cromey et al., 2002a, Chamberlain and Stucchi, 2007). The settling velocities of fecal material and pellets, based primarily on laboratory studies, are large, 40 mm/s and 100 mm/s respectively, so the depositional footprint of this waste material usually does not extend more than several hundred meters from the pen (Chen et al., 1999; Cromey et al., 2002a; Sutherland et al., 2006). The far-field, which extends up to several kilometers away from farming operations, has received less attention (Droppo et al., 2007; Chamberlain and Stucchi, 2007; Reid et al., 2009). Transport of waste to the far-field may occur by advection of finer, slower-sinking, suspended particles away

from the pens or by post-depositional resuspension and transport of degraded feces and pellets from under the net pens. Measurements of finer, slower-sinking particles near salmon aquaculture pens are lacking, however, which limits understanding of potential far-field impacts.

In the ocean, the settling of the fine-grained particulate material is affected by the process of flocculation, which is the aggregation of small particles into larger, faster settling agglomerations known as "flocs" (Kranck, 1973, McCave, 1984, Kranck, 1985, Milligan and Kranck 1992; Milligan et al., 2007). The controls on flocculation include particle encounter rate, which depends nonlinearly on concentration, particle contact efficiency and stickiness, and particle break-up due to turbulence (Hill, 1996, Milligan and Law, 2005; Hill et al., 2013). Large particle concentrations, large particle stickiness, and low-to-moderate turbulent shear increase flocculation rates, which in turn increase the settling velocity and associated vertical flux of fine grained material to the seabed. In contrast to faster sinking waste material such as pellets and fecal material, flocs in-situ generally have settling velocities of order 1 mm s^{-1} (Hill et al., 2001; Fox et al. 2004; Curran et al. 2007).

Based on interpretation of particle size distributions in a core collected near a site of salmon net pens in the L'Etang Inlet in the Bay of Fundy in New Brunswick, Canada, Milligan and Law (2005) showed that an increase in the fraction of fine sediment deposited in flocs coincided in time with the emplacement of pens. Grain size distributions in grab samples of surficial sediments showed that floc deposition increased throughout the areas of mud

deposition in the inlet, both in the near- and far-fields. Milligan and Law (2005) attributed the increase in floc deposition to increases in particle concentration and stickiness associated with salmon aquaculture. They inferred that concentration increased because of the introduction of fine particles shed from feed and feces, and stickiness increased because of the organic nature of the introduced particles. The study of Milligan and Law (2005) provides evidence that small particles associated with salmon feed and waste interact with natural suspended particles to form flocs that can be transported from the near-field to the far-field.

Transport of flocs away from aquaculture sites may degrade the health of a bay or inlet because contaminants are generally transported in the marine environment within flocs (Milligan and Loring, 1997; Milligan and Law, 2013). Because flocs typically contain large amounts of organic material, as well, they are a preferred source of food for suspension-feeding organisms such as scallops, clams, and mussels (Cranford et al., 2005; Kach and Ward, 2008; Ward et al., 2008). Incorporation of contaminants into flocs therefore makes the contaminants readily available for ingestion by filter feeding organisms.

Elevated levels of trace metals and organic matter have been documented in several studies around salmon aquaculture operations (Schendel et al., 2004; Smith et al., 2005; Sutherland et al., 2006; Dean et al., 2007; Milligan and Law, 2013). In these studies elevated concentrations of metals such as zinc (Zn) and phosphorus (P) have been linked to feed pellets and fecal material, while elevated concentrations of copper (Cu) have been linked to increases in

anthropogenic inputs such as anti-fouling paints. Metals in excess concentration above background such as molybdenum (Mo) and cadmium (Cd) have been linked to the precipitation of authigenic phases, usually in the presence of anoxia in the sediments associated with the large organic loading to the seabed around fish farms (Smith et al., 2005). Floc transport away from net pens may transport these contaminants into the far-field, potentially affecting ecosystem health.

The relationships between flocculation, settling, and contaminants indicate that understanding of floc size, settling velocity and density may be required for accurate modeling of the far-field fate of aquaculture wastes, but in situ measurements of these parameters at aquaculture sites are limited (Reid et al. 2009). Understanding these parameters will not only improve predictive modelling capability for the far-field, but it will also enhance the design and integration of Integrated Multi-trophic Aquaculture Systems (IMTA), in which particle wastes are utilized by farmed suspension feeders like mussels, and excess nutrients are utilized by farmed macroalgae (Reid et al. 2009). Particle size and packaging information is needed to help determine which species can be grown at an IMTA site, and particle settling and transport information is needed to determine optimal locations for particle interception by selected species.

This study used optical instrumentation to measure the particle size, particle packaging, and settling velocity of material in suspension at an area of active salmon farming. These data were combined with physical forcing data such as current velocity, wind speed and direction and water temperature to

explore the mechanisms controlling the particle size at the farm site. The size-versus-settling velocity data were fit with a model developed by Khelifa and Hill (2006) to determine the effective in-situ density of particles, and a floc size versus density relationship was constructed.

2. Methods

2.1 Overview

The particle size, settling velocity, and particle packaging of suspended material was measured in-situ at an area of active salmon aquaculture in Charlie Cove, southwest New Brunswick, Canada (Fig. 1). Charlie Cove is sheltered from the outer Bay of Fundy by small islands around the site. The bathymetry at the site is sloped with water depths ranging from 18m at the landward side to 33m at the seaward end. The average water depth is approximately 23 m. Tidal range is 6 meters during spring tides. The aquaculture site occupies an area that is about 400m in length by about 200m in width. It is made up of 8 circular pens with 50m diameters in two parallel rows of four (Fig. 1). At the landward end is an IMTA site where mussels are grown on lines adjacent to the pens.

For one week in November 2008, a custom digital floc camera (DFC), a Sequoia Scientific LISST 100X type C (LISST) and digital video camera (DVC) with attached settling column were deployed at the Charlie Cove salmon aquaculture site. The DFC and LISST were mounted side by side on an aluminum frame and were tied off to the outside edge of the salmon pen on the landward side of the site. The DFC and LISST were always 7m below the sea surface and measured the particle stream entering and exiting the cage site

16
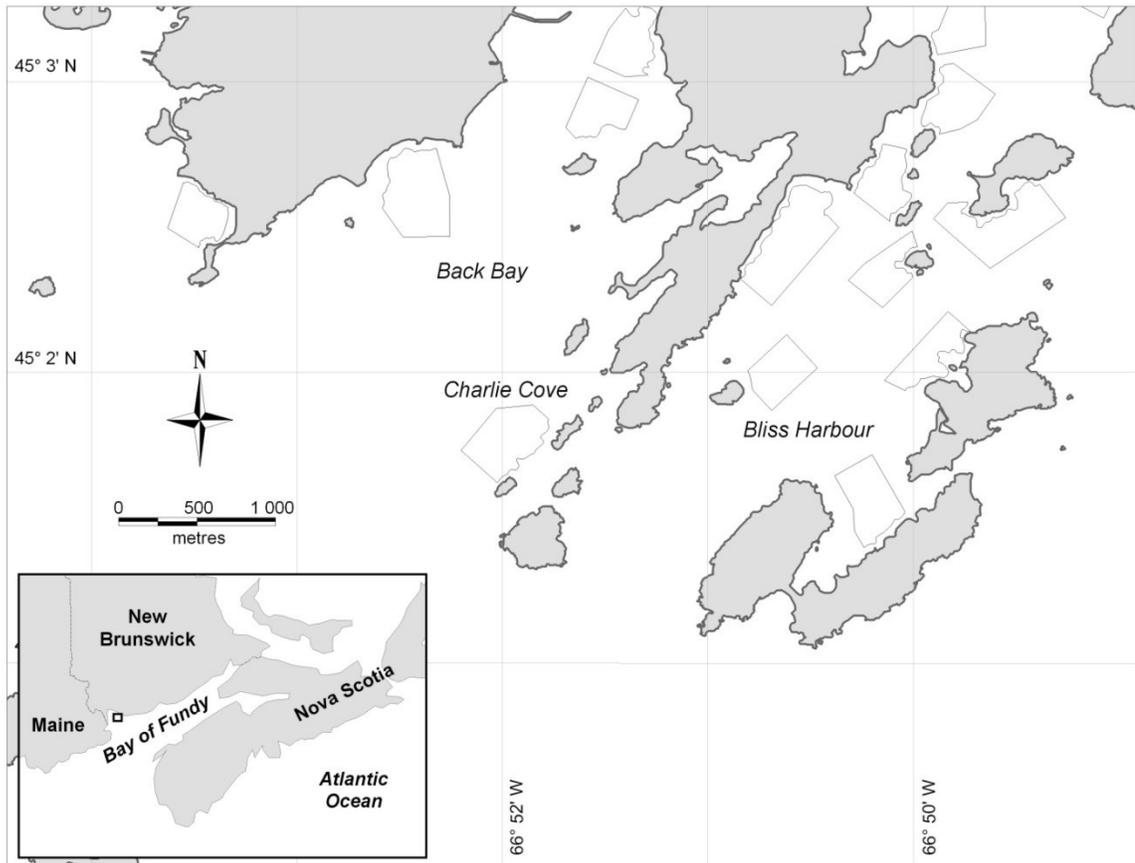
Figure 1. Map of South-West New Brunswick. Aquaculture sites are outlined by gray lines. The Charlie Cove site is labelled on the map.

depending whether the tide was flooding or ebbing. The DFC and LISST were deployed at 5pm GMT on November 24th (i.e. year day 329) and recovered 2 days later. The battery pack belonging to the DFC was changed, and the LISST and DFC particle size data were downloaded. The DFC and LISST pair were returned to the same location and water depth early on Friday, November 28th and finally recovered on Monday, December 1st (year day 336).

The DVC with settling column was mounted on a frame and placed on the seabed, directly under the outside edge of the cage, immediately below the DFC and LISST. Current velocity measurements were made throughout the study period using a 1200 KHz, RD Instruments acoustic Doppler current profiler (ADCP), which was positioned at 5m off the bottom and in a downward looking position to resolve the near bottom current velocity. The ADCP was positioned adjacent to the DVC.

2.2 Particle size distributions

The LISST measured suspended particle sizes from 2.50-500 μm. The DFC had a resolvable size range from ~45 μm to 40 mm in diameter. Data from the two instruments were merged to provide a size distribution that extended across most of the particulate size range found in the ocean (Mikkelsen et al., 2005; Curran et al., 2007; Hill et al., 2013). The LISST measured the intensity of light (670 nm) scattered by particles onto 32 logarithmically-spaced ring detectors. It also measured how much light was transmitted across a 5-cm path-length. The patterns of scattered light were inverted into particle size distributions using instrument-specific calibrations based on the scattering patterns for

particles of known size and volume concentration (Agrawal and Pottsmith, 2000; Mikkelsen et al., 2005). Assuming spherical geometry, the particle size distributions were converted to area and volume distributions. Sequoia Scientific's spherical-shape matrix was used to invert the data. LISST volume and area concentrations were estimated every 10 minutes and were calculated based on the average of 12 burst samples comprising 100 measurements each.

The DFC captured silhouette images of suspended particles every 10 minutes on the same schedule as the LISST. The field of view for the DFC was 4cm by 4cm with the depth of field set at 2.5cm. The pixel size for the DFC was approximately 15 µm and using 9 pixels (3 x 3) to define a particle, the minimum resolvable particle diameter was approximately 45 µm. For each image an area of interest (AOI) was selected that was relatively free of gradients in lighting or debris and organisms on the camera's glass plates. The images were cropped to the AOI, and for each image the threshold grey scale value used to define particles edges from the image background was defined using Otsu's method of particle edge detection to create a binary image (Otsu, 1979). The particle areas in each image were converted to equivalent spherical volumes. Particle areas and volumes were divided into 35 logarithmically spaced diameter bins. For a complete description of the image analysis and particle size distribution processing of the DFC images see Mikkelsen et al. (2004).

2.3 Entropy Analysis

Entropy analysis was used to separate particle size distributions into groups. The analysis formed groups in which similarity within groups was

maximal, as were differences among groups (Mikkelsen et al. 2007; Curran et al. 2007; Li et al. 2011). The number of groups was user-defined. There are five major processes affecting particle size in coastal waters: resuspension, deposition, aggregation, disaggregation, and advection (e.g., Hill et al., 2013). Five groups were selected to explore if there was evidence of these five processes governing size distributions during the deployment. For a complete description of entropy analysis and its application to marine particle size distributions, see Mikkelsen et al. (2007). For a description on ways to choose the number of groups for analysis, see deGelleke et al. (2013).

Particle parameters in each group were calculated and compared. Specifically, macrofloc, microfloc and single-grain fractions were calculated for each group (*cf.* Eisma, 1986; Mikkelsen et al. 2006; Curran et al. 2007). Single grains are <33μm and are transported and settle as individual grains. Microflocs are small tightly packed flocs that are composed of single grains and organic matter and are >33 μm and <133 μm. Macroflocs, are porous, loosely bound structures that are composed of microflocs, are >133 μm, and have been shown to attain diameters of several thousand μm.

2.4 Particle Size versus Settling Velocity

The size-versus-settling velocity of flocs was measured using a Sony DCR-VX2000 digital video camera (DVC) held in a stainless steel pressure housing with an attached plexiglass settling column. The DVC settling column had a baffle installed at the top to minimize the flow disturbance of settling particles. The DVC used mini DV tapes to record 80, 1-minute videos. During

the deployment the DVC captured a 1-minute video clip every 120 minutes. The

viewing volume of the DVC was 4.1 x 3.2 x 2.5 cm with a pixel size of 75 um.

For quality control in the image analysis, only particles that comprised 9 or more

pixels were analyzed, so the minimum resolution was ~220 μm (3 x 3 pixels).

Particle size and settling velocity from the DVC were calculated for each of

the 1-min clips. A sequence of four frames separated by 1 second was used to

estimate, for each particle, the equivalent spherical diameter, the settling

distance, and the settling time. In order for a particle to be included in the

analysis, the particle had to be present in 3 of the 4 frames. Floc size versus

settling velocity and floc size versus effective density relationships were

constructed for the entire deployment (Fox et al. 2004; Curran et al. 2007, Hill et

al. 2011).

2.5 Ancillary data

A 1200-KHz RDI ADCP was moored at 5m off the bottom in a downward

looking orientation and was positioned adjacent to the DVC and the DFC and

LISST. The instrument collected magnitude and direction data at 5-cm bin

intervals in the lower 4.4 m of the water. The first bin was 0.6 m below the

transducer, which was considered the instrument blanking distance. The ADCP

data were collected and averaged over 5-minute intervals.

Shear stress (τ_b) is expressed as:

$$\tau_b = \rho \, (u_*)^2 \tag{1}$$

where ρ is the fluid density and in this case taken to be 1025 kg m^{-3}, and u$_*$ is the shear velocity in m s^{-1}. Shear velocity can be estimated using the law of the wall defined by

$$u^* = kU(z) / \ln (z/z_0) \qquad\qquad (2)$$

where k is von Karman's constant (= 0.4), $U(z)$ (m s^{-1}) is the velocity at some height, z (m), above the bottom, in this case 1 m, and the roughness length, z_0 (m), was taken to be 2.0 E-4 based on Soulsby's (1983) estimate for a muddy seabed. The value for z_0 used in this study is the value used by Cromey et al. (2002b) in the resuspension module of DEPOMOD, which is a model typically used to predict the depositional footprint of net pens.

Tidal amplitude was based on the prediction from DFO Webtide (Dupont et al., 2005) for Back Bay, which is immediately adjacent to the Charlie Cove aquaculture site. Wind direction and magnitude were obtained from the Environment Canada weather station in St. Stephen, N.B., the closest to the study site and representative of prevailing conditions. Conductivity, temperature and depth (CTD) casts were performed at the site opportunistically using a Seabird 25. Water samples at the site were collected and filtered onto Millipore 8.0um filters, which have excellent trapping efficiency (Sheldon et al., 1972) and have been used to determine the disaggregated inorganic grain size in suspension (Law et al., 2008) when analyzed on a Coulter Counter Multisizer (Kranck and Milligan 1979; Milligan and Kranck, 1991).

3 Results

Winds at the study site were variable with the highest speeds originating predominantly from the east to northeast, and reaching up to 30 km hr^{-1} on the night of November 25th and morning of the 26th (year day 331). The remainder of the study had light and variable winds below 15 km hr^{-1}, usually from the northeast or southwest (Fig. 2). Due to its lack of exposure to the open waters of the Bay of Fundy, the effect of wind waves at Charlie Cove was considered negligible and therefore not included in interpretation of the nearbed velocity measurements. Tidal current velocities at the site were generally less than 20 cm s^{-1}, with a mean tidal range of 5m (Fig. 2). Current direction was generally to the northeast during flood tides and to the southwest during ebb tides. Water density estimated from periodic CTD casts at the study site was 1025 kg m^{-3} based on a water temperature of 8.5°C and salinity of 32 PSU. Suspended sediment samples collected at the site had a median, disaggregated diameter of approximately 7 μm, which is similar to the bottom sediment. The seabed sediments at Charlie Cove were fine grained mud with median diameter, (D_{50}) values under the cage and at the side of the cage of 9.2 and 8.8 μm respectively. These values were consistent over most of Charlie Cove and there were no bed forms present in the vicinity of the aquaculture operations.

The DFC only collected images for the first 2 hours of the first deployment and then failed. As a result, area and volume concentrations are based on LISST measurements alone. Particle size spectra based on area concentration and to a lesser extent volume concentration show diameter modes at approximately 6 μm and 300 μm (Fig. 3).
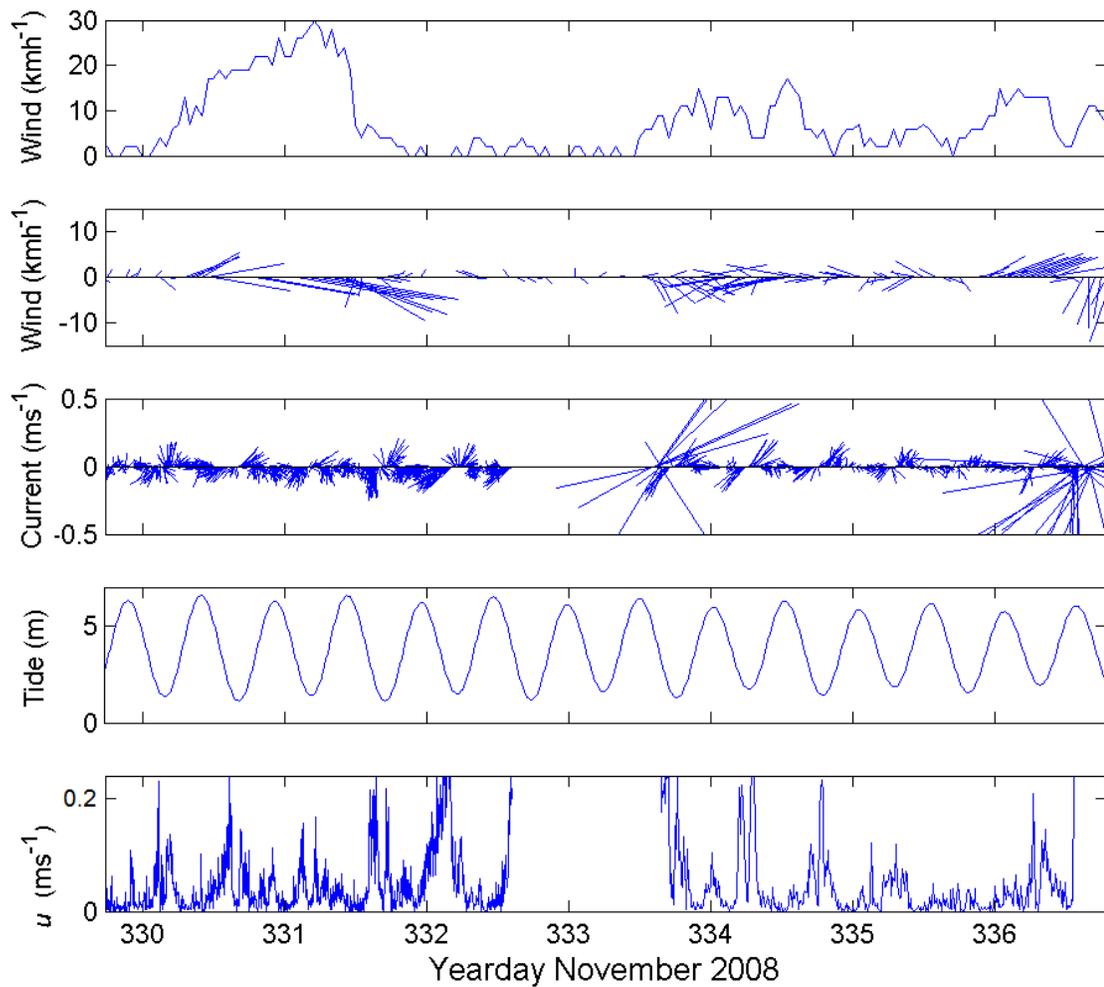
Figure 2. Forcing conditions at the study site from yearday 330 to 336, which
extends from November 25th to Dec 1st, 2008. The top panel is wind speed and
the second panel is a stick plot indicating wind speed and direction. Positive
values are winds from the south. The third panel is the current speed and
direction at the site with positive values indicating a flowing from south to north.
The fourth panel is the predicted tide at Back Bay which is immediately adjacent
to Charlie cove. The bottom panel is the velocity at 1 m above the bottom
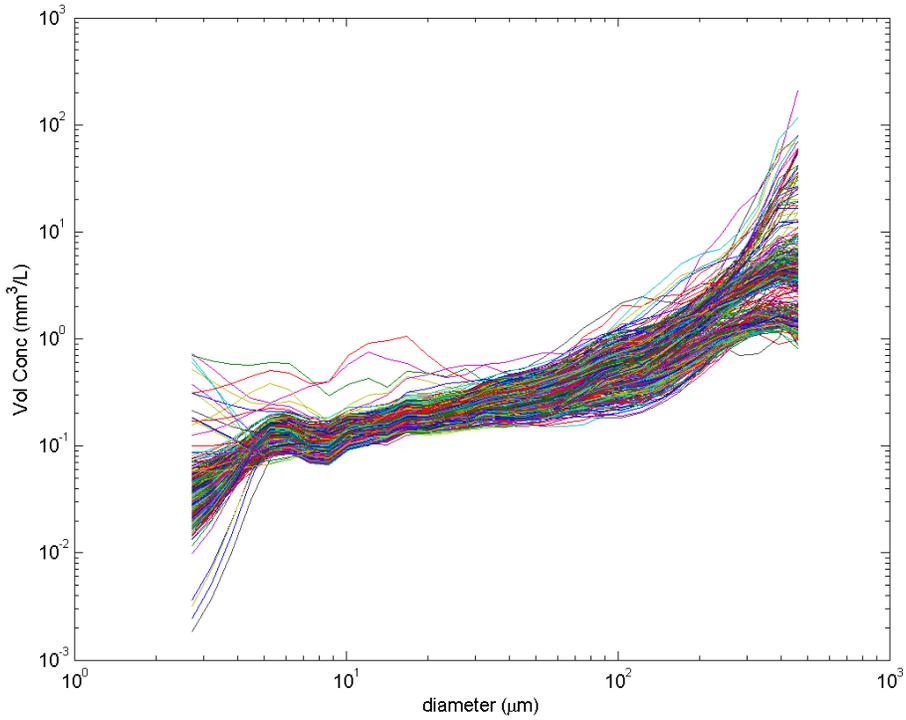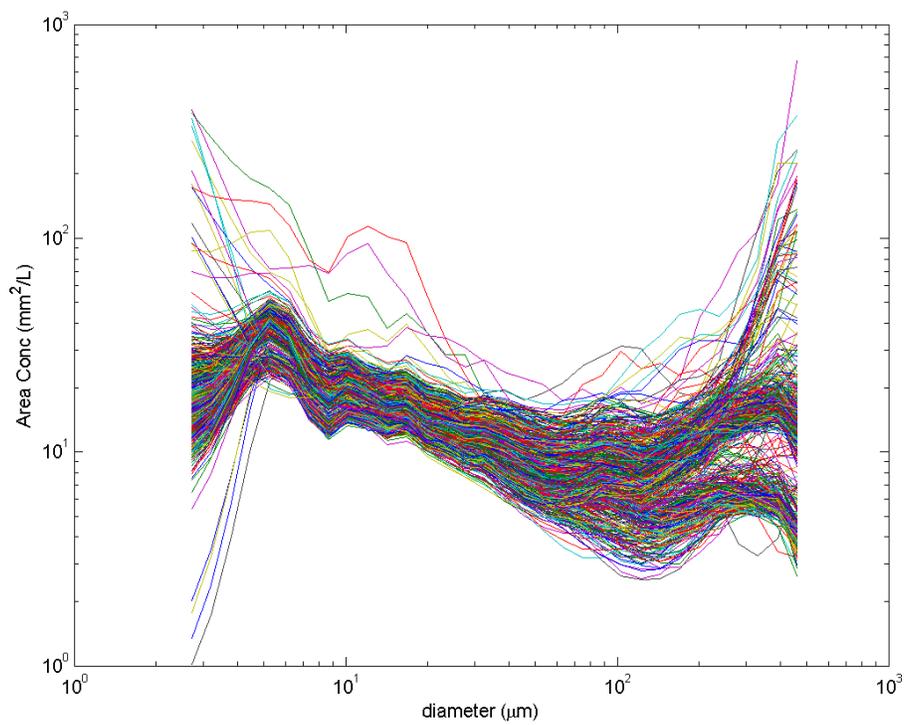
Figure 3. LISST 100X particle size distributions for both area concentration (top panel) and volume concentration (bottom panel).

Particle area and volume distributions were used to calculate single grain (< 33 μm), microfloc (33 μm to 133 μm), and macrofloc (>133 μm) fractions (Fig. 4). For the first deployment the area concentration was dominated by the single grain fraction that represented approximately 75% of the suspension, whereas, in the second deployment single grains accounted for roughly 65-70% of the suspension. The macrofloc population dominated the volume concentration in both the first and second deployment and on average accounted for 65% to 70% and then 80% of the suspension respectively (Fig. 4). Tidal signals in particle size were not evident in the time series of percentages of the single grain, microfloc and macrofloc populations. Just prior to year day 336 (Dec 1) there was a large increase in the macrofloc fraction with corresponding decrease in the single grain fraction and to a lesser extent a reduction in the microfloc fraction (Fig. 4). Over a four- to five-hour period the macrofloc population accounted for over 50% of the area concentration and over 95% of the concentration by volume (Fig. 4).

Averaged particle size distributions based on area and volume from 5 entropy groups were similar (Fig. 5). Groups 1 and 2 occurred during the first deployment, and they were finer than Groups 3 and 4, which occurred during the second deployment. Compared to Groups 1 and 2, Groups 3 and 4 had smaller single-grain and microfloc fractions and larger macrofloc fractions (Table 1). Group 5, which was the coarsest group with a macrofloc fraction of greater than 90%, appeared during the four- to five-hour period of larger particle sizes on day 336 (Fig. 5). Group 5 distributions occurred at a time when wind stress remained
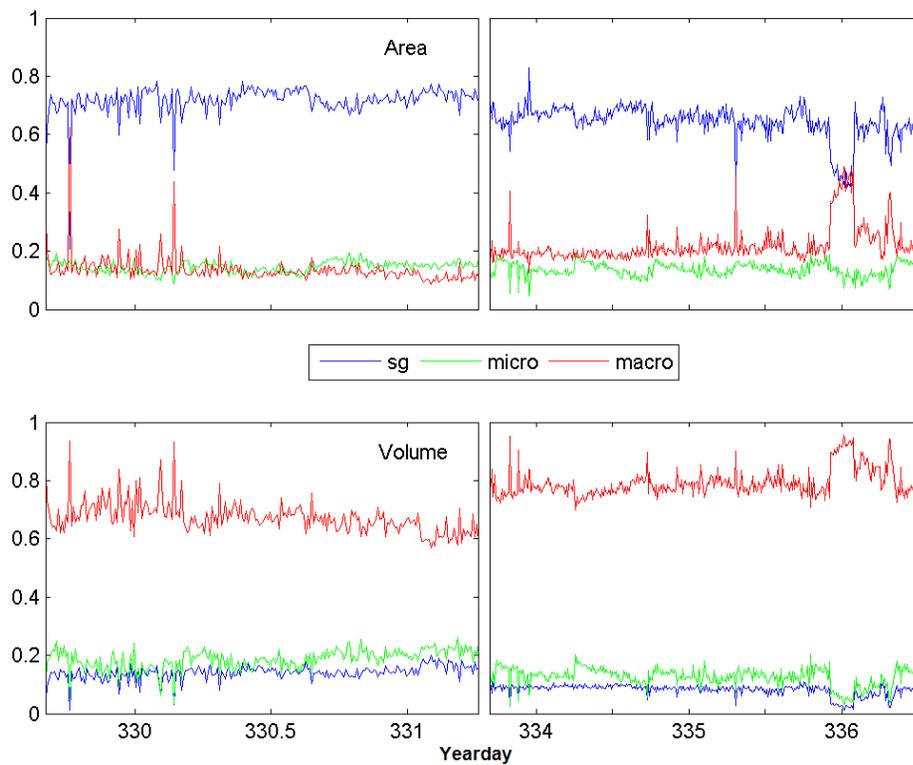
Figure 4. Time series of single grain (D < 33 μm), microfloc (33 < D <133 μm), and macrofloc (D > 133 μm) fractions in suspension for area (top panel) and volume (bottom panel) based on the LISST 100X particle size distributions.
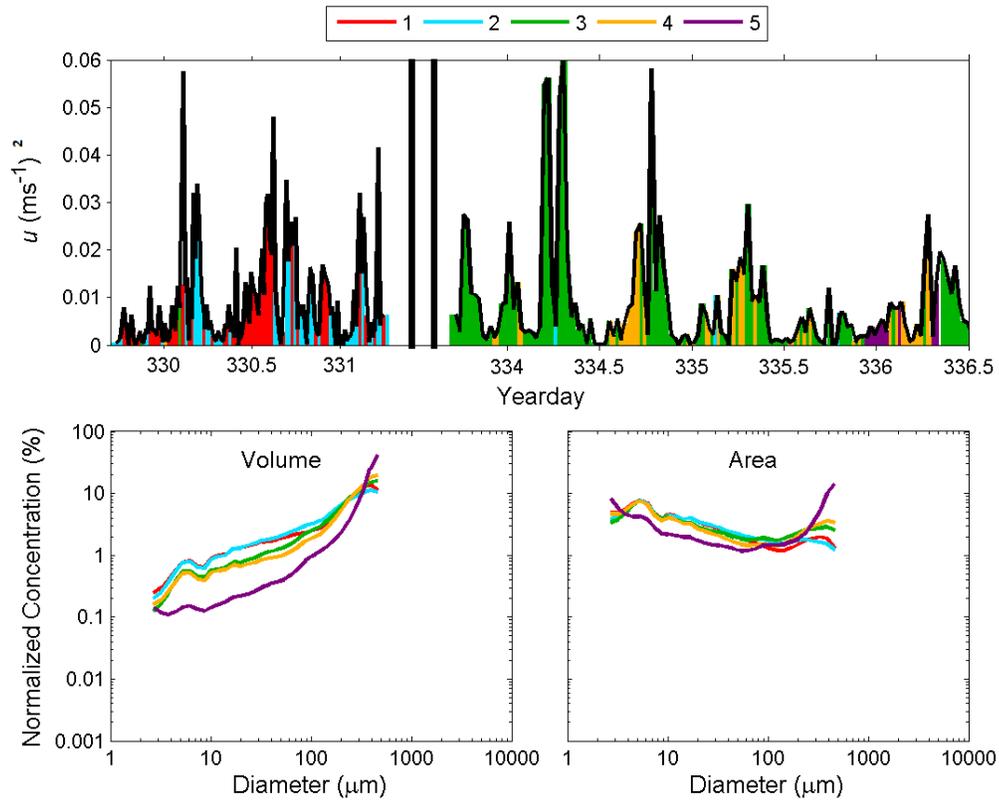
Figure 5. Particle size distributions (n= 634) sorted into 5 groups using entropy analysis. The upper panel uses colour to show particle size groupings over a time series of the square of the velocity from the ADCP for currents only throughout the deployment period. Lower panels are mean particle size distributions per group, presented as normalized volume and area concentrations.

Table 1. Results from the 5 entropy particle size groups and the percentages of single grains (SG), microflocs (Micro) and macroflocs in each group.

	Red	Blue	Green	Yellow	Purple
SG	14.4	14.2	9.0	8.2	2.7
Micro	20.4	24.8	18.3	13.8	6.5
Macro	65.2	61.0	72.7	78.1	90.8

low, close to 5 km hr^{-1} for over a day, and during the only time when current

velocities remained low < 0.10 m s^{-1} for longer than 12 hours. Overall, however,

groups did not correspond to specific stress levels or stages of the tide (Fig. 5).

The DVC produced 796 estimates of floc size versus settling velocity and

floc size versus effective density (Fig. 6). Settling velocities ranged from 0.195

mm s^{-1} to 39.9 mm s^{-1} for floc sizes that ranged from 226.1μm to 997.1 μm (Fig.

6). The average size and settling velocity for the population of flocs measured

during the deployment were 331 μm and 0.83 mm s^{-1} respectively. Of the 796

flocs observed, 20 had settling velocities > 2mm s^{-1}, and only 8, or about 1% of

the population, had floc settling velocities > 10 mm s^{-1}. The commonly observed,

order-of-magnitude scatter in settling velocities for a given particle diameter has

been attributed to variable particle packaging and composition within flocs (e.g.,

Hill et al., 1998). Particle densities were calculated with a modified form of

Stokes Law (cf. Khelifa and Hill, 2006).

The size versus settling data were fit to the model of Khelifa and Hill

(2006) (Fig. 6). The model describes settling velocity and density as a function of

aggregate size (cf. Hill et al. 2011). The model requires inputs of water density,

ρ, and dynamic viscosity, μ, which were estimated based on a mean temperature

of 8.5°C and salinity of 32 PSU. It also requires the component particle diameter,

D_c, and the diameter of the largest flocs in suspension, D_{max}. The component

particle diameter, D_c, was determined from the disaggregated inorganic grain size

distribution (DIGS) in the water samples. It was taken as the volumetric mean

diameter of the DIGS samples, which was 7 μm. The parameter D_{max} was
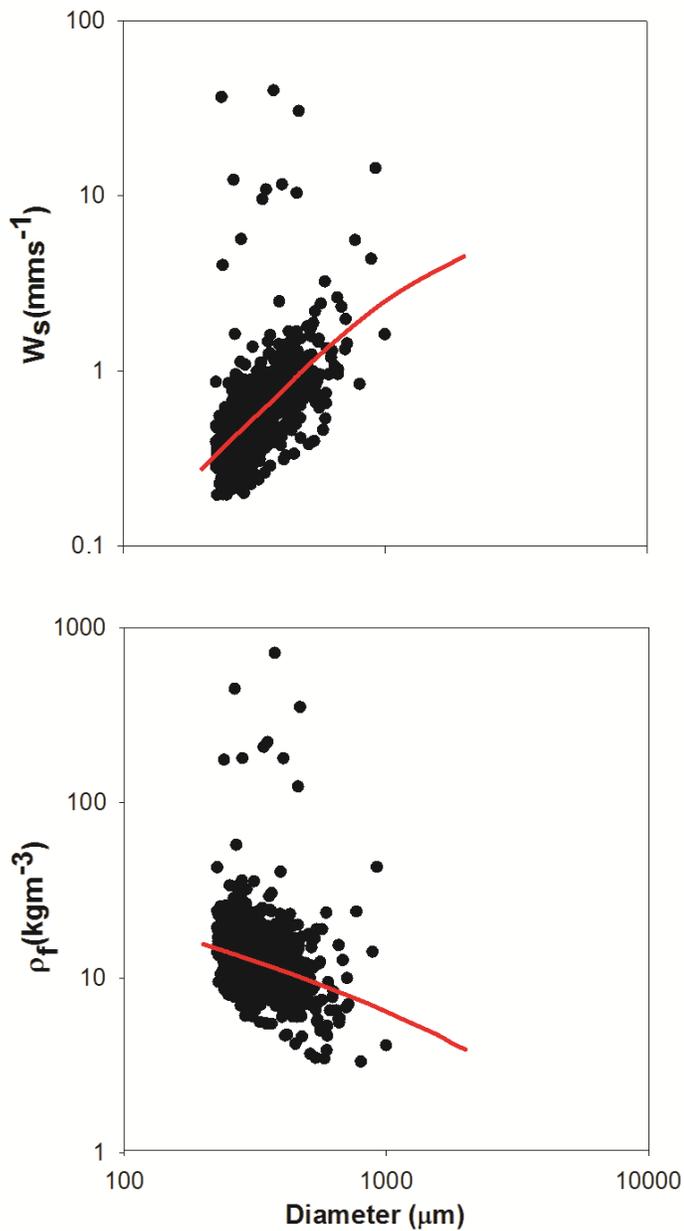
Figure 6. Unbinned particle size versus settling velocity and particle size versus effective density (panel on top and bottom). The particle effective densities were estimated using a modified Stokes' law. The red line in each of the panels represents the Kheilfa and Hill (2006) fit of the data.

determined as the 95th percentile of particle diameters observed with the DVC.

Its value was 594 μm. The model fit to the size versus settling velocity data

yielded estimates of two parameters: F_{max}, which is the fractal dimension of

largest flocs in suspension, and ρ_s, which is the density of the component grains.

The fractal dimension describes a relationship between the diameter and mass of

a particle, with the fractal dimension of largest aggregates in-situ generally falling

within a range of 1.8 to 2.4 (Hill et al. 1998; Sternberg et al. 1999 Fox et al. 2004;

Hill et al. 2011). In this study, the value of F_{max} was 2.7 and the component

particle density was 1060 kg m^{-3}.

4 Discussion

4.1 Particle size and packaging

Floc size and abundance in the ocean is controlled by five basic

mechanisms: advection, resuspension, aggregation, disaggregation, and

deposition (Jago et al. 2006; Mikkelsen et al. 2006; Hill et al. 2013). A change in

floc size or abundance due to advection is distinguishable when floc size is

decoupled from bottom stress (Jago et al. 2006). Resuspension is

distinguishable by coupling between floc size and seabed stress (Milligan et al.

2001; Fugate and Freidrichs, 2003; Hill et al. 2013). Aggregation occurs when

turbulence is low to moderate and particle concentration is large (Milligan et al.

2007). The process of aggregation occurs most often in a tidally dominated

system during slack water, when the coincidence of elevated concentration and

low-to-moderate turbulence allows flocs to grow (Jago et al. 2006).

Disaggregation is the process of floc destruction and occurs under energetic

conditions. Its signature is an inverse correlation between floc size and turbulence (Winterwerp, 1998; Hill et al. 2001; Mikkelsen et al. 2006; Mikkelsen et al.2007). Hill et al. (2001) reported that marine aggregates or flocs break up when turbulent stress is at or above 0.1 Pa. Deposition occurs when stress is low enough for flocs to settle from the water column. It is associated with decreases in concentration and overall particle size. As a suspension settles, however, a temporary increase in concentration near the seabed can occur (Milligan et al. 2001; Voulgaris and Meyers, 2004; Mikkelsen et al. 2006; Hill et al. 2011).

Particle packaging at the study site was relatively consistent during deployment 1 and again during deployment 2, but the packaging observed during the two deployments differed, with entropy groups 1 and 2 appearing in deployment 1 and groups 3 and 4 appearing in deployment 2 (Fig. 5). The single grain fraction was smaller and macrofloc fraction was larger during the second deployment. The changes in particle size were not associated with changes in bottom shear stress, which were similar during the two deployments (Fig. 2, 4, 5). Decoupling of particle size from shear stress is associated with advection of water masses with different particle populations (Jago et al., 2006).

Entropy group 5 was characterized by the largest macrofloc fraction. Size distributions in this group occurred at the end of day 335, after a period of prolonged low winds and currents (Fig. 2). The co-occurrence of large particles and low energy is diagnostic of aggregation. Interestingly the flocs in suspension at this time dominated the water column for just under five hours. Based on

average floc settling velocities of roughly 1mm s^{-1}, it would take about 5 hours to clear a 20 m water column, roughly the average depth at our study site. Alternatively, the change in particle size during this event could also be due to advection. Time series of beam attenuation can help to resolve which process was the more likely cause of the change in particle size.

Beam attenuation (C_p) has been successfully used as a proxy for mass concentration in suspension (e.g. Boss et al., 2009a). C_p generally is not sensitive to changes in particle size caused by aggregation or disaggregation, so changes in C_p usually result from resuspension, deposition or advection (Boss et al. 2009 a & b; Hill et al. 2011). In this study beam attenuation was generally just above 2 m^{-1} for the first deployment of the LISST and just below 4 m^{-1} for the second deployment (Fig. 7). This change in C_p between deployments can be explained by advection. The appearance of entropy group 5 at the end of day 335 was associated with an increase in C_p. Changes in particle size due to aggregation alone should not create significant changes in C_p, as evident by a jump in C_p from ~3 m^{-1} to 10 m^{-1} so it is likely that this event was due to advection of a water mass with different particles.

Increases in C_p occurred generally on flood tides and were generally associated with small changes in water temperature, another indication that particles could have been advected into the study site (Fig. 2, 7). Water sampling as part of a companion study (Milligan and Law, 2013) showed background suspended particulate matter below 2 mg L^{-1} during year day 330 and below 3 mg L^{-1} during year day 335. Despite the low number of water samples, the
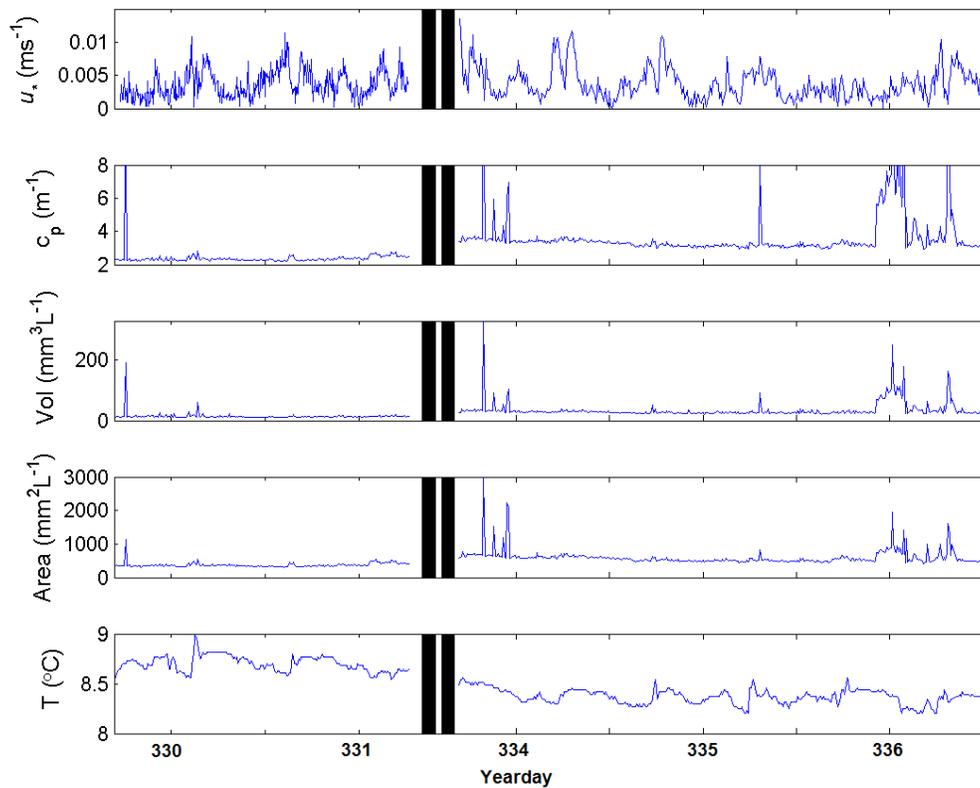
Figure 7. Time series of physical and particle variables. The top panel is a plot of shear velocity calculated over the study period using the law of the wall and a bottom roughness parameter of 2.0e-4 from Soulsby et al. (1983) for a muddy seabed. The next four panels are beam attenuation (C_p), volume concentration, area concentration and water temperature all collected by the LISST over the study period.

change in concentration supports the hypothesis that the water mass at the study site changed between the two LISST deployments.

Evidence for a limited role for resuspension in shaping particle size distributions is available in the time series of shear velocity. Shear velocity remained below 0.01 m s^{-1} for the entire deployment period and generally was lower than 0.005 m s^{-1} for long periods of time (Fig. 7). Fluff layers, primarily composed of flocs, can be resuspended by shear velocities as low as approximately 0.003 m s^{-1} (Law et al. 2008, Milligan and Law, 2013), but more consolidated marine muddy bottom sediments have been shown to resuspend at shear velocities as low as 0.006 m s^{-1} (Schaff et al, 2006) but generally require shear velocities to be greater than 0.009 m s^{-1} (Sanford and Maa, 1988, Wiberg et al. 1994; Law et al. 2008; Dickhudt et al. 2010). A bottom shear velocity of 0.009 m s^{-1} was rarely exceeded during the deployment period and when seabed shear velocity did approach 0.01 m s^{-1} during year day 334 there was no corresponding increase in floc size, abundance, or suspended mass concentration which would be indicative of resuspension at the study site (Fig. 7).

Data from NOAA Buoy 44027 (not shown) which is located 20NM SE of Jonesport, ME indicate that a large wave event (up to 6m) with long period swell (>10 sec) went through the area on the 26th – 27th (year day 331 - 332) not long before the end of the first deployment. This event offers an alternative hypothesis to that of the advection of particles and may explain the different particle sizes and beam attenuation coefficients between deployments 1 and 2. While the instruments were not in the water, the large wave event may have

resuspended bottom sediment in the region. Concentrations therefore, may have been larger during the second deployment because freshly resuspended material had not yet settled.   There were no operations directly related to aquaculture activities such as feeding or cleaning of net pens that could be hypothesized as a reason for changes in mass concentration.

4.2 Size versus settling velocity

The values of F_{max} and ρ_s from this study are higher and lower, respectively, than published literature values for these parameters. The low density of the component particles (ρ_s) suggests that they were rich in organic matter, whereas the high value of fractal dimension (F_{max}) indicates that the aggregate components were relatively tightly packed. The fractal dimensions of large flocs in-situ generally fall within a range of 1.8 to 2.4, with an average value near 2 (Syvitski et al. 1995; Hill et al. 1998; Sternberg et al. 1999; Fox et al. 2004; Hill et al. 2011). Estimated densities of component particles ranged from 1150 kg m^{-3} in a study by Hill et al. (2011) to 1600 kg m^{-3} in the study of Curran et al. (2007). One hypothesis is that the lower estimated density of component particles within aggregates at this study site could have resulted from the release of fine organic particles into the water column from salmon aquaculture operations, either in the form of fecal material or bits of broken down feed. The relatively large fractal dimension could have resulted from denser packing of feces in salmon digestive tracts or denser packing of feed during the production process. Alternatively, because this area of the Bay of Fundy is energetic, with limited inputs of fresh fine sediment, flocs may be densely packed due to multiple

resuspension and deposition cycles. Feed and fecal material could have initially settled to the seabed, became consolidated and then reworked and resuspended into the water column thus altering their initial conditions and making them small enough to be incorporated in flocs. The input of organic material may have also been from operations other than aquaculture.

Modelled floc effective densities ranged from 1030 kg/m^{-3} to 1040 kg/m^{-3} for floc sizes ranging from 200 to 2000 µm (Fig. 6). These densities were similar to those found for fecal density in studies conducted by Ogunkoya et al. (2006) and Moccia et al. (2007). Both of these studies measured the properties of rainbow trout feces in the laboratory, and the observed densities ranged between 1022 kg m^{-3} and 1052 kg m^{-3}. Marked differences between this study and those of Ogunkoya et al. (2006) and Moccia et al. (2006) were seen in the settling velocities, but they can be explained by different sizes of settling particles among studies. Unfortunately, no particle size data accompanied the other studies. Moccia et al. (2007) reported settling velocities between 43.3 mm s^{-1} and 60.6 mm s^{-1}, while Ogunkoya reported settling velocities of 27 mm s^{-1} to 34 mm s^{-1}. This study observed a maximum settling velocity of 39.9 mm s^{-1}, and only 3 of the 796 measurements were >30 mm s^{-1}, which is generally used as the lower estimate of intact salmon fecal material settling velocity based on laboratory studies under controlled conditions. Chen et al. (1999) speculated that as fecal pellets settle in the water column they may break up into smaller pieces, which would slow their settling rate. The measurements of the size settling velocity in this study were made using a settling column and video that was sitting on the

seabed in 20 m of water. Settling particles analyzed in this study would have

been subjected to water column turbulence from the time they were released

until they entered the settling column.

4.3 Possible Implications for Aquaculture Waste Transport

A review of the biophysical properties of salmonid feces and implications

for waste dispersal models and IMTA by Reid et al. (2009) stated that information

in the literature was limited on particle size, density, and the settling velocity of

material at aquaculture cage environments. The estimated floc fractal

dimension, which describes the packaging of material in suspension, in this study

was higher than in previous studies in the marine environment (Mikkelsen et al.

2006; 2007, Curran et al. 2007; Hill et al. 2011; Hill et al. 2013). Also, the density

of the component particles in flocs was lower at this study site compared to other

floc populations measured in a variety of marine environments (Mikkelsen et al.

2006; 2007, Curran et al. 2007; Hill et al. 2011; Hill et al. 2013). Interestingly,

they were similar to densities of aquaculture waste material described previously

in laboratory studies (Ogunkoya et al 2006; Moccia et al. 2006). Together these

observations provide indirect support for the hypothesis that particles associated

with finfish aquaculture activities are incorporated into easily transported flocs

(Milligan and Law, 2005).

Floc sizes in this study were generally *< 600* μm based on observations

from the DVC, with an average size of ~340 μm. Average floc settling velocities

were approximately 1 mm s^{-1}, and although compositional data were not

available, the flocs may have contained small bits of food or fecal material based

on their estimated density. With an average water depth of 20 m and a floc settling velocity of 1 mm s^{-1}, it would take 20,000 seconds, or about 5 hours, for a particle to settle to the seabed. At Charlie Cove current velocities are regularly >10 cm s^{-1}. The horizontal distance a particle would travel would be on the order of 2 km based on a horizontal velocity of 10 cm s^{-1} and a settling time of 20,000 seconds. The 2-km distance is larger than the normally defined near field zone (<500 m) where aquaculture activities have documented effects on the environment. The 2 km estimated horizontal distance of travel for settling flocs is likely a minimum because it does not include post-depositional resuspension and transport of these organic-rich flocs.

A recent study by Graydon et al. (2012) around an aquaculture site in the southwest Isles region of N.B. showed the incorporation of aquaculture derived waste material from feed pellets (canthaxanthin) in sea urchins at 1 km from the active salmon farming cage site, both near the surface and at 1 m off the bottom. The 1 km represented the farthest distance measured in that study. Graydon et al. (2012) hypothesized that a background concentration of pigments may exist from widespread dispersal of salmon derived particles from all the salmon farms in the area. Sara et al. (2006) used isotopic analysis to detect aquaculture waste material in the water column and in the seabed. They found evidence of farm derived material at distances up to 1 km, also the furthest distance measured. Sara et al. (2006) proposed that post-depositional resuspension and transport of waste explained the occurrence of waste in the far-field. If feed pellets are broken down either by the fish themselves during feeding or by hydrodynamic

processes and subsequently incorporated into flocs like those observed in this study, the calculations above show that transport distances of wastes could be greater than 1 km.

The modelling of aquaculture waste solid fraction has focused on the deposition of fecal material and feed pellets to the seabed. Models indicate that enhanced flux of these materials is limited to the near field area < 500m from the cage edge (Findlay and Watling, 1994; Cromey et al. 2002a; Chamberlain and Stucchi, 2007). Typical settling velocities used to model these components, are 40 mm s^{-1} (feces) and 100 mm s^{-1} (feed), respectively. These particles were not completely resolved in this study because of the maximum observable settling velocity by the DVC as configured approached that of fecal settling as previously determined in laboratory studies. Feces and feed have been observed in-situ and obviously need to be included in aquaculture waste models. Observations here indicate that flocs captured near an aquaculture site were different from those observed in other marine environments. They sank at roughly 1 mm s^{-1} and may provide a mechanism for exporting aquaculture derived waste material to the far-field. Based on these findings, flocs should also be considered in aquaculture waste transport models. Models such as DEPOMOD or other transport models could include material that sinks at 1 mm s^{-1}, in addition to the already included feed pellets (100 mm s^{-1}) and fecal material (40 mm s^{-1}).

To fully elucidate the particle size, packaging, composition and settling velocity of material around aquaculture sites, further studies are required. Isotopic analysis as performed by Sara et al. (2006) may prove useful for

quantifying the amount of aquaculture-derived particles in each of the proposed classes of waste material (i.e. those that settle at 100, 40 and 1 mm s^{-1}). These studies should be conducted in areas in close proximity to farming operations and at background sites remote from farming operations.

The inferred dominant process influencing floc properties during this study was advection. Clear indicators of resuspension, aggregation, disaggregation, and deposition were not detected. The dominance of advection may have been due to the relatively sheltered study site that had moderate tidal currents and water depths that limited the effects of wave resuspension. It would be beneficial to cover the entire range of hydrodynamic conditions that could be experienced at farming operations in the southwest Isles region of New Brunswick. In this region winter storms produce high winds and large waves that have the potential to resuspend and transport waste material from under a cage site. This full range of hydrodynamic conditions would help to capture and quantify the 5 mechanistic processes that control particle size and transport.

5 Conclusions

Particle size and packaging are controlled in the marine environment by the processes of advection, resuspension, aggregation, disaggregation and deposition. At the Charlie Cove site in the macrotidal Bay of Fundy, particle size and concentration were controlled generally by advection, although resuspension of material between the first and second deployments could not be ruled out.

The size versus settling velocity data collected with the DVC and attached settling column were fit to the model of Khelifa and Hill (2006) to produce a floc

size versus density relationship. Component particles had an estimated density of 1060 kg m^{-3}, and the fractal dimension of the largest particles was 2.7. These parameters suggest that the flocs observed at the site were tightly packed and had low densities typical of organic matter. These values differ from those in the published literature where observations were made in the absence of aquaculture related activities. The effective densities of particles observed in this study were comparable to those obtained from studies on fish fecal matter observed in previous lab studies.

The average settling velocity of aggregates observed in this study was of order 1 mm s^{-1}. This settling velocity combined with current velocities of order 10 cm s^{-1} would mean that flocs could have been transported over distances of ~2 km. We propose that flocs, which settle on the order of 1 mm s^{-1}, in addition to settling fecal material and feed, be included in aquaculture waste transport models to elucidate the entire particle population.

Acknowledgements

Chapter 3

This chapter is a manuscript published in Aquaculture Environment Interactions. Citation is below:

Law, B.A., Hill, P.S., Milligan, T.G., Zions, V.S., 2016. Erodibility of aquaculture waste from different bottom substrates. Aquaculture Environment Interactions, 8, 575-584. doi:10.3354/aei00199

Erodibility of aquaculture waste from different bottom substrates
Law, B.A.[1,2,*], Hill, P.S.[2], Milligan, T.G.[1], Zions, V.[1]

[1] FISHERIES AND OCEANS CANADA, BEDFORD INSTITUTE OF OCEANOGRAPHY, DARTMOUTH, NOVA SCOTIA, CANADA, B2Y 4A2

[2] DEPARTMENT OF OCEANOGRAPHY, DALHOUSIE UNIVERSITY, HALIFAX, NOVA SCOTIA, CANADA, B3H 4J1

* Corresponding author
Brent Law
Habitat Sedimentologist
Fisheries and Oceans Canada
Bedford Institute of Oceanography
1 Challenger Drive, Dartmouth, Nova Scotia
Canada, B2Y 4A2
Brent.Law@mar.dfo-mpo.gc.ca
Telephone | Téléphone 902-426-8548
Facsimile | Télécopieur 902-426-6695
Government of Canada | Gouvernement du Canada

Abstract

A laboratory study was carried out to examine the effect of bed sediment texture on the erodibility of salmon aquaculture waste fecal material and salmon feed pellets. Erodibility measurements of this material were made using a Gust microcosm erosion chamber and artificially composed substrates of mud, sand, sand and gravel, sand and cobble, and cobble. Results show that cumulative mass eroded (CME) and erodibility constant (M) can vary by up to an order of magnitude depending on substrate composition, with a mud substrate having higher values than that of substrates composed of sand, gravel and cobble. Findings from this study suggest that bottom sediment texture plays a major role in aquaculture waste resuspension and subsequent transport and that predictive models of the transport of aquaculture waste should include the erosion dynamics of bottom texture.

1. Introduction

With the expansion of the aquaculture industry, concerns have been raised over the fate of aquaculture waste material, primarily feed pellets and fecal matter from salmon farming. Models that predict the transport and fate of particles in the coastal ocean are required by Habitat Managers, Fisheries and Aquaculture Managers, and other government regulators to understand marine water quality, contaminant transport, coastal erosion, and the cumulative effects from anthropogenic influences. Models presently being used for finfish aquaculture do not predict waste transport accurately because they lack data with which to parameterize the cohesive nature and transport properties of fecal material, waste pellets, and their interaction with particulate matter in suspension and on the seabed.

Research related to aquaculture waste has dealt primarily with deposition immediately under or adjacent to salmon net pens. Modelling and field studies have focused on near-field effects from organic enrichment, while the far field has received far less attention. The near field is considered to be the area within a few hundred meters of farming operations, while the far field can extend kilometers away. Models to predict the depositional footprint from salmon and other finfish farms using the settling characteristics of waste solids have become increasingly accurate (Panchang et al., 1997; Cromey et al., 2002; Chamberlain and Stucchi, 2007). Models that predict the subsequent resuspension and transport of waste material, however, are lacking (Droppo et al., 2007; Chamberlain and Stucchi, 2007; Reid et al., 2009). Development of coupled

hydrodynamic-sediment transport models that can address the far field will require parameterization of the factors responsible for influencing the erosion of aquaculture waste material. Measurements of the erodibility of waste particles associated with aquaculture are lacking, which limits understanding of potential far-field transport and possible environmental impacts.

Wave and current stress exerted on the seabed provide the work necessary to erode particles from the seabed, whereas particle size and density, bed roughness, cohesion, porosity, consolidation, and biological activity control the erosion resistance of the seabed (Amos et al. 1992, 1997; Maa et al., 1998; Sanford and Maa, 2001, Wiberg et al., 2013). Overall understanding of cohesive sediment resuspension is incomplete because it is governed by not only hydrodynamic forces and the force of gravity, but also by cohesion, which depends on biological and electrochemical variables (Black et al., 2002; Droppo, 2007). The highly organic nature of aquaculture wastes could significantly impact their erodibility.

Boundary shear stress is defined as the force per unit of area that flowing water exerts on the seabed. Particles at the surface of the seabed move when the downstream (i.e. fluid drag) and upward (i.e. fluid lift) forces overcome the forces keeping a particle in contact with the bed (Wiberg and Smith, 1987). The stress on the bed required to induce motion is the critical erosion shear stress, which is denoted τ_c (Einstein, 1950; Partheniades, 1962; Amos et al., 1992; Tolhurst et al., 1999). There have been many investigations of the erosion of non-cohesive (e.g., Shields, 1936; Soulsby, 1997) and cohesive seabeds

(Winterwerp, 1989; Amos et al., 1992, 1997). In the broadest terms non-cohesive sediments have mean grain sizes > 63µm, and cohesive sediments or "muds" are dominated by fine-grained particles that are < 63µm. More recently, attention also has been given to erosion of sand-mud mixtures that show complex behaviours influenced strongly by the fraction of mud in the mixture (van Ledden et al., 2004; Law et al., 2008; Wiberg et al., 2013). Little research has focused on the erosion of aquaculture waste solids.

The model DEPOMOD was developed to predict the solids waste accumulation on the seabed associated with fish farming activity (Cromey et al., 2002). While primarily addressing the initial deposition of waste, DEPOMOD also employs a simple resuspension module to redistribute waste particles according to near-bed currents. The resuspension module uses the erosion formula:

$$Me = M \left(\frac{\tau b}{\tau c} - 1 \right) \tag{1}$$

where Me is the eroded mass (kg m^{-2} s^{-1}), τb (Pa) is the applied bottom stress, τc (Pa) is the critical stress for erosion, and M is an erodibility constant (kg m^{-2} s^{-1}). In the module the values of M and τc are hard coded to be 7.0 x 10^{-7} kg m^{-2} s^{-1} and 0.0179 Pa (9.5 cm s^{-1} flow speed), respectively. DEPOMOD does not consider variation in bottom substrate and its effect on erodibility.

To examine the effect of bottom type on erosion, aquaculture wastes were placed on top of sediment cores that contained different substrates. The cores were eroded in the lab with a Gust microcosm erosion chamber. The bottom substrates used were representative of a range of seabed types found under

aquaculture sites. The methods used were the same as those used in the field for making direct measurements of sediment erodibility. Results are presented in terms of the erodibility parameter, M, and the critical erosion stress (i.e. τc) required to mobilize waste particles.

2. Methods

2.1 Overview

Cores representing different bottom types were made in 10.8 cm core barrels. Five different bottom types were used: mud, sand, sand and gravel, sand and cobble, and cobble (Fig. 1). In each core, seawater was added to a depth of 10 cm above the sediment surface. For each substrate type, waste material from salmon was allowed to settle onto the surface of the core. The salmon waste was collected from the tanks at the Coldbrook, N.S. fish hatchery. Salmon fecal material comprised intact and disintegrated fecal material. It was added gently to the tops of the artificial cores 2 hours before erosion studies commenced to allow sufficient time for the material to settle. The mass of fecal material added to each erosion experiment was determined by gravimetric analysis. The erodibility of salmon feed pellets was examined by depositing pellets on the different surfaces. Each core was then fitted with a Gust Erosion Chamber to determine the erosion shear stress and mass eroded.

2.2 Gust Chamber

The Gust chamber is an erosion simulator that comprises a polycarbonate housing with a rotating disk, a removable lid, and water input and output connections. It fits

Fig. 1. Downward looking photos onto the bottom substrate used in each of the erosion chamber experiments. In order starting at the top left panel is cobble, sand and gravel, sand, sand and cobble and consolidated mud. The diameter of the cores is the same as that of a slo-core tube, which is 10.8 cm.

directly on top of a core tube. By controlling both the rotation rate of the disk and

the rate at which water is pumped through the device, a uniform shear stress is

applied across the sediment surface. Shear stresses applied to cores were 0.01,

0.08, 0.16, 0.24, 0.32, 0.40, 0.48, and 0.60 Pa. Shear stress at each level was

applied until an attached turbidity meter recorded values that corresponded to

background concentrations, which was 30 minutes for the 0.01 Pa stress, and 20

minutes for each successive shear stress. Background water, which was seawater

filtered at 0.45 µm to remove particles, was pumped into the chamber and

withdrawn from an outlet in the lid to maintain the desired shear stress. The water

exiting the chamber, which contained eroded particles, was pumped from the

chamber through the turbidity meter, collected in a 2 L flask and filtered for

suspended particulate matter (SPM). The turbidity meter and SPM data were used

to calculate cumulative mass eroded and critical erosion shear stress (τc) for each

core. For a complete description of the Gust chamber, its function and calibration,

see Gust and Muller (1997); Tolhurst et al. (2000); and Stevens et al. (2007).

2.3 Substrates

The bottom substrates were chosen to be representative of the seabed

types in which salmon aquaculture is active in Canada or where new sites may

be developed (Fig. 1). The mud core was formed from mud collected in St.

Peters Bay, Prince Edward Island. The mud had a median diameter, d50, of 10

µm. The mud core was pre-eroded without waste in order to obtain a smooth,

consolidated mud bed which was used in the erosion studies. This treatment

prevented mixing of resuspended substrate mud with waste particles. The sand

used in the experiment was from Lawrencetown Beach, Nova Scotia and had a d50 of ~ 250 µm. The gravel was a quarry grade, and 65 % of the mass had diameters between 2 and 2.5 mm, and 85 % of the particles by mass had diameters greater than 1.5 mm. The cobble classification had only a small percentage of actual cobble (i.e. > 64 mm), most of the sediment in this class was actually larger gravel between 20 and 50 mm, which came from Lawrencetown beach, NS, but the classification of cobble was used to distinguish it from smaller gravel used in these experiments. All classifications of grain size are based on the Wentworth scale.

For each substrate type and waste material, the experiments were performed 6 times. The salmon fecal material erosion studies were performed in triplicate in the summer and again in triplicate in the winter to determine if there were seasonal differences in the waste material resuspension due to decreased feeding and metabolic process in the winter. There were no discernable differences in the resuspension dynamics in terms of erosion rate or cumulative mass eroded, so winter and summer data sets were combined.

Experiments with salmon feed pellets were carried out in the same manner using mud, sand, and cobble substrates. Feed pellets that were 5 mm in diameter and 9 mm in diameter were used to represent a range of pellets fed to small and large salmon during the grow out process. Critical stress for motion was based on when at least one of the pellets moved, and rolling and saltating classifications were based on when half of the pellets were in that specific motion. In these experiments rolling means the movement of pellets along the

core top while saltating means the bouncing of pellets. The horizontal transport numbers listed herein are based on the majority of pellets moving around the core at an equal spacing from the core wall. Wall effects are not accounted for and only general trends are reported.

2.4 Erosion Calculations

The mass eroded per unit area at each shear stress step was calculated by multiplying the SPM for each shear stress step, which was determined by gravimetric filtration, by the total volume of water collected for each stress step, and then dividing by the area of the eroded surface (0.0092 m^2). The cumulative mass eroded (CME) in kg m^{-2}, is the sum of the mass eroded for each shear stress step. CME was normalized by the % of waste material recovered in each erosion experiment to account for small differences in the amount of waste material added to the core tubes. The erodibility parameter (i.e. M) was determined based on equation (1) above and is an average value calculated up to and including a bottom shear stress of 0.60 Pa. An average erodibility parameter, M, is presented as a means to compare the results of this study with the parameters used in DEPOMOD.

3. Results

Critical erosion shear stress, defined as the stress at which waste material was initially resuspended from the surface, was determined to be 0.01 Pa for all bottom types (Figure 2; Table 1). The erodibility of salmon aquaculture waste solids from different bottom substrates resemble that of a Type I (i.e. depth
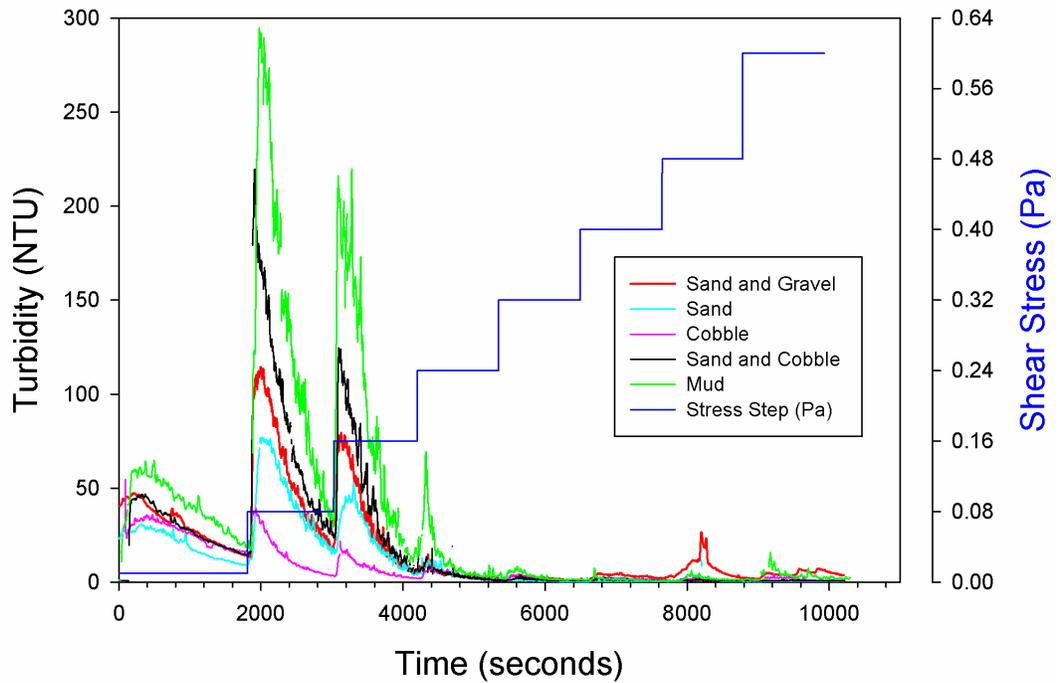
Fig. 2. A plot of turbidity versus time from the Gust erosion studies of salmon aquaculture waste material. The plot was generated from the Campbell turbidity sensors attached to the erosion chamber. Different colours indicate different bottom substrates.

Table 1. Salmon Waste Parameters N=6

Substrate	tau_c (Pa)	M (kg m^{-2} s^{-1})
Sand Avg	0.01	3.50E-07
Std Dev		1.50E-07
Mud Avg	0.01	1.30E-06
Std Dev		4.90E-07
Cobble Avg	0.01	4.50E-08
Std Dev		1.80E-08
S&G Avg	0.01	6.00E-07
Std Dev		1.90E-07
S&C Avg	0.01	5.80E-07
Std Dev		2.70E-07

limited) erosion (Amos et al., 1992; Fig. 2). A plot of turbidity, which is a proxy for suspended mass concentration, with time for increasing bottom shear stresses in the Gust chamber shows an erosion pattern in which once the new shear stress is applied to the bottom substrate, the concentration of waste solids rapidly increases as they are eroded from the bed and then decrease exponentially as resuspended wastes exit the well-mixed chamber via the exhalant flow (Fig. 2). Visual observation of waste solids eroded from the different bottom substrates suggests that aggregated waste particles dominate at lower shear stress (i.e. 0.01 Pa and 0.08 Pa; Fig. 3).

Comparison of 5 different bottom substrates indicates that more wastes were eroded from muddy substrates than from sandy and gravel substrates (Fig. 2). The erosion experiments also showed that little to no erosion of waste solids or bottom substrate occurred above 0.32 Pa, which was evidenced by low turbidity (Fig. 2). In all but the erosion experiments conducted on a muddy seabed, there was evidence that some of the waste solids remained even after the complete erosion experiments, which were conducted up to and including 0.60 Pa (Fig. 4). On average > 97 % of salmon waste material added to the mud substrate was eroded, while < 25 % of the material added to the cobble substrate was removed (Fig. 4). The substrates composed of sand averaged about 65 % removal from the bed (Fig. 4). These percentages were determined by dividing the CME by the total amount of waste material added to each core.

Average cumulative mass eroded (CME) in kg m^{-2} up to and including the 0.60 Pa stress step for the salmon waste experiments was 0.030 kg m^{-2} +/- 0.013

Fig. 3. Photo of a core showing the erosion of waste material at low stress (i.e. 0.08 Pa). The large suspended particles are organic-rich flocs.
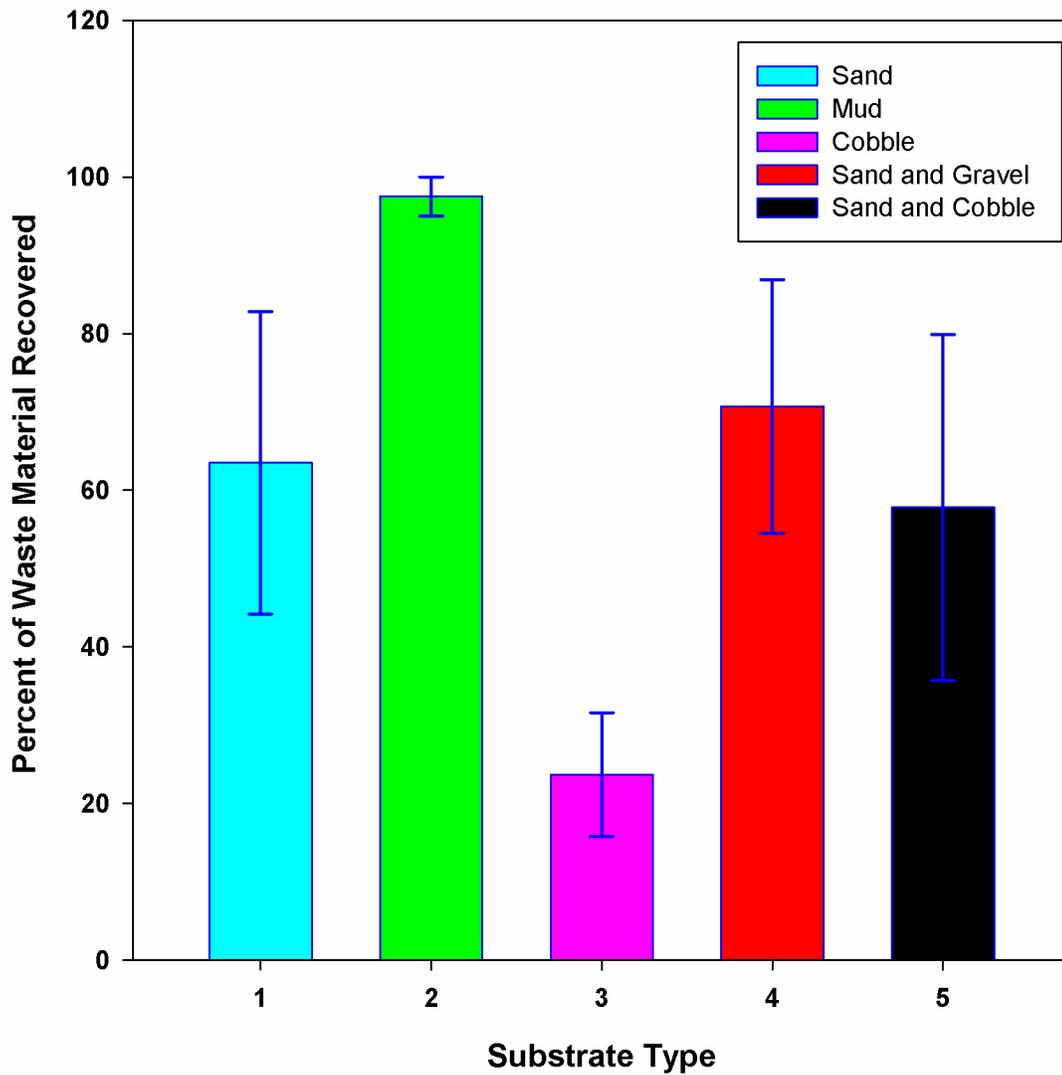
Fig. 4. A plot of the average percent of waste material recovered from the N=6 erosion experiments completed on each substrate. Error bars represent one standard deviation.

kg m^{-2} for the sandy bottom substrate (Fig. 5). The average CME for a muddy

seabed was 0.116 kg m^{-2} +/- 0.041 kg m^{-2}, 0.055 kgm^{-2} +/- 0.017 kg m^{-2} for a

seabed composed of sand and gravel, 0.049 kg m^{-2} +/- 0.023 kg m^{-2} for a sand

and cobble seabed and for a cobble (mostly larger gravel) seabed CME was

0.005 kg m^{-2} +/- 0.002 kg m^{-2} (Fig. 5). The CME from the cobble substrate was

only 5 % as large as the CME from the mud substrate. The sand substrate

yielded CME values that were approximately 4 times less than the mud

substrate, while the sand and gravel and sand and cobble had CME values

around half of that of the mud substrate.

Critical shear stress for motion of feed pellets varies depending on bottom

type and pellet size (Table 2; Table 3). For 5 mm feed pellets the critical erosion

shear stresses were 0.03 Pa, 0.08 Pa, and 0.20 Pa for mud, sand, and cobble

respectively. For 9 mm feed pellets the critical erosion shear stresses were 0.04

Pa, 0.08 Pa, and 0.28 Pa for the mud, sand, and cobble substrates respectively.

Horizontal transport speeds in mm s^{-1} on the different substrates and different

stresses were calculated based on the number of revolutions the feed pellets

made in the Gust chamber over a given period of time divided by the outside

circumference of the tube (Table 3; Table 4). Generally, transport speeds ranged

from 10 mm s^{-1} to 75 mm s^{-1} for feed pellets on the mud and sand substrates but

were negligible on the cobble substrate. Pellets in the cobble moved slightly

from one crevice to another with time but later became lodged in the substrate.
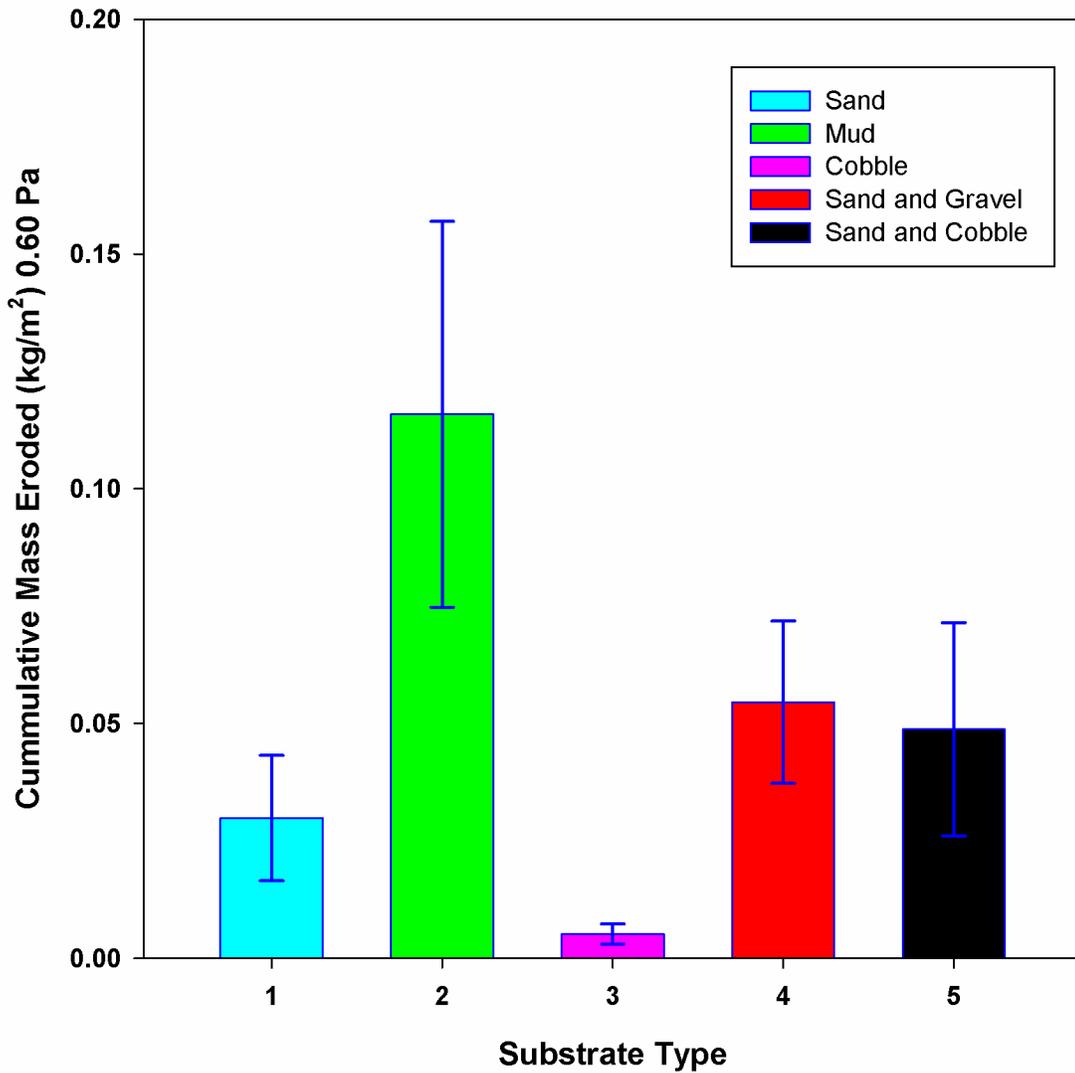
Fig. 5. A plot of cumulative mass eroded in Kg/m² up to and including the 0.60 Pa shear stress step for the N=6 erosion experiments using salmon fecal waste material. Results are normalized to % recovery of waste material. Error bars represent one standard deviation.

Table 2. 5.0 mm Salmon feed pellet transport parameters.

Substrate	tau_c (Pa)	Horizontal Transport (mm s^{-1})	Comments
Mud (consolidated)	0.03	~ 10 from 0.08 to 0.16 Pa ~ 20 to 30 from 0.16 to 0.24 Pa ~ 60 to 75 after 0.24 Pa	rolling at 0.08 Pa, saltating at 0.24 Pa breakup begins at 0.16 Pa
Sand	0.08	~10 from 0.08 to 0.16 Pa ~ 20 to 30 from 0.16 to 0.24 Pa ~75 after 0.24 Pa	rolling 0.16 to 0.24 Pa, some pellets bury in sand between 0.24 and 0.32 Pa, from 0.48 to 0.60 Pa pellets unbury from sand and saltate vigorously and start to really break apart breakup begins at 0.16 Pa
Cobble	0.2	Nil	trapped in stress refuge

Table 3. 9.0 mm Salmon feed pellet transport parameters.

Substrate	tau_c (Pa)	Horizontal Transport (mm s^{-1})	Comments
Mud (consolidated)	0.04	~ 10 from 0.08 to 0.16 Pa ~ 20 to 30 from 0.16 to 0.24 Pa ~ 60 to 75 after 0.24 Pa	rolling at 0.08 Pa, saltating at 0.24 Pa breakup begins at 0.16 Pa
Sand	0.08	~10 from 0.08 to 0.16 Pa ~ 20 to 30 from 0.16 to 0.24 Pa ~75 after 0.24 Pa	rolling 0.16 to 0.24 Pa, some pellets bury in sand between 0.24 and 0.32 Pa, from 0.48 to 0.60 Pa pellets unbury from sand and saltate vigoursly and start to really break apart breakup begins at 0.16 Pa
Cobble	0.28	Nil	trapped in stress refuge

4. Discussion

4.1 Tau Critical

Critical erosion shear stress based on incipient motion was determined to be 0.01 Pa for salmon waste fecal material (Figure 2; Table 1). This value is similar to that previously proposed by Cromey et al. (2002b) who used synthetic tracer beads to simulate salmon waste and reported a tau critical value of 0.0179 Pa, which is most commonly referenced as a "hard coded" value for resuspension in DEPOMOD. This stress corresponds to a flow velocity of approximately 9.5 cm s^{-1}. The numbers reported in this study and that of Cromey et al. (2002b) are similar to other published values for floc erosion (Amos et al., 1997; Thomsen and Gust, 2000; Law et al., 2008; Milligan and Law, 2013). More consolidated cohesive seabeds have higher tau critical values, ranging from 0.03 Pa to 0.08 Pa (Sanford and Maa, 2001; Stevens et al., 2007; Dickhudt et al., 2010; Wiberg et al., 2013). In this study, material first eroded at 0.01 Pa, but the bulk of waste material mass resuspended at the subsequent erosion stress step of 0.08 Pa (Fig. 2). This behaviour is similar to erosion experiments documented in field studies (Stevens et al., 2007; Dickhudt et al., 2010; Wiberg et al., 2013).

The critical erosion stress for feed pellets, for a cobble bed, was significantly larger than that of the sand and mud seabeds. This result is caused by the wedging of pellets in cracks and crevices in the rocks, where they are sheltered from fluid drag and lift (Table 2 & 3). The critical stress values obtained in this study for motion on sandy and muddy substrates were similar to those reported for rolling and saltating by Sutherland et al. (2006), which corresponded to flow

velocities of 16 cm s^{-1} to 20 cm s^{-1} and 32 cm s^{-1} to 40 cm s^{-1}, respectively. Feed

pellet breakup occurred at an applied stress of 0.16 Pa, which corresponds to flow

velocity for pellet breakup reported by Stewart and Grant (2002). As shear stress

increased above 0.24 Pa, pellets swelled and began to saltate, and breakup

became evident (Table 2 & 3).

4.2 Bottom Type

The cumulative mass of salmon fecal material eroded from a mud bed

was an order of magnitude greater than that eroded from a cobble bed (Table 1;

Figure 5). The three substrates composed primarily of sand behaved similarly,

with mass eroded falling between that of cobble and mud substrates (Figure 5 &

6). Figure 6 represents the CME for salmon waste material eroded as a function

of increasing shear stress. Other studies of sediment transport have presented

their results in this manner to look at changing erosion patterns with increasing

shear (Sanford and Maa, 2001; Stevens et al., 2007; Dickhudt et al., 2010;

Wiberg et al., 2013). The difference between this study and those mentioned

above, which primarily looked at the erosion of cohesive seabeds, is that after

0.32 Pa shear in this study there was no longer the increase in the erosion of

bottom material that was found in the other studies (Fig. 6). In natural bottom

sediments the erosion of the seabed increases with increasing shear stress

(Amos et al., 1988; 1992; Maa et al., 1998). The lack of erosion at higher shear

stresses in this study occurred because of the fixed amount of waste available for

erosion (Wiberg et al., 1994; Law et al. 2008; Fig. 6). In this study almost the
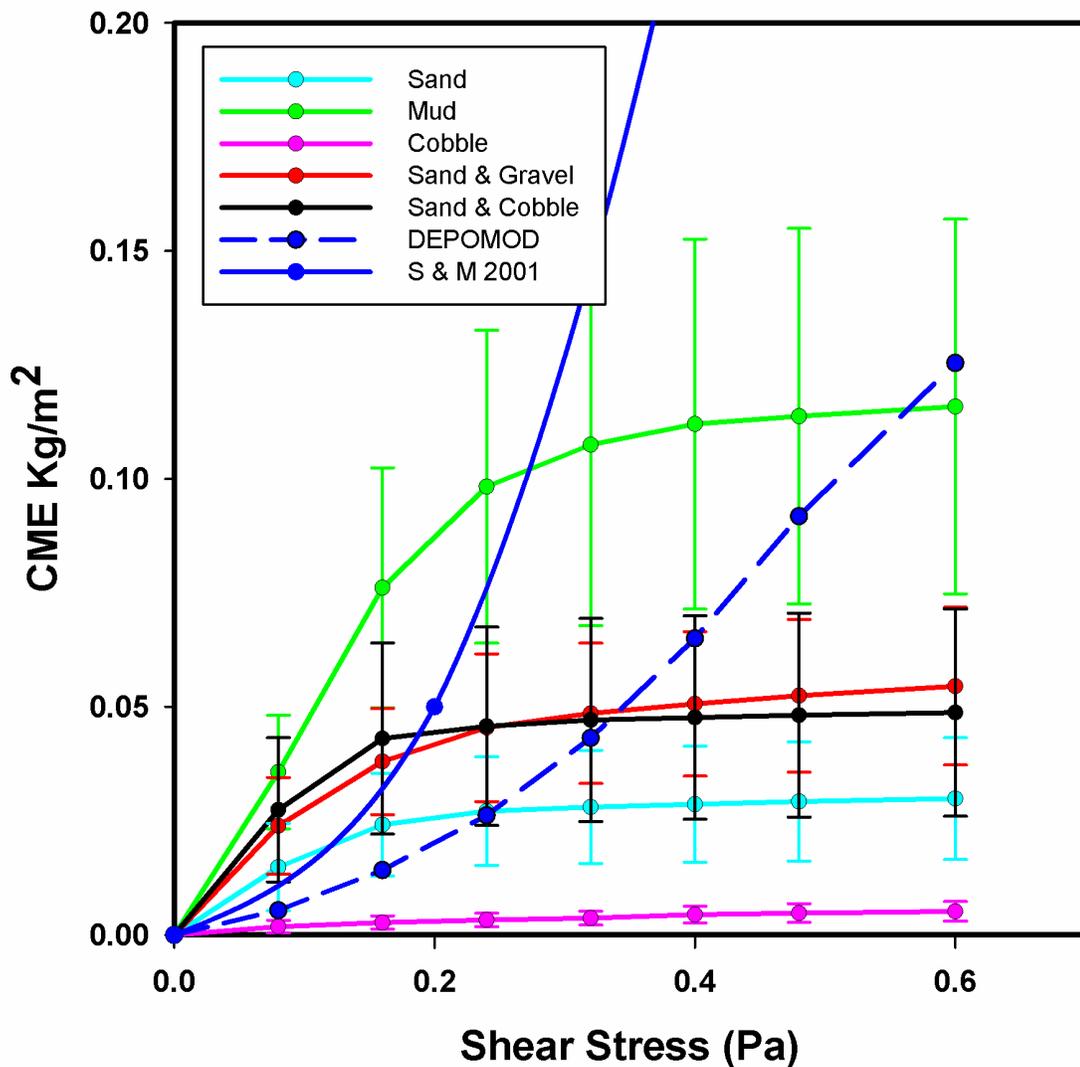
Fig. 6. A plot of cumulative mass eroded in Kg/m² versus shear stress for the N=6 salmon fecal waste material erosion studies. In addition, a DEPOMOD prediction is included based on elapsed time and an erodibility parameter of 7.0 E-7 Kg/m²s. The plot describing data of Maa et al., 1998 which is described in detail in Sanford and Maa (2001) is also included for comparison.

entire mass was eroded from a consolidated, flat, muddy seabed, whereas all coarser substrates acted to limit erosion.

Soulsby (1983) investigated bed roughness length and its effect on drag coefficient. A muddy seabed had an estimated bed roughness length of 2.0 E-4 m and a corresponding drag coefficient at 1 m off the bottom, $C_{100,}$ of 2.2 E-3, while a gravel seabed had a bottom roughness length of 3.0 E-3 m and a drag coefficient, C_{100} of 4.7 E-3. The bottom roughness length was about an order of magnitude greater between the muddy and gravel bed, yet it did not yield an order of magnitude difference in drag coefficient, which may help explain some of the order of magnitude difference in erodibility seen in our study between the muddy and cobble (larger gravel) seabed. One possible reason for the difference could be due to the fact that the median diameter, d50, of the mud used in our study was 10 μm and a smaller diameter than the study of Soulsby (1983), which would reduce the drag coefficient and may help explain some of the order of magnitude difference in erosion. A second possible explanation is that the cohesive nature of fecal material is variable and acts to limit erosion. Droppo et al. (2007) showed that aquaculture material can act to stabilize the seabed and increase erosion resistance. This seems less likely in this study as the fecal material added to cores was always from the same source and only sat on the tops of cores for two hours prior to erosion studies, which likely provides insufficient time to stabilize the seabed. A third and more plausible explanation as to why a mud bed erodes more material (i.e. a higher erosion rate) seems to be due to the fact that fecal material becomes trapped between cobbles and is sheltered from erosion behind larger

sand and gravel grains. In the sand cobble and sand gravel mixtures much of the interstitial space between larger grains is occupied by sand, but research has shown that particulate matter can be incorporated into sand beds as a result of bedform induced interfacial flows (Heuttel et al; 1996). The presence of gravel and cobble in these mixed substrates could also lead to the generation of turbulence that would enhance bottom stress leading to greater erosion than from the sand bed alone.

4.3 Erodibility Parameter (M)

In sediment transport models, in the absence of site-specific erosion measurements, the erodibility parameter, M, governs the removal rate of material from the seabed when a bed stress greater than a critical stress is applied. In this study, M, represents an average erodibility parameter from 0.01 Pa to 0.32 Pa, the range over which aquaculture waste fecal material was removed from the seabed. The values of M ranged over an order of magnitude from approximately 1.3 E-6 kg m^{-2} s^{-1} for the mud substrate to 4.5 E-8 kg m^{-2} s^{-1} for the cobble substrate for the erosion of salmon waste material (Table 1). M ranged from 2 to 8 E-6 kg m^{-2} s^{-1} in the study of Sanford and Maa (2001), which is a re-analysis of Maa et al. (1998), to 1.4 E-6 kg m^{-2} s^{-1} in the study of Sanford et al. (1991), to 7.0 E-7 kg m^{-2} s^{-1} in the DEPOMOD study of Cromey et al. (2002b). The erosion studies of Maa et al. (1998) and Sanford et al. (2001) were generally performed on muddy cohesive seabeds while the study of Cromey et al. (2002b) used synthetic tracer beds of similar size and settling velocity to represent aquaculture fecal material. A study by Harris et al. (1993) calculated M to be 3.0 E-5 kg m^{-2} s^{-}

[1] in an area with high critical shear velocity, indicative of a sandy environment. Broadly, M varies over several orders of magnitude in a wide range of environments.

The values of M from Sanford et al. (2001) would overestimate the erosion of waste material from this study (Fig. 6). At shear stresses greater than 0.32 Pa, the cores in this study were depleted of waste material, or waste material was unavailable for erosion (i.e. trapped in the stress refuges or bed armoured), whereas in the Sanford et al. (2001) study, the seabed continued to be a source of resuspended mass as the bottom stress increased (Fig. 6). The value of M used in the Cromey et al. (2002b) study modeled the erodibility of waste in our study from that of a cobble seabed up to 0.24 Pa, and then diverged with good estimation of erodibility for the seabed composed of sand in our study from 0.40 Pa to 0.60 Pa, the highest seabed stresses used in this study (Fig. 6). Using a single value of M in DEPOMOD, although simplistic for modelling, becomes problematic, because as long as the bottom stress exceeds a single value of critical stress the model continues to erode waste material at a constant rate (i.e. M) with time, and no depletion of the bed or waste material occurs.

4.4 Modelling

Recent sediment transport modelling efforts increase τ_c with depth into the substrate to limit the amount of material that can be eroded until a new critical stress is exceeded (Stevens et al., 2007; Sanford et al., 2008). This study using artificially created cores to examine aquaculture fecal material erodibility showed similar erodibility characteristics, where an increase in tau critical was required to

continue to resuspend and remove waste fecal material from the bed (Fig. 3 & 6).

After 0.32 Pa all the deposited material had either been eroded from the bed or

was prevented from being eroded by becoming trapped in crevices, buried or

armoured by heavier grains or waste (Fig. 6). The fecal waste material was

given only a limited time to settle (i.e. 2 hours) and was in quiescent conditions

with no stress applied during the settling process. It is assumed therefore that

the removal of waste material from the substrates used in this study was a result

of armouring by heavier sediment grains or waste and not due to consolidation /

dewatering effects. The slowest settling material would have been the first

removed from the erosion experiments followed by faster settling material,

predominantly larger fecal material assuming a similar density.

Sanford and Maa (2001) proposed a linear formula for erosion with

changing tau critical with depth (z), which takes the form of the equation:

$$Me = M\left(\tau b - \tau c(z)\right)$$
(2)

Using this linear formula, the erosion results of this study could be modelled but

only up to 0.32 Pa of bottom stress if the correct erodibility parameter M and tau

critical with depth were used. Equation 1 above, as presently used in the

resuspension module of DEPOMOD, would not predict accurately the erosion of

waste material from the seabed in our study even if a correct value of M was

used. The use of a constant erosion rate while τ_c is exceeded results in an

overestimate or underestimate of erosion depending on the flow velocity over the

seabed. It is cautioned that this study only represented a small number of

erosion experiments with waste material (i.e. N = 6) and was not completed in-situ where hydrodynamics would play a major role in shaping bottom sediment texture and control the initial deposition of waste products. However, results from this experiment closely resemble those of Milligan and Law (2013) which were for cores collected next to salmon aquaculture cages. This study does also not take into consideration the consolidation time required for waste fecal material to be incorporated into the seabed and how the interaction of waste with the seabed plays a role in the resuspension dynamics. Law et al. (2014) showed that small particles that were highly organic and possibly indicative of waste material could be incorporated in flocs once they were deposited on the seabed or incorporated into floc structures if components of waste material were broken down into very small constituents. If incorporation into floc derived material occurred, then this waste material would be easily transported even at the lowest stress used in this study.

Figure 7 represents the best fit to the average cumulative mass eroded curves based on the data collected in this study. A simple exponential rise to maximum equation following:

$$y = a\,(1 - b^x) \tag{3}$$

explains the majority of the erosion data (i.e. R^2 = 0.99, p< 0.0001). The parameters a and b represent the maximum CME eroded for each bottom type and the rate of removing material from each bottom type respectively (Table 4). The larger "b" value indicates that it approaches the value "a": faster. Muds approach "a" quickly because the waste is eroded completely and has no spot to
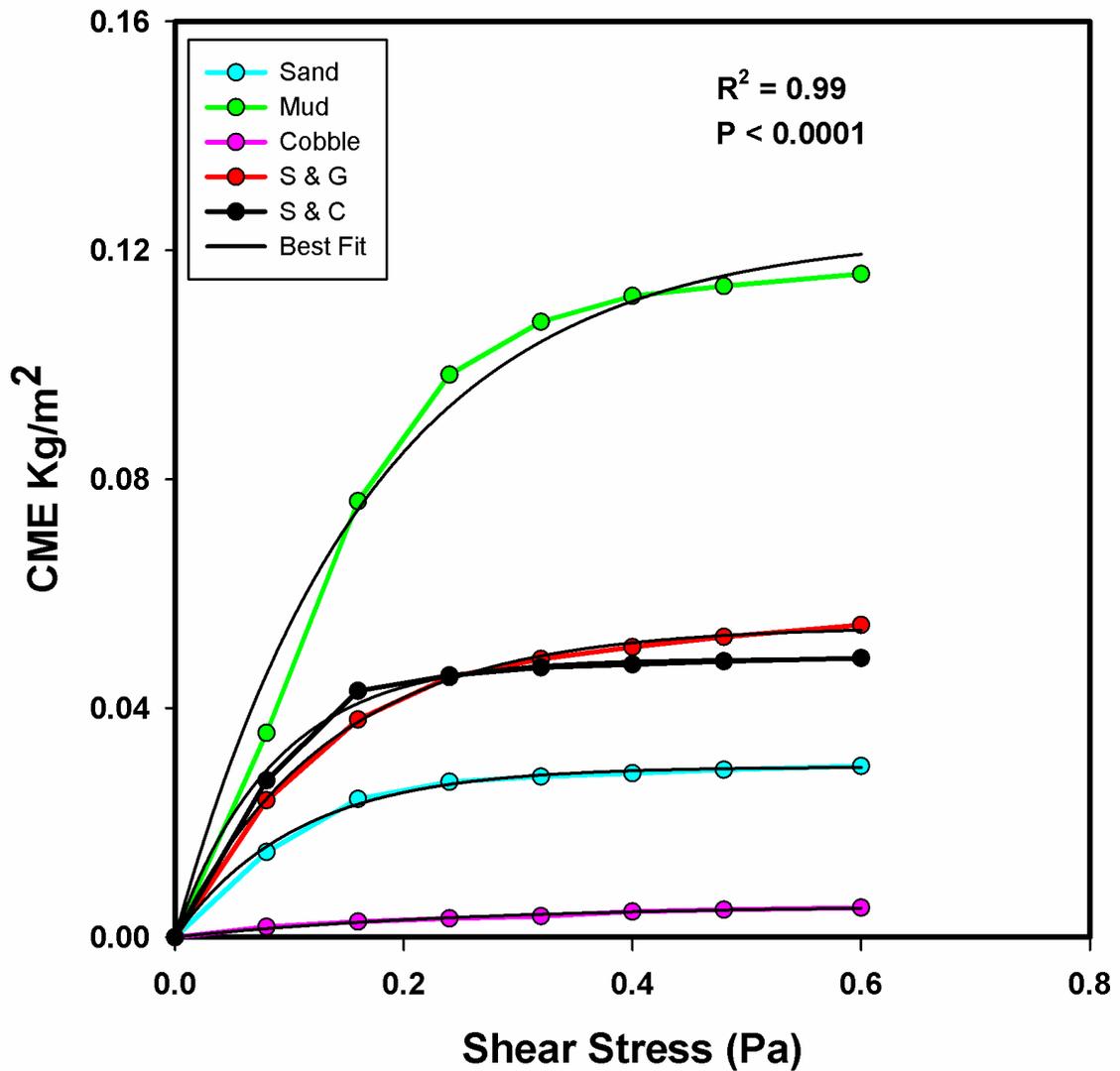
Fig. 7. The best fit plot of cumulative mass eroded in Kg m^{-2} versus shear stress for the N=6 salmon fecal waste material erosion studies. The fits are based on the simple exponential rise to maximum equation, $y = a(1-b^x)$.

Table 4. Parameters for modelled fits of CME vs Shear Stress.

Bottom Type	a	b	R^2	p
Mud	0.123	0.00290	0.99	< 0.0001
Sand & Gravel	0.054	0.00060	0.99	< 0.0001
Sand & Cobble	0.049	0.000013	0.99	< 0.0001
Sand	0.03	0.000076	0.99	< 0.0001
Cobble	0.006	0.02100	0.99	< 0.0001

hide or way to become armoured by the bed. Cobble approaches "a" quickly because most of the material available for resuspension gets driven into the bed (i.e. crevices) at low stress and only the easily eroded flocculated material gets eroded. Sands act between that of mud and cobble with active bed exchange driving some of the waste into the bed with about half of the material being resuspended and removed. It is possible equation 3 above could be used in aquaculture waste transport models to simulate the erosion of waste from differing seabed types by using the appropriate values for a and b under conditions where supply from the bed is limited.

In addition to waste fecal material it is necessary for waste feed pellets to be treated separately in aquaculture waste transport models. Presently, the resuspension component of DEPOMOD treats waste fecal material and feed pellets as a single entity with one erosion parameter (Cromey et al., 2002b). Chamberlain and Stucchi (2007) hypothesized that the seabed geochemistry as a result of organic loading at their study sites was affected by feed pellet deposition even though their model output suggested that all waste material would be transported out of their model domain when the resuspension component of DEPOMOD was turned on. Evidence from this study as well as the study of Sutherland et al. (2006) suggest that much higher shear stress values are required to transport feed pellets than the single number of 0.0179 Pa "hard coded" in the DEPOMOD model. In addition, thought should be given to the exposure of feed pellets to the marine environment. Stewart and Grant (2002) showed in laboratory studies that most feed pellets break down and

disintegrate in much smaller constituents within approximately 30 days of being in the water.

At present the deposition of aquaculture waste material in DEPOMOD is governed by a settling velocity for fecal material of 3.4 mm s^{-1} and for feed pellets of 100 mm s^{-1}. The resuspension of these materials is treated with one erosion parameter and 1 single value for τ_c. If DEPOMOD or a newer updated version is to be used as the community aquaculture waste transport model, then provisions should be made to include multiple groups of material each with their own settling velocities and critical stresses for erosion. The groups could also include their own transport parameters such as (M) and would need to be related to the amount of waste input to aquaculture sites. Future erosion work using experiments both in lab and in-situ at aquaculture sites will help further refine waste transport parameters.

4.5 Implications

Recent work on size sorting during the erosion of cores from the Gulf of Lions, France (Law et al., 2008) and in Seal Harbour, NS (Milligan and Law, 2013) suggests that increases in clay (sediment particles < 4 µm in diameter) changes resuspension dynamics. In sediments that contain > 7.5 % clay, a wide range of sizes are eroded at reduced but equal rates. Sediments with a smaller clay fraction exhibit greater erodibility and size-selective sorting over the entire particle size range. Sediment with a small clay fraction can be winnowed of its fine fraction during erosion, but sediments with a larger clay fraction cannot.

When muddy sands are eroded, the smallest sediment sizes are winnowed from the bed, essentially cleaning the sands. In contrast, when muds are eroded, size sorting is reduced substantially. In short, after deposition, sands are "cleaned" by physical disturbance, but muds resist any further sorting. Even if muds are repeatedly resuspended and transported over great distances, they maintain their poorly sorted character and small mean grain size. Further research on bedform induced interfacial flows have shown the ability of the flow to transfer suspended particles from the boundary layer and into surficial sediments which produce structural heterogeneity of the seabed (Huettel et al., 1996; Chen et al., 2010). It was evident in this research that coarse substrates such as cobble, sands, and gravel have the ability to retain aquaculture waste even at higher shear stresses. Implications may then exist in areas of open cage aquaculture over coarse substrate that bed dynamics may change from one of non-cohesive to cohesive. Further research on this topic is warranted.

5. Conclusion

Bottom sediment substrate plays a role in the erodibility of aquaculture waste material. An order of magnitude difference exists in the cumulative mass eroded of waste fecal material and subsequently the erosion parameter, M, between a mud and cobble seabed. A seabed composed of sand erodes between that of cobble and mud. Feed pellets experience large differences in τ_c, the stress required for motion, between the same seabed types. It is therefore critical that waste fecal material and feed pellets be treated as separate entities in aquaculture waste transport models. Future work should focus on the

72

consolidation time of waste material and its incorporation into the seabed and subsequent re-working. Erosion studies should also take place at areas of active aquaculture sites with differing bottom types to validate the results seen in this laboratory study. Refining transport parameters and future model validation will help increase our predictive capacity of waste transport to the far field and help understand possible ecosystem response.

Acknowledgments

Chapter 4

This chapter is a manuscript that has been submitted to Aquaculture Environment Interactions.

Spatial and temporal variation in erodibility of surficial sediment at areas of active salmon aquaculture

Law, B.A.[1, 2,*], Hill, P.S. [2]

[1] FISHERIES AND OCEANS CANADA, BEDFORD INSTITUTE OF OCEANOGRAPHY, DARTMOUTH, NOVA SCOTIA, CANADA, B2Y 4A2

[2] DEPARTMENT OF OCEANOGRAPHY, DALHOUSIE UNIVERSITY, HALIFAX, NOVA SCOTIA, CANADA, B3H 4J1

* Corresponding author
Brent Law
Habitat Sedimentologist
Fisheries and Oceans Canada
Bedford Institute of Oceanography
1 Challenger Drive, Dartmouth, Nova Scotia
Canada, B2Y 4A2
Brent.Law@mar.dfo-mpo.gc.ca
Telephone | Téléphone 902-426-8548
Facsimile | Télécopieur 902-426-6695
Government of Canada | Gouvernement du Canada

Abstract

Cores collected with an intact sediment-water interface were coupled to a Gust erosion chamber to examine the effect of increasing shear stress on bottom sediments in areas of salmon aquaculture. Cores were collected along transects of stations at a cohesive and a non-cohesive seabed site. Organic matter percentage in bottom sediments near aquaculture sites (< 200 m from operations) correlated with the cumulative mass eroded. As the percentage of organics increased the mass eroded decreased over the sampling periods. Two-way ANOVA indicated that a significant increase ($p<0.05$) in organic matter percentage in bottom sediments occurred at both sites over the times of the sampling, which were coincident with the periods from when the aquaculture sites were first stocked with salmon smolt until just before fish were removed for market. Along the sampled transect at the cohesive site, the percentage of organics in bottom sediment increased significantly out to 200 m from the site. At the non-cohesive site, organic fraction in the sediment only increased at locations that were immediately adjacent to the cage site. Organic matter flux in kg m^2 d^{-1} doubled over the time of the study at both sites and values suggest that material would have been available for resuspension and transport from both sites. The ability to parameterize the movement of this material in transport models will increase predictive capacity regarding dispersal of farm wastes, which may help to increase the environmental sustainability of salmon aquaculture in the marine environment.

Keywords: aquaculture, erodibility, waste transport, bottom substrate

1. Introduction

By 2007 over 75% of the world's natural fish stocks were over-exploited (FAO, 2007). To meet the demand of the world for fish and to lessen the pressure on over-exploited fish stocks, aquaculture has experienced rapid growth over the last quarter century. As of 2012, finfish aquaculture supplied about 1/5th of the world's fish with demand expected to increase significantly over the next several decades (FAO, 2012).

Until recently, research related directly to particulate salmon aquaculture waste has dealt primarily with deposition immediately under or adjacent to net pens (Smith et al., 2005; Graydon et al., 2012; Bannister et al., 2016). Modelling and field studies have focused on near-field effects from organic enrichment, while the far field has received less attention. The near field is considered to be the area within a few hundred meters of farming operations, while the far field can extend kilometers away. Models to predict the depositional footprint from salmon and other finfish farms using the settling characteristics of waste solids have become increasingly accurate (Panchang et al., 1997; Cromey et al., 2002 a and b; Chamberlain and Stucchi, 2007). Models that predict the subsequent resuspension and transport of waste material, however, are inaccurate (Droppo et al., 2007; Chamberlain and Stucchi, 2007; Reid et al., 2009). Development of coupled hydrodynamic-sediment transport models that can address the far field will require parameterization of the factors responsible for influencing the erosion of aquaculture waste material. Measurements of the erodibility of waste particles

associated with finfish aquaculture are also lacking, which limits understanding of potential far-field transport and possible environmental impacts.

Particles at the sediment-water interface move when the downstream (i.e. fluid drag) and upward (i.e. fluid lift) forces overcome the forces keeping particles in contact with the seabed (Wiberg and Smith, 1987). The critical erosion shear stress, which is denoted τ_c, is the stress required at the seabed to initiate the motion of particles (Einstein, 1950; Partheniades, 1962; Amos et al., 1992; Tolhurst et al., 1999). In the broadest terms non-cohesive sediments have mean grain sizes > 63μm, and cohesive sediments or "muds" are dominated by fine-grained particles that are < 63μm. Overall, there have been many investigations of the erosion of both non-cohesive (eg. Shields 1936; Soulsby 1997) and cohesive seabeds (e.g. Winterwerp 1989, Amos et al, 1992; 1997). More recently, attention has been given to the erosion of sand-mud mixtures that show complex behaviours influenced strongly by the fraction of mud in the mixture (van Ledden et al., 2004; Stevens et al., 2007; Law et al., 2008; Wiberg et al., 2013).

Generally, the stress exerted by waves and/or currents on the seabed provides the work necessary to erode particles from the seabed, whereas particle size and density, cohesion, porosity, consolidation, and biological activity determine the erosion resistance of the seabed (Amos et al. 1992, 1997; Maa et al., 1998; Sanford and Maa, 2001, Wiberg et al., 2013). Understanding of cohesive sediment resuspension is incomplete because it is governed not only by hydrodynamic forces and the force of gravity, but also by cohesion, which depends on biological and electrochemical variables (Black et al., 2002, Droppo,

2007). Recent work on size sorting during the erosion of cores from the Gulf of Lions, France (Law et al., 2008) and in Seal Harbour, NS (Milligan and Law, 2013) suggests that increases in clay (sediment particles <4 um in diameter) change resuspension dynamics. In sediments that contain > 10% clay, a wide range of sizes are eroded at reduced but equal rates. Sediments with a smaller clay fraction exhibit greater erodibility and size-selective sorting over the entire particle size range. Sediment with a small clay fraction can be winnowed of its fine fraction during erosion, but sediments with a larger clay fraction cannot. When muddy sands are eroded, the smallest sediment sizes are winnowed from the bed, essentially cleaning the sands. In contrast, when muds are eroded, size sorting is reduced substantially. In short, after deposition, sands are "cleaned" by physical disturbance, but muds resist any further sorting. Even if muds are repeatedly resuspended and transported over great distances, they maintain their poorly sorted character and small mean grain size.

The input of fecal material and feed from salmon aquaculture increases the amount of "sticky organic material" and hence cohesion in the water column and in the sediments surrounding aquaculture sites. Milligan and Law (2005) showed decadal changes in floc limit, which is a parameter derived from grain size distributions, from sediments collected in bays with intensive open-cage salmon aquaculture. The increased floc limit in bottom sediments was linked to increased organic loading, which ultimately increased flocculation and the settling of fine-grained material to the seabed (Milligan and Law, 2005). These changes were accompanied by increased sediment accumulation and an increase in

organic matter in the seabed (Smith et al., 2005). Increases in deposited organic matter can also lead to the formation of microbial mats. These mats form when oxygen is depleted in the sediments and overlying water column and can become widespread in sulfide rich waters (Grant and Gust, 1987). The formation of mats on the seabed is associated with a process known as "biostabilization" (Krumbein et al., 1994). This process occurs when organisms such as algae, fungi, microbes, combined with exo-polymeric substances (EPS) "glue down' or stabilize the sediment bed (Droppo, 2007). This process occurs rapidly in the organic-enriched sediments around active aquaculture operations (Droppo et al., 2007). The addition of fine sediment to the seabed by aquaculture operations therefore has the potential to alter the texture of bed sediment and change the erosion dynamics of bottom sediments near pens.

This study used cores collected with an intact sediment-water interface coupled to a Gust erosion chamber to examine the effect of increasing shear stress on bottom sediments collected at areas of salmon aquaculture. Cores were collected and eroded from along a transect of stations at both a cohesive and non-cohesive seabed site. The goal of this study was to document the spatial and temporal change in erodibility (i.e. cumulative mass eroded, CME) of bottom sediments and to understand possible mechanisms responsible for these changes.

2. Methods

2.1 Overview

The CME of cores collected with an intact sediment-water interface was measured at two areas of active salmon aquaculture: 1) in Jordan Bay, southwest Nova Scotia, Canada and 2) in Passamaquoddy Bay, southwest New Brunswick, Canada (Fig. 1). Jordan Bay is located on the Atlantic coast of Nova Scotia and is exposed to wind waves and longer period swell. The Jordan Bay aquaculture site is located in the outer part of the Bay (43 42.0 N, 65 11.7 W) and is close to Blue Island (Fig 1). The average water depth at the site is approximately 17 m, and the average tidal range is 1.5 meters (Fig 3). The aquaculture site occupies an area that is about 500 m in length by about 200 m in width. It is made up of (20) circular pens with in two parallel rows of 10 (Fig. 1). The sediment at the site is non-cohesive. It comprises fine sand with d50 values of approximately 125 μm, and the clay fraction is less than 2%. Passamaquoddy Bay is sheltered from the outer Bay of Fundy by islands around the site, primarily Deer Island. The Navy Islands aquaculture site in Passamaquoddy Bay (45 01.9 N, 67 00.4 W) is located in the southwest corner of the Bay (Fig 1). The average water depth at the site is approximately 23 m and has an average tidal range of 7 meters (Fig. 2). The aquaculture site occupies an area that is about 500 m in length by about 200 m in width. It is made up of (15) circular pens in two parallel rows of eight and seven respectively (Fig. 1). The seabed at the site is primarily mud with median diameters (d50) of approximately 9.5 μm with a small sand fraction, (< 2%). The sediments are cohesive, with an average clay (< 4 μm) fraction of greater than 20%.
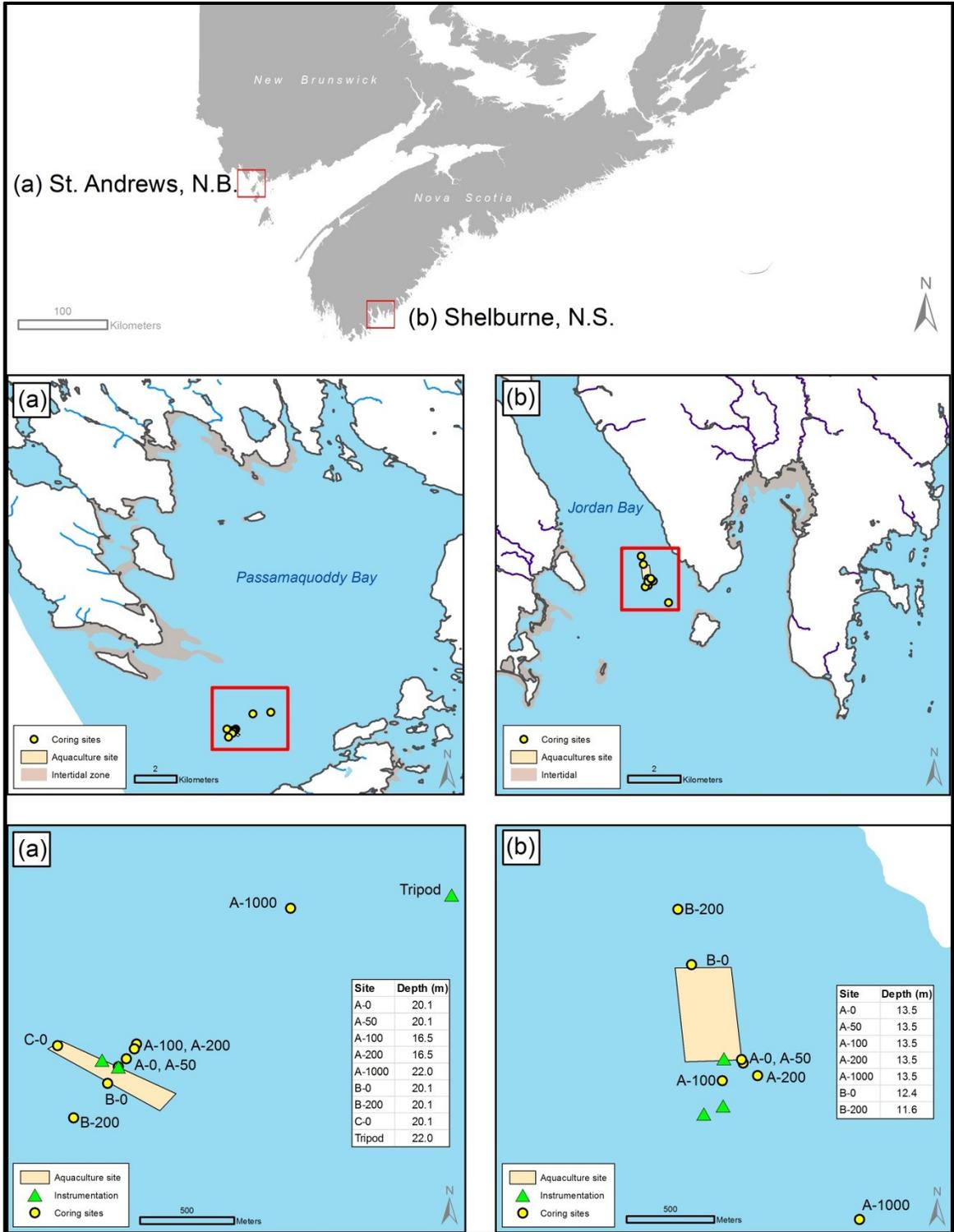
Figure 1. Map of the two study areas.
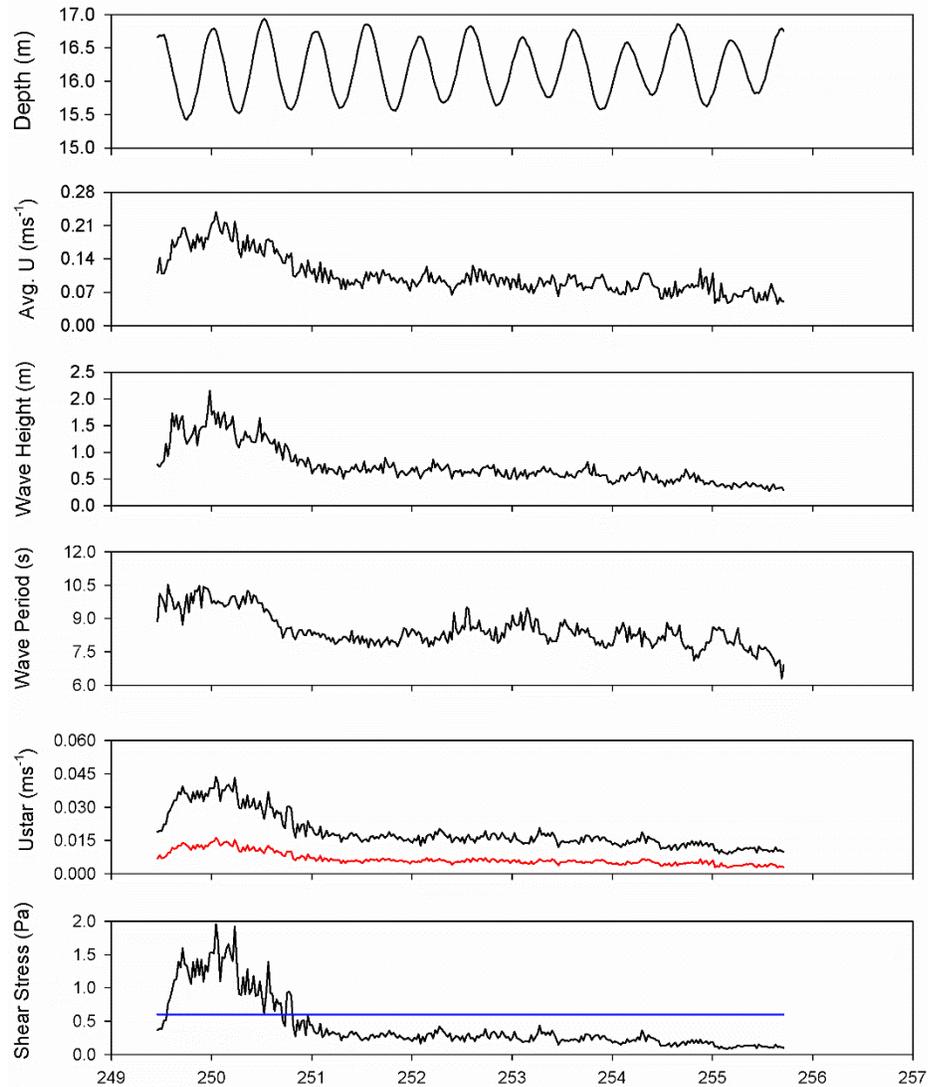
Figure 2. Jordan Bay physical oceanography data from September 2016 from near cage. Top panel is water depth (m) from the CTD; second panel is the average current speed (m s^{-1}); third panel represents significant wave height (m), fourth panel is the wave period (s); fifth panel is calculated combined wave current shear velocity (m s^{-1}) in black and current-only shear velocity (m s^{-1}) in red; bottom panel is the calculated shear stress (Pa) in black and the max shear stress of the Gust Erosion experiments (Pa) in blue.
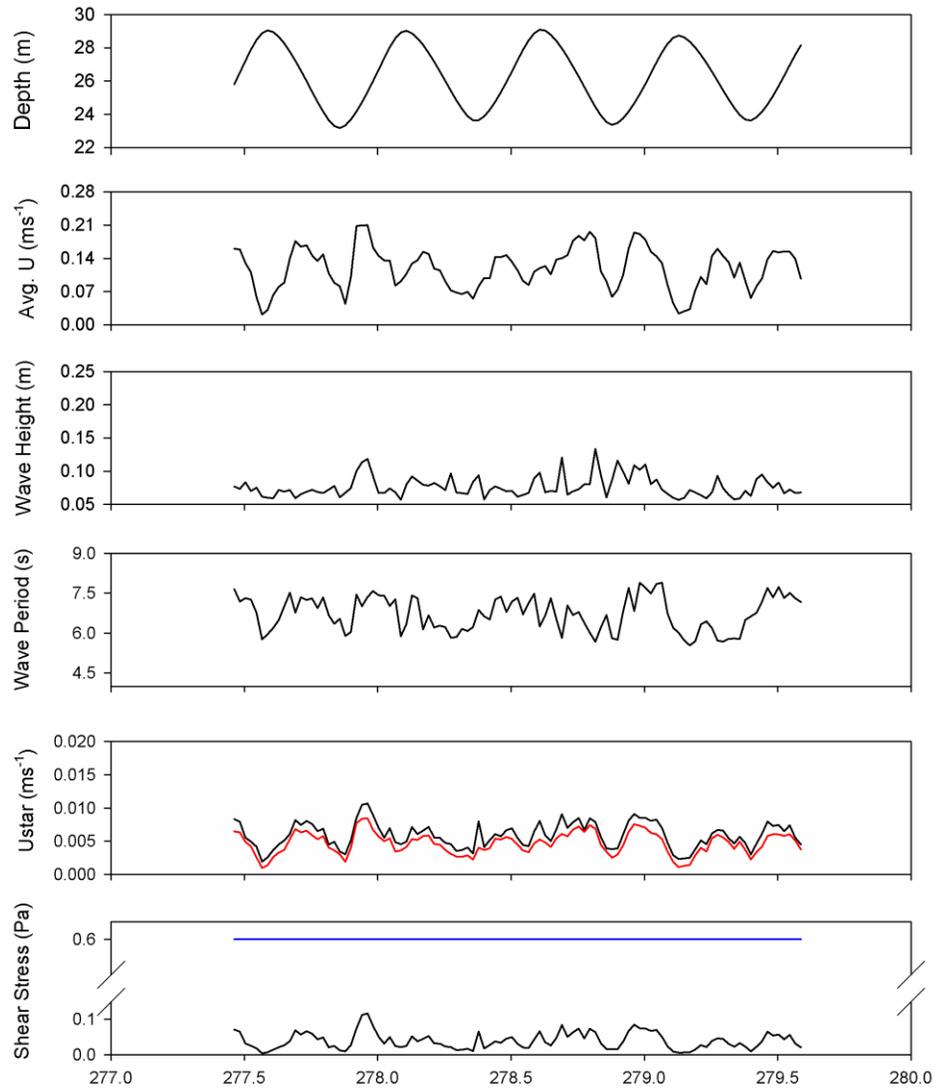
Figure 3. Navy Island physical oceanography data from October 2016 from near cage. Top panel is water depth (m) from the CTD; second panel is the average current speed (m s^{-1}); third panel represents significant wave height (m), fourth panel is the wave period (s); fifth panel is calculated combined wave current shear velocity (m s^{-1}) in black and currents-only shear velocity (m s^{-1}) in red; bottom panel is the calculated shear stress (Pa) in black and the max shear stress of the Gust Erosion experiments (Pa) in blue.

The Navy Island and Jordan Bay aquaculture sites were both stocked with juvenile salmon in April / May 2015. Cores were collected and eroded during approximately one-week field excursions in May 2015, October 2015 and October 2016 at the Navy Islands site and in June 2015, September 2015 and September 2016 at the Jordan Bay site. The cores were collected using a mini-slo corer and coupled to a Gust microcosm erosion chamber. Cores were collected along a series of stations from 0 m (i.e. at the cage site) to 1000 m (i.e. reference site) along a transect based on the mean direction of the currents at both locations. Additional stations were sampled throughout the sampling periods to encompass the opposite side of the site to help provide additional information on sediment characteristics as time for sampling permitted.

2.2 Mini slo-corer

The mini slo-corer is a reconfiguration of the large slo-corer developed by Bothner et al., (1998) for studies of trace metal levels associated with sewage outfalls in Boston Harbour and was used to collect all bottom sediment samples. The mini slo-corer is a hydraulically damped gravity corer that uses 50 kg of lead to push a polycarbonate barrel slowly into the seabed to collect bottom core samples. The key feature of the slo-corer is its ability to collect sediment cores without disturbing the sediment water interface, thereby preserving flocculated mobile material at the surface. Other corers (e.g. box and gravity) and grab samplers (e.g. Eckman and Van-veen) do not preserve an intact sediment water interface due to their impact on the seabed when sampling (Milligan and Law, 2013).

2.3 Gust Chamber

The Gust chamber is an erosion simulator that comprises a housing with a rotating stirring disk, a removable lid, and water input and output connections. It fits directly on top of a slo-core tube. By controlling both the rotation rate of the stirring disk and the rate at which water is pumped through the device, a uniform shear stress can be applied across the sediment surface. Shear stresses applied to cores for this study were 0.01, 0.08, 0.16, 0.24, 0.32, 0.40, 0.48 and 0.60Pa with the first step of 0.01Pa being used to flush tubing and the Gust chamber. Shear stress at each level was maintained until an attached turbidity meter recorded values that corresponded to background concentrations, which usually required 30 min for the 0.01Pa and 20 min for each successive shear stress. This relatively rapid decrease in concentration with time at a given shear stress is indicative of depth-limited erosion, also known as Type I erosion (e.g., Sanford & Maa 2001), such that the critical shear stress of the bed increases with depth. Background water, collected near the seabed from which the core was taken, was pumped into the chamber and withdrawn from an outlet in the lid to maintain the desired shear stress. The water that was pumped through the turbidity meter from the chamber subsequently was collected in a 2L flask and filtered for suspended particulate matter (SPM) and particle size analysis. The turbidity meter and SPM data were used to calculate erosion rate, cumulative mass eroded and the depth-dependent critical erosion shear stress (τ_c) for each core using the Gust Chamber processing software and following the erosion formulations of Sanford and Maa (2001), which allows τ_c to increase with depth,

thus properly representing depth-limited erosion. For a complete description of the Gust chamber, its function and calibration, see Gust and Muller (1997); Tolhurst et al. (2000); and Stevens et al. (2007).

2.4 Cumulative Mass Eroded

The mass eroded per unit area at each shear stress step was calculated by multiplying the SPM for each shear stress step minus the background SPM, which was determined by gravimetric filtration, by the total volume of water collected for each stress step, and then dividing by the area of the eroded surface (0.0092 m^2). The cumulative mass eroded (CME) in kg m^{-2}, was calculated as the sum of the masses eroded for each shear stress step.

2.5 Sediment Analysis

Organic matter percentages from bottom sediments collected from the top 0.5 cm to 1.0 cm from slo-cores were determined using loss on ignition by combusting the sediment at 450 ^{0}C for 6 hours to determine organic matter masses (Kristensen 1990). The before-minus-after combusted weight of the sediment divided by the total dry weight multiplied by 100 represents the total organic matter percentage of the sample.

Organic matter flux values were determined based on a programmable sediment trap that collected up to 12 samples at the cage edge near the 0 m transect station, each over 6-hour periods, during the study. The samples were used to calculate an average flux in g m^2 d^{-1} for the entire sampling period.

The Disaggregated Inorganic Grain Size (DIGS) of the bottom sediments was determined for both the cohesive and non-cohesive sediments. Organic

matter was removed by adding 35% hydrogen peroxide (H_2O_2) to the sample. Samples then were disaggregated with a sapphire-tipped ultrasonic probe prior to analysis. Grain-size analysis of cohesive samples from the Navy Island site were run on a Coulter Counter Multisizer 3 electro-resistance particle size analyzer (Milligan and Kranck, 1991; Law et al., 2008), and non-cohesive samples collected at the Jordan Bay site were analyzed using a Beckman Coulter LS 13320 laser diffraction particle size analyzer.

Bed solids volume fraction, $\varnothing_{stot,}$ was determined by dividing the volume of solids in the bed sediment by the total volume. A known volume of sediment was subsampled in a syringe and then dried to determine water content. The solids volume fraction of the mud matrix, $\varnothing_{sm,}$ in the bed sediment was determined based on the < 63 μm fraction from the grain size analysis of bottom sediments using the Coulter Counter and Coulter Laser. For more information on $\varnothing_{stot,}$ $\varnothing_{sm}$, see Sanford (2008) and Dickhudt et al. (2010).

2.6 Physical Oceanography data

An upward-looking Acoustic Doppler Current Profiler, ADCP (2 MHz, Nortek Aquadopp) was deployed on a bottom-mounted frame at each aquaculture site, 100 m from the 0m coring location. The ADCP was positioned 0.15 m above the seabed. Data were collected in burst mode at 8 Hz and 4800 samples. This frequency of sampling allowed data collection for 10 minutes every 30 minutes and enabled the measurement of both current velocities and orbital velocities due to waves. Shear velocities from currents were estimated using the Law of the Wall equation and a wave-current-interaction model

developed by Grant and Madsen was used to determine the combined wave-current shear stress at the seabed (Grant and Madsen 1986; Madsen 1994). Significant wave heights were collected using an RBR duet-Temperature and Depth, wave gauge sampling at 16Hz with 2048 samples per burst every 5 minutes. An RBR CTD XR-620 was configured to make measurements of salinity, temperature and pressure every 5 minutes by averaging data collected at 6 Hz for 30 seconds.

2.7 Statistics

Statistical analyses were performed in SigmaStat of the SigmaPlot graphics software, which is a part of the Systat software package. Spearman correlations were used to test for correlation between sediment variables after the data were tested for normality using a Shapiro-Wilk test. Two-Way ANOVA was carried out using station distance and time of sampling as the variables and using data for CME and organic matter percent for both the Jordan Bay and Navy Island locations. Comparisons both between and within variables based on significance of interactions was carried out using a Holm-Sidak test. In addition, significance of interaction was explored using Student-Newman-Keuls and Bonferroni and revealed similar results and therefore only Holm-Sidak results are presented.

3.0 Results

3.1 Physical Oceanography

Seabed shear stresses at Jordan Bay were dominated by wave activity (Fig 2). In September 2016 seabed shear stress averaged 0.42 Pa. Stress

remained above 0.08 Pa for the length of the study, and it was greater than 0.24

Pa for over 50% of the deployment period (Fig 2). Seabed shear stresses at

Navy Island were dominated by the tide (Fig 3). During the October 2016 field

campaign, bottom shear stress averaged 0.039 Pa and remained under 0.08 Pa

for > 93 % of the deployment period. Seabed shear stress at both study

locations had similar values for the other study time periods compared with the

last 2016 sampling. Significant wave heights at Navy Island are very small

compared to Jordan Bay, ranging from 0.03 m to 0.13 m with an average of 0.07

m (Fig. 3), whereas, significant wave heights in Jordan Bay were sometimes in

excess of 2 meters (Fig 2). As a result of such small wave heights, orbital

velocities from waves were often negligible at the Navy Island site. Current

velocities at both Jordan Bay and Navy Island were similar with maximum current

velocities of approximately 0.20 m s^{-1} (Fig 2 and 3). Salinity was more variable at

the Navy Island site compared to Jordan Bay over the three study periods and

ranged from a low of 30.7 PSU in May 2015 to a max of 32.7 PSU in October

2016 with an average of 31.8 PSU (Fig 3), whereas Jordan Bay had salinity of

31.3 PSU and varied by less than 0.5 PSU over the three study time periods (Fig

2).

3.2 Cumulative Mass Eroded

Critical surface erosion shear stress, defined herein as the stress at which

material was initially resuspended from the surface, was determined to be 0.01 to

0.02 Pa. In both Jordan Bay, which is an area with a non-cohesive sediment

seabed, and Navy Island, which is an area with a cohesive seabed, the initial

erosion of material occurred at low shear stress. Visual observation of material eroded from the different bottom substrates suggests that flocculated particles dominated at lower shear stresses (i.e. 0.01 Pa and 0.08 Pa). The primary difference in erodibility of bottom substrate, between the sites was that at the non-cohesive site, little erosion occurred over all but the last two steps (i.e. 0.48 Pa and 0.60 Pa), whereas at the cohesive site, a similar amount of material eroded over each consecutive stress step.

The CME at Jordan Bay from the 0-m stations on either side of the cage were always about an order of magnitude less during the June 2015 and Sept 2015 sampling and were 5 times lower at the 0-m stations as compared to the 1000-m station in the September 2016 sampling (Fig 4, Table 1). At the initial site visit to Navy Island in May 2015 all stations had similar CME with the 50-m station eroding approximately 2 times that of the 0-m and 1000-m station (Fig 5, Table 2) In subsequent sampling periods in October 2015 and again in October 2016 there was greater than an order of magnitude difference in cumulative mass eroded between the 0-m station and 1000-m station, with the 0-m station eroding significantly less mass (Fig 5, Table 2).

3.3 Sediment Characteristics

At Jordan Bay*,* although the range of the mass fraction of sand (i.e. fs sand) shifted slightly, the mass fraction of sand in bottom sediments averaged 0.91 for each of the three sampling periods (Table 3). In addition, while the mud fraction in some bottom sediment samples increased over the three study periods from June 2015 to September 2016, the minimum amount remained

constant over the three samplings, resulting in very little change to the average mud fraction (Table 3). The parameters ϕstot and ϕsm are representative of the bed solids volume fraction and of the solids volume fraction of the mud matrix respectively and are parameters used in the modelling of bed erosion and deposition processes. Indicative of a sandy environment ϕstot averaged 0.78 in June 2015 and 0.71 in September 2016 while the average value of ϕsm was 0.24 in June 2015 and 0.19 in September 2016 (Table 3).

At Navy Island the mass fraction of sand was always between 0.00 and 0.04 for minimum and maximum respectively and averaged 0.01, 0.01, and 0.02 during the May 2015, October 2015, and October 2016 study periods (Table 4). The mud fraction (i.e. < 63 μm) ranged from 96 % to 100% in the bottom sediment samples and averaged approximately 99 % over the three study periods (Table 4). Indicative of a muddy environment ϕstot averaged 0.37 in May 2015, 0.40 in October 2015, and 0.35 in October 2016 while the average value of ϕsm was 0.37 in May 2015, 0.39 in October 2015 and 0.34 in October 2016 (Table 4).

Jordan Bay, N.S.
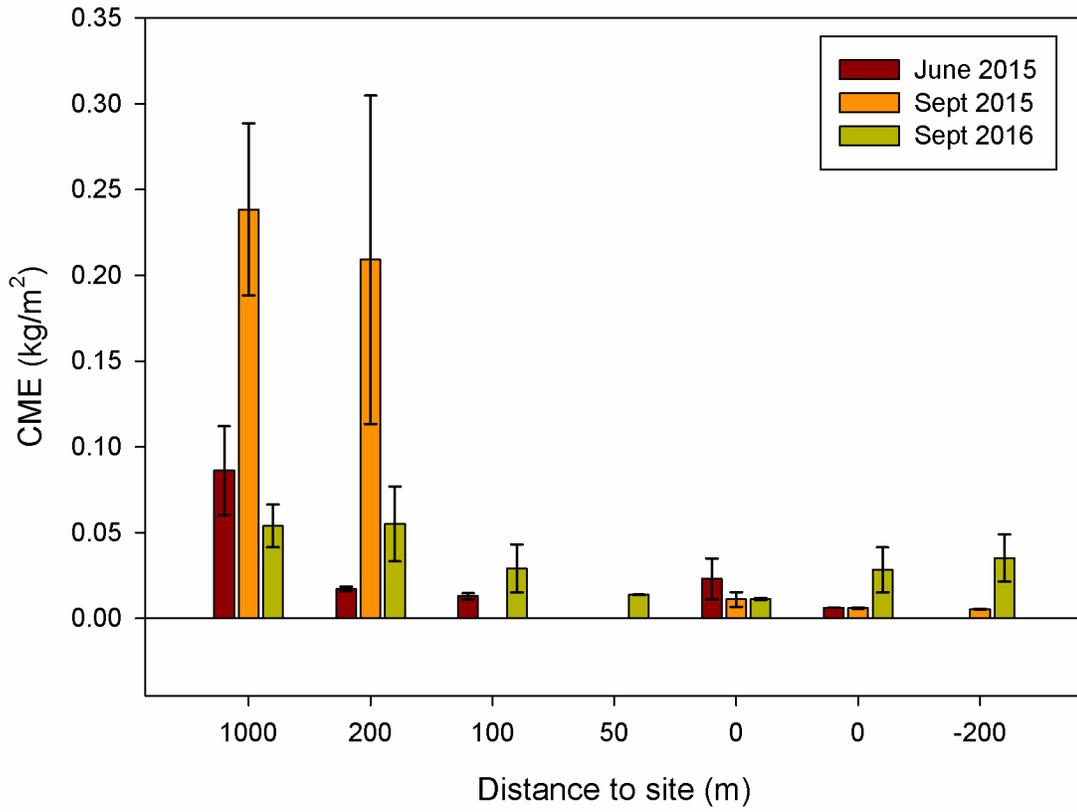
Figure 4. Jordan Bay cumulative mass eroded (kg m^{-2}) from all samplings.

Table 1. Average cumulative mass eroded (CME) values for Jordan Bay.

Distance (m)	AVG CME (kg/m2)	STD Dev (Kg/m^2)	Jordan Bay Date
0	0.0230	0.0119	Jun-15
100	0.0130	0.0017	Jun-15
200	0.0172	0.0014	Jun-15
1000	0.0862	0.0259	Jun-15
0 (opp)	0.0063	0.0001	Jun-15
0	0.0111	0.0043	Sep-15
200	0.2091	0.0957	Sep-15
1000	0.2384	0.0501	Sep-15
0 (opp)	0.0061	0.0004	Sep-15
200 (opp)	0.0054	0.0002	Sep-15
0 m	0.0113	0.0007	Sep-16
50 m	0.0138	0.0002	Sep-16
100 m	0.0292	0.0140	Sep-16
200 m	0.0551	0.0218	Sep-16
1000 m	0.0540	0.0125	Sep-16
0 (opp)	0.0283	0.0132	Sep-16
200 (opp)	0.0352	0.0137	Sep-16
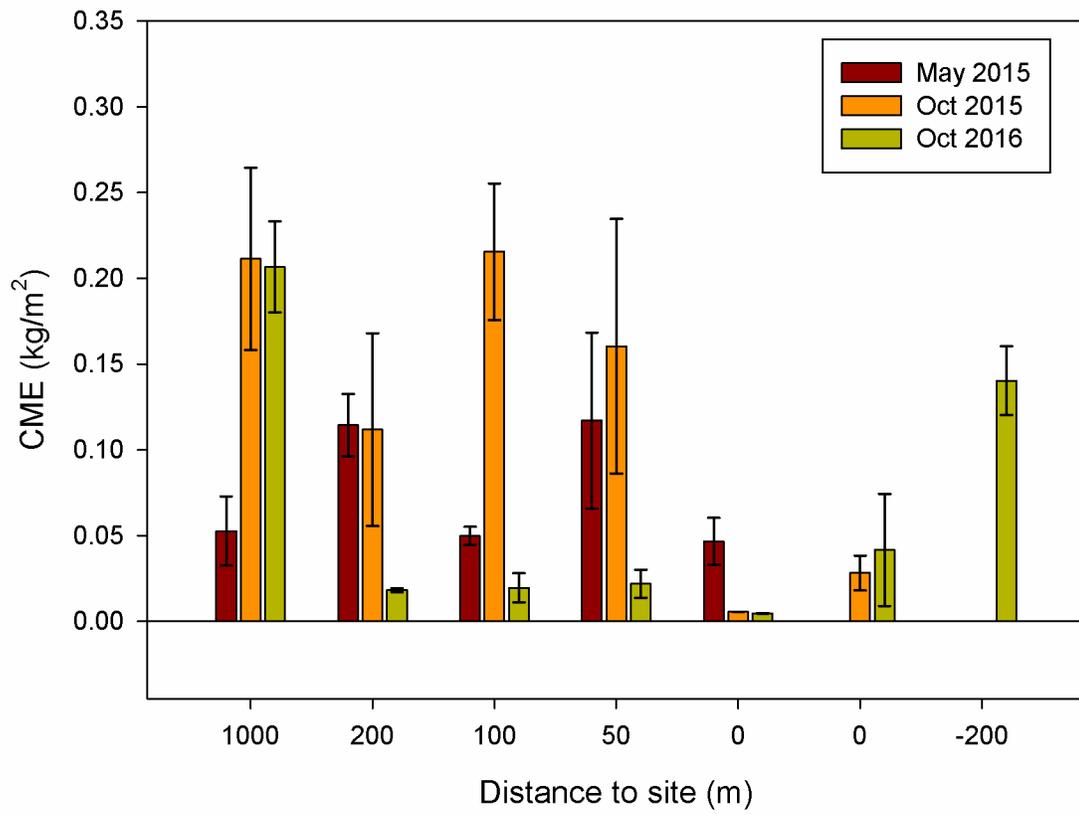
Figure 5. Navy Island cumulative mass eroded (kg m^{-2}) from all samplings.

Table 2. Average cumulative mass eroded (CME) values for Navy Island.

Distance (m)	AVG CME (kg/m2)	STD Dev (Kg/m^2)	Navy Island Date
0	0.0467	0.0137	May-15
50	0.1171	0.0512	May-15
100	0.0499	0.0053	May-15
200	0.1144	0.0181	May-15
1000	0.0527	0.0202	May-15
0 m	0.0056	0.0001	Oct-15
50 m	0.1605	0.0742	Oct-15
100 m	0.2155	0.0398	Oct-15
200 m	0.1118	0.0562	Oct-15
1000 m	0.2114	0.0531	Oct-15
0 (opp)	0.0283	0.0101	Oct-15
0	0.0047	0.0002	Oct-16
50	0.022	0.0082	Oct-16
100	0.0196	0.0085	Oct-16
200	0.0182	0.0011	Oct-16
1000	0.2067	0.0265	Oct-16
0 (opp)	0.0417	0.0327	Oct-16
200 (opp)	0.1404	0.0200	Oct-16

Table 3. Jordan Bay sediment characteristics

Jun-15	Max	Min	Avg
WC (%)	26.2	19.7	21.8
ϕ stot	0.8	0.74	0.78
fs sand	0.94	0.87	0.91
ϕ sm	0.30	0.19	0.24
< 63 µm (%)	12.9	6.4	8.91
< 4 µm (%)	1.33	1.01	1.16
Organic (%)	0.86	0.47	0.57
Sep-15			
WC (%)	N/A	N/A	N/A
ϕ stot	N/A	N/A	N/A
fs sand	0.94	0.87	0.91
ϕ sm	N/A	N/A	N/A
< 63 µm (%)	13.2	6.40	8.80
< 4 µm (%)	2.02	1.00	1.25
Organic (%)	1.19	0.48	0.63
Sep-16			
WC (%)	31.3	21.3	28.6
ϕ stot	0.77	0.69	0.71
fs sand	0.94	0.85	0.91
ϕ sm	0.31	0.13	0.19
< 63 µm (%)	15.9	6.40	9.20
< 4 µm (%)	1.71	0.93	1.13
Organic (%)	1.79	0.50	0.63

3.3 2-Way Anova (Holm-Siddak) and Spearman Correlations

Two-way ANOVA was performed to examine the interactions of sampling distance from the center of the aquaculture cage sites and sample date on CME. At Jordan Bay there was a significant effect of station distance, $F_{(3, 12)} = 23.16$, $p<0.001$ and sample date, $F_{(2, 23)} = 14.63$, $p<0.001$ on CME (Table 5). Post hoc analysis of comparisons of factor showed significant differences in CME among stations largely driven by station distance within the September 2015 sampling. At Navy Island there also was a significant effect of station distance, $F_{(4, 15)} = 3.979$, $p<0.021$ and sample date, $F_{(2, 15)} = 5.55$, $p<0.016$, on CME (Table 6). Post hoc analysis of comparisons of factor showed only significant differences in CME among the stations at 0-m and at 1000-m.

Spearman correlations, the measure of strength of linear associations between variables, were run for each of the sediment characteristics from the bottom sediments collected at Jordan Bay and Navy Island (Table 7; Table 8). Table 4. Navy Island sediment characteristics.

The sediment data were combined over all three sampling periods. Values of CME were negatively correlated with the % organics found in the muddy bottom sediments at Navy Island (i.e. R = -0.695, $p<0.001$) (Table 8). The negative correlation coefficient means that as the percentage of organics in bottom sediments increased, the amount of mass eroded in the erosion experiments decreased. Organic matter flux in g m^2 d^{-1} approximately doubled at both locations over the study periods (Fig 6).

Table 4. Navy Island sediment characteristics.

May-15	Max	Min	Avg
WC (%)	67.6	56.9	63.1
ϕ stot	0.43	0.35	0.37
fs sand	0.02	0.000	0.01
ϕ sm	0.43	0.32	0.37
< 63 μm (%)	100	98.3	99.3
< 4 μm (%)	26.1	22.9	24.4
Organic (%)	5.80	5.36	5.55
Oct-15			
WC (%)	69.1	53.1	61.6
ϕ stot	0.47	0.33	0.40
fs sand	0.02	0.00	0.01
ϕ sm	0.47	0.33	0.39
< 63 μm (%)	100	97.7	98.7
< 4 μm (%)	25.8	20.3	22.3
Organic (%)	7.50	5.60	6.30
Oct-16			
WC (%)	69.8	61.7	65.9
ϕ stot	0.38	0.30	0.35
fs sand	0.04	0.00	0.02
ϕ sm	0.38	0.30	0.34
< 63 μm (%)	100	96.3	98.5
< 4 μm (%)	26.1	20.8	23.0
Organic (%)	8.60	5.74	6.88

Table 5. Source Table JB ANOVA for CME.

Source	DF	SS	MS	F	P
Station Distance	3	0.0672	0.0224	23.016	<0.001
Sample Date	2	0.0285	0.0142	14.63	<0.001
Distance x Date	6	0.052	0.00867	8.902	<0.001
Residual	12	0.0117	0.000974		
Total	23	0.159	0.00693		

Table 6. Source Table NI ANOVA for CME.

Source	DF	SS	MS	F	P
Station Distance	4	0.0583	0.0146	3.979	0.021
Sample Date	2	0.0406	0.0203	5.55	0.016
Distance x Date	8	0.0708	0.00885	2.418	0.067
Residual	15	0.0549	0.00366		
Total	29	0.225	0.00775		

Table 7. Jordan Bay Spearman Correlations. P-values are shown below the correlation coefficients and are represented significance by; <0.05 gets *, < 0.01 gets **, and < 0.001 gets ***. The pairs of variables with positive correlation coefficients and P values tend to increase together and. for the pairs with negative correlation coefficients and P values, one variable tends to decrease while the other increases.

Jordan Bay	Φstot	>63 um fraction	fs mass sand fraction	Φsm	< 4 um fraction (%)	Organic Content (%)	CME (kg/m2)
Water Content (%)	-1.000	-0.155	-0.155	-0.778	-0.170	0.380	0.330
	***			***		**	
Φstot		0.155	0.155	0.778	0.170	-0.380	-0.330
				***		**	
<63 um fraction			-1.000	0.357	0.648	0.141	0.292
			***	*	***		
fs mass sand fraction				-0.357	-0.648	-0.141	-0.292
				*	***		
Φsm					0.551	-0.284	-0.096
					***	*	
< 4 um fraction (%)						0.361	-0.147
						*	
Organic Content (%)							-0.064

Table 8. Navy Island Spearman Correlations. P-values are shown below the correlation coefficients and are represented significance by; <0.05 gets *, < 0.01 gets **, and < 0.001 gets ***. The pairs of variables with positive correlation coefficients and P values tend to increase together and. for the pairs with negative correlation coefficients and P values, one variable tends to decrease while the other increases.

| Navy Island	Φstot	>63 um fraction	fs mass sand fraction	Φsm	< 4 um fraction (%)	Organic Content (%)	CME (kg/m2)
Water Content (%)	-1.000	-0.030	-0.030	-0.990	0.616	0.263	-0.259
	***			***	***		
Φstot		0.030	0.030	0.990	-0.616	-0.263	0.259
				***	***		
<63 um fraction			-1.000	0.052	0.104	-0.244	-0.115
			***				
fs mass sand fraction				-0.051	-0.103	0.238	0.125
Φsm					-0.607	-0.280	0.265
					***	*	
< 4 um fraction (%)						-0.013	-0.070
Organic Content (%)							-0.695
							***
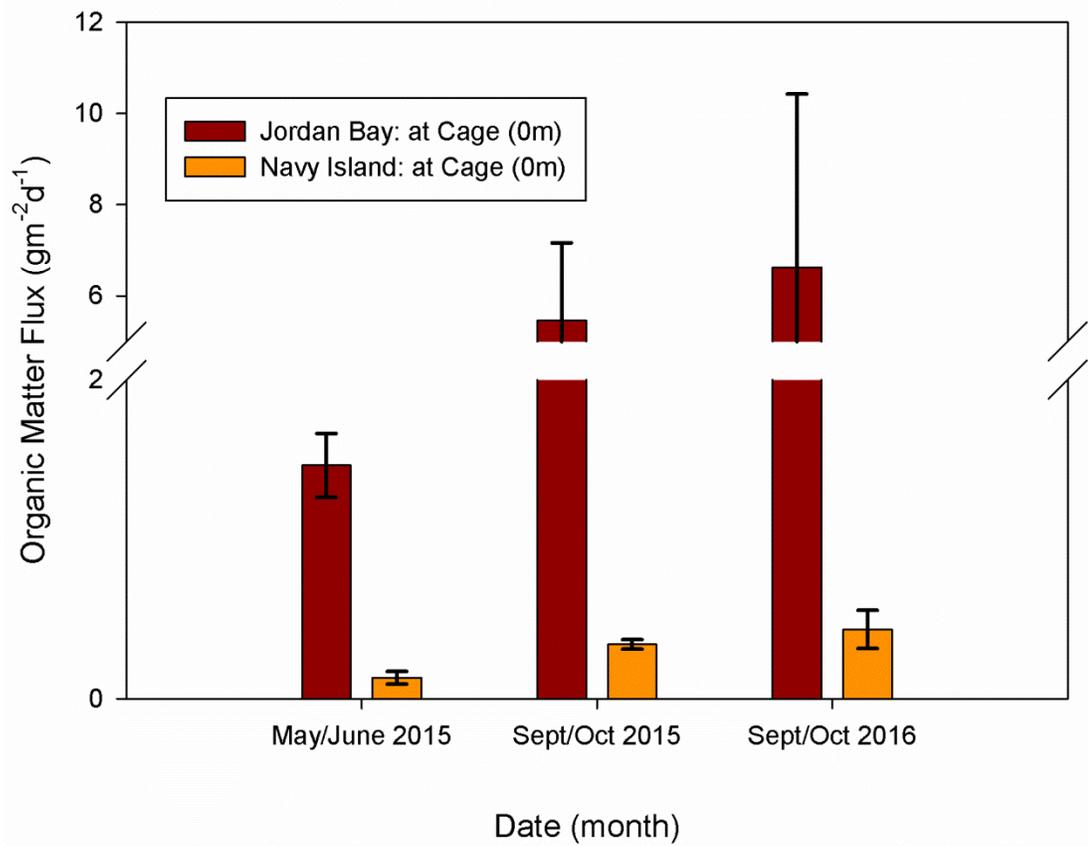
Figure 6. Jordan Bay and Navy Island organic matter flux from all samplings

Table 9. Source Table JB ANOVA for Organic concentration.

Source	DF	SS	MS	F	P
Station Distance	5	2.27	0.454	15.97	<0.001
Sample Date	2	0.715	0.358	12.582	<0.001
Distance x Date	10	0.368	0.0368	1.296	0.27
Residual	36	1.023	0.0284		
Total	53	4.377	0.0826		

Table 10. Source Table NI ANOVA for Organic concentration.

| Source	DF	SS	MS	F	P
Station Distance	4	8.781	2.195	24.563	<0.001
Sample Date	2	9.123	4.562	51.042	<0.001
Distance x Date	8	4.428	0.554	6.193	<0.001
Residual	30	2.681	0.0894		
Total	44	25.014	0.568		

Jordan Bay, N.S.
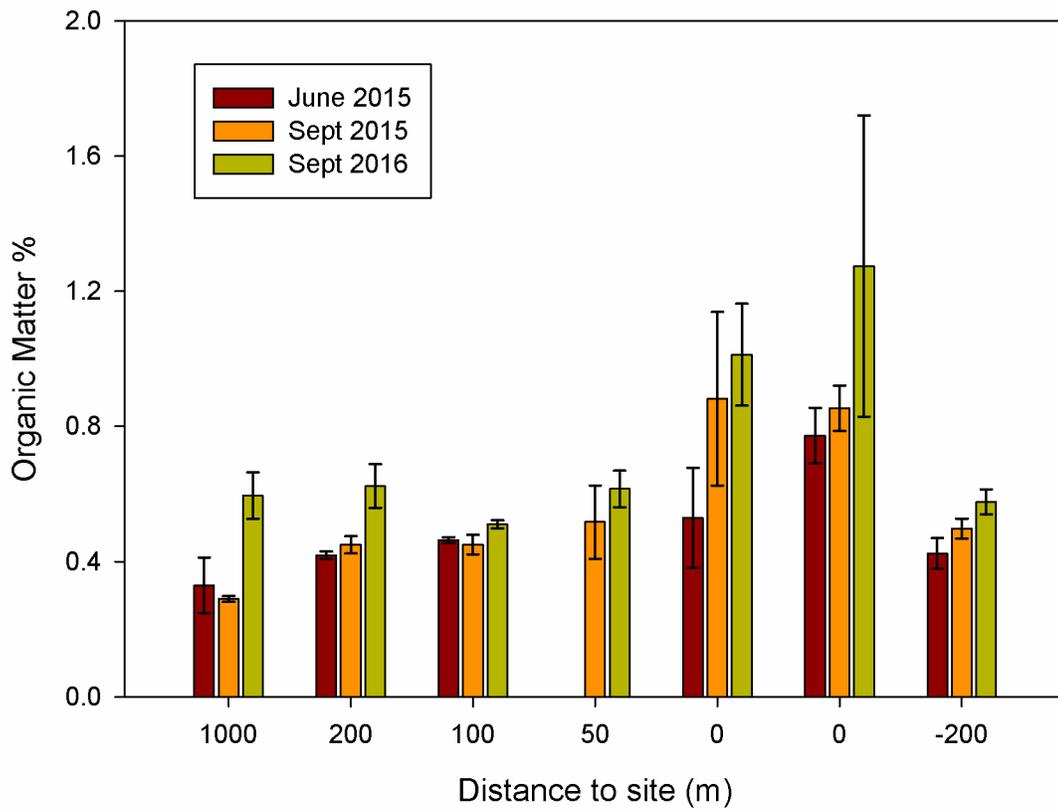
Figure 7. Jordan Bay bottom sediment organic matter percentage from all samplings.
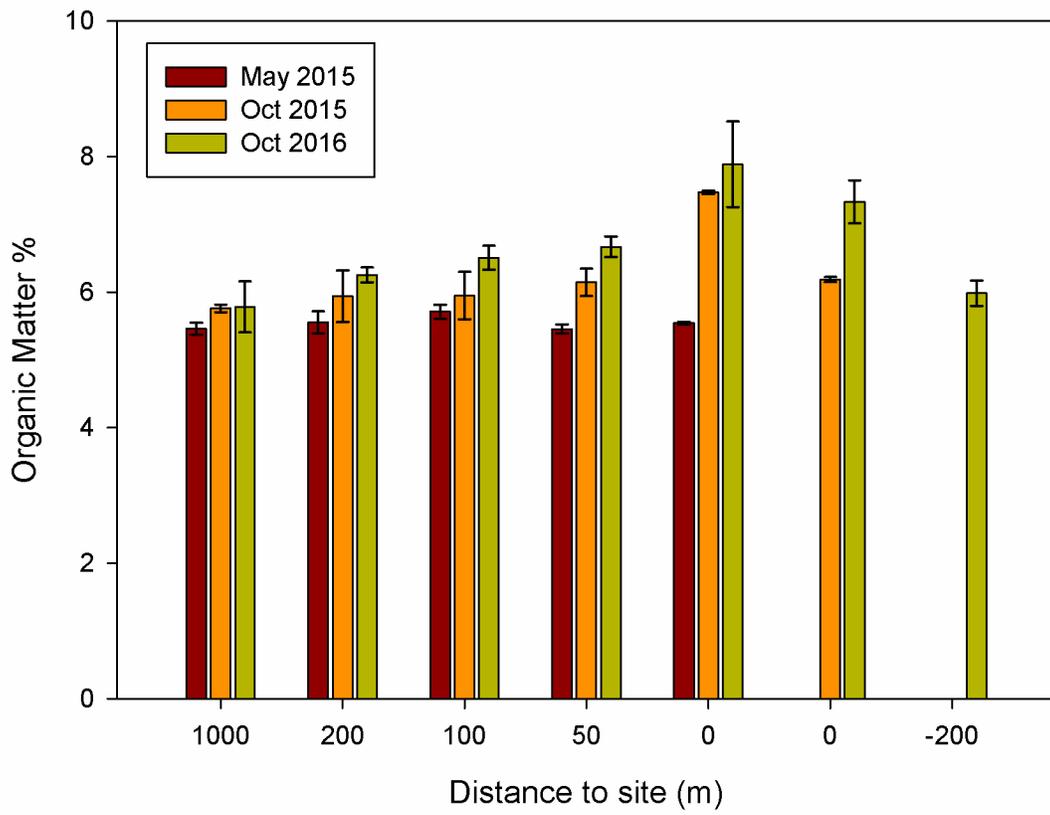
Figure 8. Navy Island bottom sediment organic matter percentage from all samplings.

To further investigate the interactions of sample distance from aquaculture operations and sample date on organic matter % a two-way ANOVA was performed. At Jordan Bay there was a significant effect of station distance, $F_{(5,36)} = 15.97$, $p<0.001$ and sample date, $F_{(2,36)} = 12.582$, $p < 0.001$ on organic % in bottom sediments (Table 9). Post hoc investigation of comparisons for factor revealed that stations immediately at the cage site both on the North and South side experienced increases in fraction of organics over the course of the sampling period (i.e. from May 2015 to September 2016) and that the stations at 0-m on both sides of the cage site were significantly different from the other stations (Fig. 7). At the Navy Island site there was also a significant effect of sample distance, $F_{(4,30)} = 24.563$, $p<0.001$ and with sample date, $F_{(2,30)} = 51.042$, $p<0.001$ on organic percentage (Table 10). Investigation of comparisons for factor revealed that there was significant difference in organic matter percentage between the 0-m, 50-m and 100-m stations and the 200-m and 1000m stations. In addition, there was a significant increase in organic matter percentage of bottom samples from the first sampling in June 2015 to October 2015 and then again to the final sampling in October 2016. Overall, stations from at the cage site out to 200 m away from the cage on the sample transect had significant change in terms of increased organic matter concentration from the start to the end of the samplings (Fig. 8).

4.0 Discussion

4.1 Near Field vs. Far Field

A significant ($p<0.05$) increase in organic matter percentage in bottom sediments occurred at Navy Island, the cohesive sediment site, out to 200 m from aquaculture operations along the sampled transect from the beginning of the sampling when fish were added to the site until the end of sampling which was just prior to fish being removed and sent to market. At the non-cohesive site at Jordan Bay, a significant ($p<0.05$) increase in organic matter was observed only at the 0-m stations on both the north and south side of the cage site over the 16-month sampling period when fish grew from smolt to near market size. Distances out to 200 m represent the near field of aquaculture operations. Organic matter flux in g m^2 d^{-1} collected at the time of each sampling approximately doubled at both locations during the grow out process (Fig 6) with higher values observed at the Jordan Bay non-cohesive site. This difference may be due to the fact that the number of cages and subsequently the number of fish at the Jordan Bay site were higher than at Navy Island site, roughly 450,000 - 600,000 fish as compared to 600,000 - 1,000,000 respectively, based on a standard stocking density of 30,000 – 50,000 fish per cage (Cranford et al., 2017). Additionally, naturally occurring organic matter may be higher at the Jordan Bay site although background water samples collected for the "Gust" erosion experiments from adjacent to the cages at both locations had similar organic matter values of 10-20 %, of the particulate matter, determined by loss on ignition (unpublished data). Finally, resuspension may play a role in the observed higher organic matter at the more energetic Jordan Bay site.

At Jordan Bay wave energy was greater. Higher energy presumably was responsible for greater dispersal of particulates coming from the aquaculture site, so only directly under the site, where flux was largest, was organic enrichment detected. Farther away from the site, depositional flux was smaller than erosional flux, so the organic content of the seabed did not increase. At Navy Island, the erosional flux from waves and currents was low, so increased organic matter in the seabed was observed farther away from the aquaculture site. Increased sediment oxygen demand does occur at aquaculture sites as a result of increased deposition of organic matter (Hargrave et. al., 1993, Droppo et al., 2007). Strain et al. (2005) estimated that up to 50% of organic matter deposited in the vicinity of salmon aquaculture cages, at a cohesive site, would be respired by the benthos. Grant et al. (1991) showed that areas of fine-grained substrate had increases in organic content, bacterial biomass, and community metabolism, which led to a benthic oxygen demand on average of 2.7 times that of coarser grained sand. Therefore, bacterial degradation and assimilative capacity of fine grained sediments would be expected to be higher in fine grained cohesive sediments at the Navy Island site.

4.2 Erodibility

The erosion of material from cores collected in-situ at both the Jordan Bay and Navy Island site occurred at shear stresses as low as 0.01 Pa to 0.02 Pa, a value exceeded in-situ at both locations, even by typical currents working on the seabed (Fig 2 & 3). The material eroded was highly organic (i.e. 40% to 60% as determined by LOI) at the 0.01 Pa and 0.08 Pa shear stress step, and visual

observations indicated that it was flocculated. Milligan and Law (2013) observed

similar floc erosion of organic material from areas of active salmon aquaculture.

As the stress increased in the erosion experiments from approximately 0.24 Pa

and up to 0.60 Pa, more bottom sediment was eroded and the organic

percentage in that sediment decreased. Even at the high shear stress steps (i.e.

0.48 Pa and 0.60 Pa), however, the percent of organics in the material eroded at

both Jordan Bay at the 0-m stations north and south and at Navy Island stations

out to 200 m on the main transect remained high (i.e. 10% to 15%) compared

with the bed sediments sampled with the slo-corer (Figs 7 and 8).

The Gust chamber erodes the most recently deposited bed material,

which because of the aquaculture at the sites, was higher in organic content than

the background sediment. Dickhudt et al. (2010) estimated that only 1-2 mm of

the bed sediment was eroded during erosion experiments performed in muddy

environments with the same erosion device. Samples collected for organic

matter analysis used approximately 0.5-1 cm of the top of the bed sediment,

which may help explain the increased organic matter percentage in Gust

samples compared with the bed sediment values. In addition, research has

shown that flow through permeable beds can transfer suspended particles from
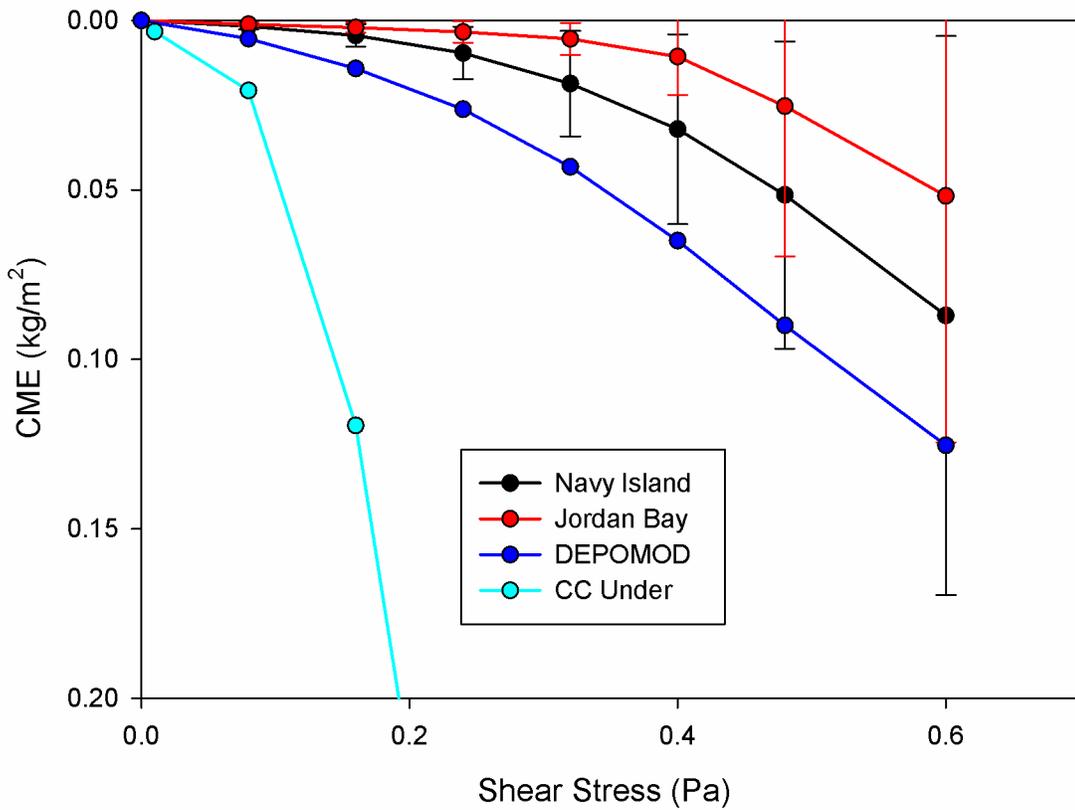
Figure 9. Average CME from Jordan Bay and Navy Island from all samplings. DEPOMOD also shown as average CME using the DEPOMOD erodibility parameter, M, value of 7.0 x E-7 as well as data from Milligan and Law (2013) from Charlie Cove aquaculture site in Southwest New Brunswick (CC Under).

the boundary layer into surficial sediments (Huettel et al., 1996; Chen et al., 2010). This material could then be available for resuspension in the erosion studies, thereby enriching the Gust samples in organic matter.

DEPOMOD is a model that was developed to predict the solids waste accumulation on the seabed associated with fish farming activity (Cromey et al., 2002a). While primarily addressing the initial deposition of waste, DEPOMOD also employs a simple resuspension module to redistribute waste particles according to near-bed currents (Cromey et al., 2002b). The resuspension module uses the erosion formula:

$$Me = M \left(\frac{\tau b}{\tau c} - 1 \right) \qquad (2)$$

where, Me is the erosion rate (kg m^{-2} s^{-1}), τ_b (Pa) is the applied bottom stress, τ_c (Pa) is the critical stress for erosion, and M is an erodibility parameter (kg m^{-2} s^{-1}). The value of M governs the removal rate of material from the seabed when a bed stress greater than a critical stress is applied. In the module the values of M and τ_c are set at 7.0×10^{-7} kg m^{-2} s^{-1} and 0.0179 Pa (9.5 cm s^{-1} flow speed), respectively. To compare DEPOMOD predictions to observations, CME at each stress step was calculated by multiplying the DEPOMOD Me for that step by the time over which that stress was applied (1200 s).

Based on our observations from this study, employing the standard DEPOMOD parameter values over-estimates the erosion of bottom material (Fig 9). Chamberlain and Stucchi (2007) also found that DEPOMOD eroded too much mass, so they recommended that the resuspension module in DEPOMOD be turned off during simulations and that DEPOMOD be used solely to determine

the depositional footprint of aquaculture operation. Chang et al., (2011) when comparing DEPOMOD output to measured sulfides also found a similar result to the study of Chamberlain and Stucchi (2007).

Overestimation of cumulative mass eroded by DEPOMOD is linked to improper characterization of erosion. Sanford and Maa (2001) proposed a linear formulation for erosion, with τ_c as an increasing function of depth. This type of erosion limits the amount of sediment available at a given stress step, as observed in the erosion of cores in this study. According to the Sanford and Maa (2001) formulation, more sediment becomes available for resuspension only by increasing the boundary shear stress. In DEPOMOD the mass transport of material continues at the rate governed by the erodibility parameter, M, as long as the critical bottom stress for erosion is exceed. An additional problem with DEPOMOD is that all particles types (i.e. recently deposited flocs, fecal material, feed pellets) are assigned the same critical stress for erosion.

4.3 Modelling and Transport

Recent modelling efforts to understand and predict the transport of finfish waste from aquaculture operations to the near and far field has evolved mostly from single point near field currents (Cromey et al., 2002a) to spatially explicit 3D current fields with higher resolution grids near farm sites (Wu et al., 2014; Bannister et al., 2016; Broch et al., 2017). Bannister et al., (2016) validated their coupled hydrodynamic-active particle tracking model of organic waste dispersal in fjord systems by using observed particulate organic matter flux values from in-situ sediment traps. They concluded that by using a range of fecal settling

material values (i.e. mm s^{-1}) from various size fish their results improved predicted deposition compared to a model with a single value for settling velocity (Cromey et al., 2002b).

Law et al. (2014) used in-situ measurements to hypothesize that farm-produced particles packaged in flocs that settle at roughly 1 mm s^{-1} can be transported to the far field. Broch et al. (2017) used a coupled hydrodynamic-mass transport model to simulate the dispersal and deposition of fish farm waste (i.e. fecal material) at three separate locations in Norway, including a fjord, an exposed coastal location, and a semi-exposed location. They included floc-derived material (i.e. smaller size <2 mm) with appropriate settling velocities. Using the DREAM model with resuspension to transport material, model output was significantly improved when compared to observations of waste/mud thickness collected as part of the Norwegian mandatory benthic surveys of fish farms (Broch et al., 2017). The DREAM model also included waves based on the wind field in the erosion process which was important in the costal exposed and semi-exposed sites.

This study, based on observations of mass eroded at aquaculture sites from a cohesive and non-cohesive farm site show several important factors that should be considered in aquaculture waste transport modelling. First, the organic content of bed sediments affects erosion. Second, organic content of bed sediments near aquaculture operations increases when fish are present. Higher organic content in turn leads to lower erosion rates when the bed becomes enriched, which represents a positive feedback. The perturbation

113

caused by the addition of fish, leads to increased organic matter concentration in the bed sediment, which leads to decreased erosion of bed material, which leads to a greater increase in organic matter until a maximum is reached or the organic supply is turned off. Third, the effect of increasing organic matter in bed sediments is diminished but does not vanish in non-cohesive sediments, such as the sandy seabed sediments at Jordan Bay. Finally, transport models need to include waves at sites such as Jordan Bay, because it is the erosive force of waves that increases seabed stress and ultimately resuspends material from the seabed and makes it available to transport by currents. The erosion experiments in this study went up to 0.60 Pa and are representative of typical coastal settings and can erode up to several millimeters of the seabed. At times when wind waves are large and occur in aquaculture areas with exposed sites and shallower water, waves can be responsible for large resuspension and transport events. Figures 2 and 3 show the difference in seabed stress between an area that is dominated by tidally induced versus wave induced stress, with the latter showing an order of magnitude difference. This difference could be responsible for eroding several cm's into the seabed, thus removing and transporting large amounts of organic matter out of the area and subsequently resetting the seabed.

4.4 Implications / Way Forward

Understanding the mass transport of aquaculture waste material to the far field is important for the sustainability of the industry and to help with social licence and acceptability of waste inputs in the marine environment. Graydon et

al. (2012) used feed pigments to determine an area of influence out to 1000 m from aquaculture operations, and they hypothesized that low concentrations of small, farm-derived particles may exist on a bay-wide scale. Law et al. (2014) showed that relatively organic-rich, flocculated particles indicative of aquaculture waste material, were present at aquaculture sites and suggested these particles as a pathway to the far field. The coupled hydrodynamic-transport modelling studies of Bannister et al. (2016) and Bach et al. (2017) showed that organic material from aquaculture operations can reach several kilometers into the far field. As the use of particle reactive chemical constituents to combat disease and other factors such as sea lice continue to be used in open-pen aquaculture, it is even more important to understand waste transport and other transport pathways. Predictive modelling using 3D spatially explicit currents coupled with waves and sediment transport / particle transport models will need to be refined and validated. The use of tracers, such as fatty acids, stable isotopes, pigments, etc. combined with measurements of particle properties (e.g. settling velocity, critical stress for erosion) and hydrodynamics will be required to increase our predictive capacity and for model validation.

5.0 Conclusion

As the percentage of organics retained in bottom sediments increased at two active aquaculture sites, the mass eroded decreased. A significant increase in organic matter percentage in bottom sediments occurred at both the cohesive and non-cohesive site over the time of the sampling, which corresponded to a period when the aquaculture sites were first stocked with salmon smolt until just

before fish were removed for market. At the cohesive site the percentage of organics in bottom sediment increased significantly out to 200 m from the site. At the non-cohesive site a significant increase was detected only at the 0-m north and 0-m locations, which were immediately adjacent to the cage site. At the non-cohesive site waves during fall and winter storms could be responsible for large resuspension events. Understanding differences in the erodibility of cohesive and non-cohesive seabeds and implementing appropriate parameters for resuspension and transport in models will improve predictive capacity in the movement of aquaculture derived waste products.

Acknowledgements

Chapter 5

This chapter comprises material to be published in a DFO technical report. Law was responsible for writing this chapter, providing all data and analysis related to non-modelled runs. Law also provided all parameters related to the transport of the 4 modelled classes consisting of fines, flocs, fecal material and feed pellets. Drozdowski was responsible for BBLT model runs and providing model output.

Proof-of-Concept Application of the Benthic Boundary Layer Transport (BBLT) model to Salmon Aquaculture Waste Dispersal

Law, B.A.[1, 2,*], Drozdowski, A.[1], Hill, P.S. [2]

[1] Fisheries and Oceans Canada, Bedford Institute of Oceanography, Dartmouth, Nova Scotia, Canada, B2Y 4A2

[2] Department of Oceanography, Dalhousie University, Halifax, Nova Scotia, Canada, B3H 4J1

* Corresponding author
Brent Law
Habitat Sedimentologist
Fisheries and Oceans Canada
Bedford Institute of Oceanography
1 Challenger Drive, Dartmouth, Nova Scotia Canada,
 B2Y 4A2
Brent.Law@mar.dfo-mpo.gc.ca
Telephone | Téléphone 902-426-8548
Facsimile | Télécopieur 902-426-6695
Government of Canada | Gouvernement du Canada

ABSTRACT

Dispersal from a fin-fish aquaculture facility in Jordan Bay, N.S., Canada was simulated using the Benthic Boundary Layer Transport model (BBLT). The currents and waves were measured during the fall of 2014 and along with calculated bottom shear stress were used as model inputs. Four waste classes were considered: fines, flocs, fecal waste and feed pellets, each with distinct settling velocities and critical erosion shear stresses. BBLT was used to simulate a 46-day continuous release scenario. The resulting concentration of each class within the cage site varied by approximately 5 orders of magnitude. The four classes mean concentration in bottom 10 cm under the cage were 0.003, 0.082, 122.4 and 234.6 g/m^3 respectively. Spatial patterns reveal the concentration of the fines to be relatively uniform inside and within a few hundred meters of the cage, and to fall by 1/10 a few kilometers away. Floc concentrations fall to 1/10 within a 100 m of the cage and by 1/1000 within a few kilometers. For fecal waste, concentrations fall by 1/10 directly outside the cage and may be undetectable a few kilometers away. Feed Pellet removal is somewhat more complicated due to the episodic deposition and advection of the sediment patch. However, just like for the fecal waste the concentration drops by at least an order of magnitude directly outside the cage and by as much as 1/1000 within a few hundred meters. The general direction of travel is to the south. The higher concentrations of fines and flocs in the far field as compared to fecal material and pellets represent a transport mechanism for constituents such as trace metals, pesticides and organics which have an affinity for the large surface areas of fine-grain sediments.

1.0 Introduction

With the expansion of open net pen salmon farming industry, environmental concerns have been raised over the fate of aquaculture waste material, primarily feed pellets and fecal matter. To date, research has focused primarily on the deposition of organic waste immediately under or adjacent to salmon net pens. Both modelling and field studies have focused on near-field effects from organic enrichment, while the far field has received far less attention. The near field is considered to be the area within a few hundred meters of the cage sites while the far field extends kilometers away from farming operations. Models to map the depositional footprint from salmon and other fin-fish farms using the settling characteristics of waste solids have become increasingly accurate (Panchang et al., 1997; Cromey et al., 2002a, Chamberlain and Stucchi, 2007). Models that map the subsequent resuspension and transport of waste material have been less successful (Droppo et al., 2007; Chamberlain and Stucchi, 2007; Reid et al., 2009; Keeley et al., 2013).

Quantifying the dispersal of finfish aquaculture waste through the use of modelling is necessary to predict the potential habitat impacts from farm systems and for evaluating siting criteria (Panchang et al., 1997; Cromey et al., 2002a; Reid et al., 2009). The accumulation of fecal material and feed pellets under cage sites and within a few hundred meter of farm sites is relatively well understood. The settling velocity of fecal material and pellets is large, approximately 40 mm/s and 100 mm/s respectively, so the depositional footprint of this waste material is relatively small and easily defined. In contrast, flocs

have settling velocities on the order of 1 mm s^{-1} (Hill et al., 2001) and can be easily transported to the far field, several km's from aquaculture operations (Law et al., 2014). Under stress, flocs can break up, resulting in settling velocities nearing that of the component particles that are almost always in suspension. These important parameters around aquaculture sites are poorly constrained in present models, yet they have potential to impact the far field (Sutherland et al., 2006; Droppo et al., 2007).

The model DEPOMOD was developed to predict the solids waste accumulation on the seabed associated with fish farming activity (Cromey et al., 2002a). It is the most established and widely used depositional model for predicting salmon farm effects, largely because it has been validated in a wide range of environments and is considered to be robust and credible (Keeley et al., 2013). While primarily addressing the initial footprint due to the deposition of waste products, by employing a settling velocity of ~ 100 mm s^{-1} for feed pellets and ~ 40 mm s^{-1} for fecal material, DEPOMOD also employs a simple resuspension module to redistribute waste particles according to near-bed currents. The resuspension module uses the values of M, an erodibility parameter, and τc, a critical stress for erosion, that are hard coded to be 7.0 x 10^{-7} kg m^{-2} s^{-1} and 0.0179 Pa (9.5 cm s^{-1} flow speed), respectively. The results of using the resuspension module of DEPOMOD has had mixed success due to the fact that the model does not always accurately predict the removal of material and its transport from the seabed (Cromey at al., 2002b; Chamberlain and Stucchi, 2007; Chang et al., 2011; Keeley et al., 2013).

The benthic boundary layer transport model (BBLT) was originally developed and used to study suspended particulate drilling waste dispersal (Hannah et al., 1995). Sediment dynamics within BBLT are modelled with a modified Rouse profile (Rouse 1937). DEPOMOD resuspends a fixed amount of the seabed based on stress in excess of the critical stress and then advects this mass of seabed using the near-bed velocity used to estimate that stress. This strategy will over-predict the transport of larger waste particles that only move very near the seabed, and it will under-predict the transport of smaller waste particles that are generally mixed higher into the boundary layer where flow speeds are larger. In addition, DEPOMOD only has only value for τc of approximately 0.02 Pa, which is substantially lower than previously reported literature values for feed pellet transport and would also contribute to over-prediction of large waste particle transport (Sutherland et al., 2006; Law et al., 2016). Recent work from Law et al. (2014) showed that slower sinking, organic-rich particles, indicative of broken down food waste and fecal material, are abundant at active salmon aquaculture farms and may represent a vector for organics to the far field. BBLT was developed in part to examine the effects of shear dispersion and vertical mixing on particle distributions around discharge sites.   DEPOMOD does not consider these effects which is justified by its focus on fast settling particles. To examine the dispersal of slower sinking particulate wastes, however, requires a more sophisticated tool such as BBLT.

BBLT was used primarily in the offshore environment (Hannah and Drozdowski, 2005; Tedford et al., 2002, 2003), to determine the fate and sub-

lethal biological impacts of drilling muds released during the drilling phase of oil and gas platforms. There has been limited near-shore work undertaken using BBLT as well. BBLT has been used to conduct an environmental assessment of the discharge of effluent solid waste and for the construction activities associated with a submarine cable crossings (AMEC E&E Division, 2007; AMEC E&E Division, 2011). Moreover, Petrie et al. (2004) have used BBLT in a study of Sydney Harbour, where they found a tendency for fine sediment to accumulate near the head of the harbour, which is broadly consistent with the distribution of pollutants found in the sediment. The applicability of BBLT to the near-shore is limited by spatial variability of the currents, which in the presence of topographic features can vary significantly in magnitude and direction over 100's of meters. Attempts to overcome spatial variability have resulted in BBLT3D which works under the same principles but uses 3-dimensional current fields produced by circulation models (Drozdowski, 2009). This method is more computationally demanding and is often limited by the availability of reliable, validated and adequately resolved circulation models. Recently, Niu et al. (2014) performed a case study to compare BBLT with another sediment transport model, ParTrack (Rye et al., 1998) and although ParTrack and BBLT are formulated quite differently, they produced comparable results.

This study collected a time series of current and wave measurements at an area of active salmon aquaculture, on a sandy bottom, non-cohesive site in Jordan Bay, in southwest Nova Scotia. The analyzed current and wave data were used to force the BBLT model. Additional input parameters of settling

velocity and critical shear stress of salmon waste particles were used to simulate the resuspension and transport of this material. The goal of this study was to determine the applicability of the BBLT model for use in predictive salmon aquaculture waste modelling studies.

2.0 Methods

2.1 BBLT Description and Features

BBLT was based on the following conceptual model of suspended sediment transport (Fig 1). First, consider an initial distribution of sediment (Fig 1, time 1) followed by an increase in bottom currents and bed stress which suspends an additional amount of sediment (Fig 1, time 2). The distribution of suspended sediment is stretched in the horizontal by vertical shear in the currents and redistributed vertically by vertical mixing (Fig 1, time 3). When the currents wane, sediment settles back to the bottom and has a broader distribution than it would have in the absence of shear dispersion and mixing (Fig 1, time 4). Shear dispersion is therefore the primary mechanism in BBLT for redistributing sediment in the horizontal because of the interaction between vertical mixing and vertical shear (Fig 2).

In the formulation of BBLT sediment "packets" have a settling velocity associated with them. These sediment packets are supplied by resuspension from the bottom. The overall model distribution of the sediment packets in the vertical follows the modified Rouse profile, which is based on balance between upward turbulent diffusion and downward sinking.

DISPERSION AND TRANSPORT OF SUSPENDED SEDIMENT IN THE BENTHIC BOUNDARY LAYER
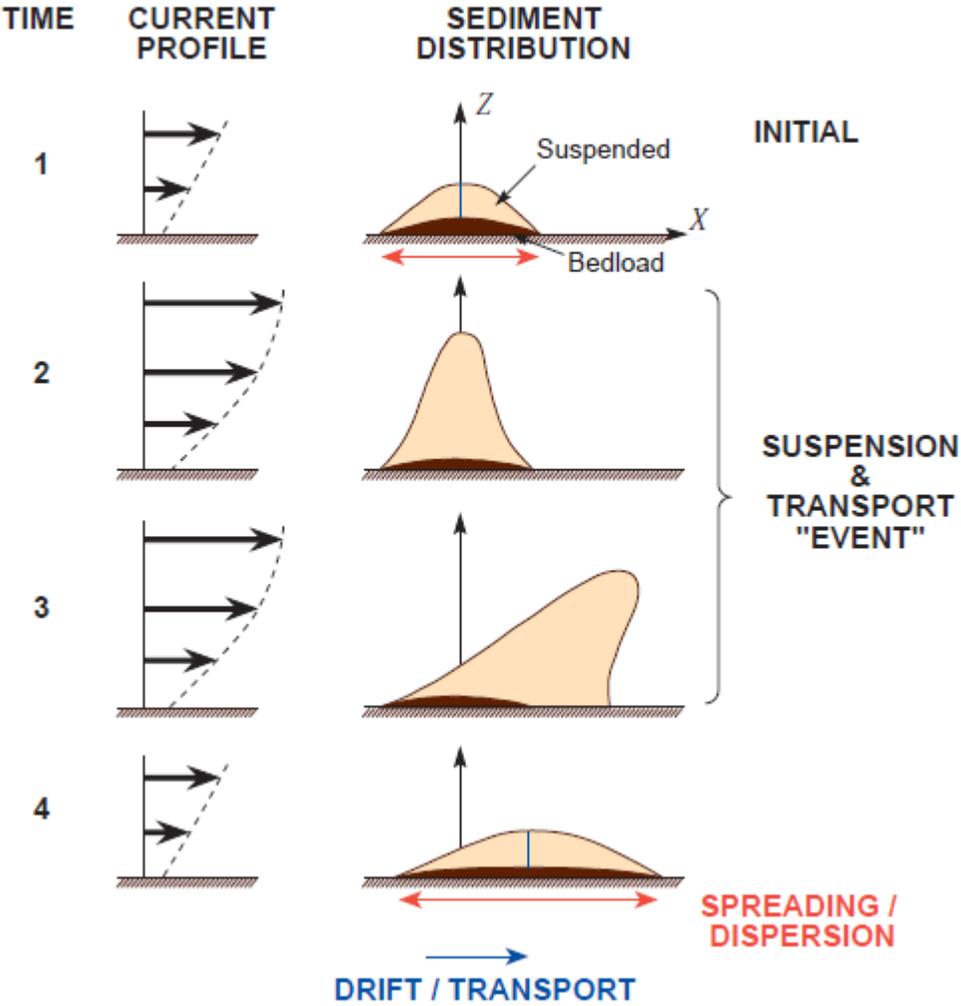

Figure 1. Conceptual model of how suspended sediment transport is modelled in BBLT. Vertical shear in horizontal currents in the benthic boundary layer lead to horizontal drift and shear dispersion. (Courtesy of Drozdowski et al., 2004).
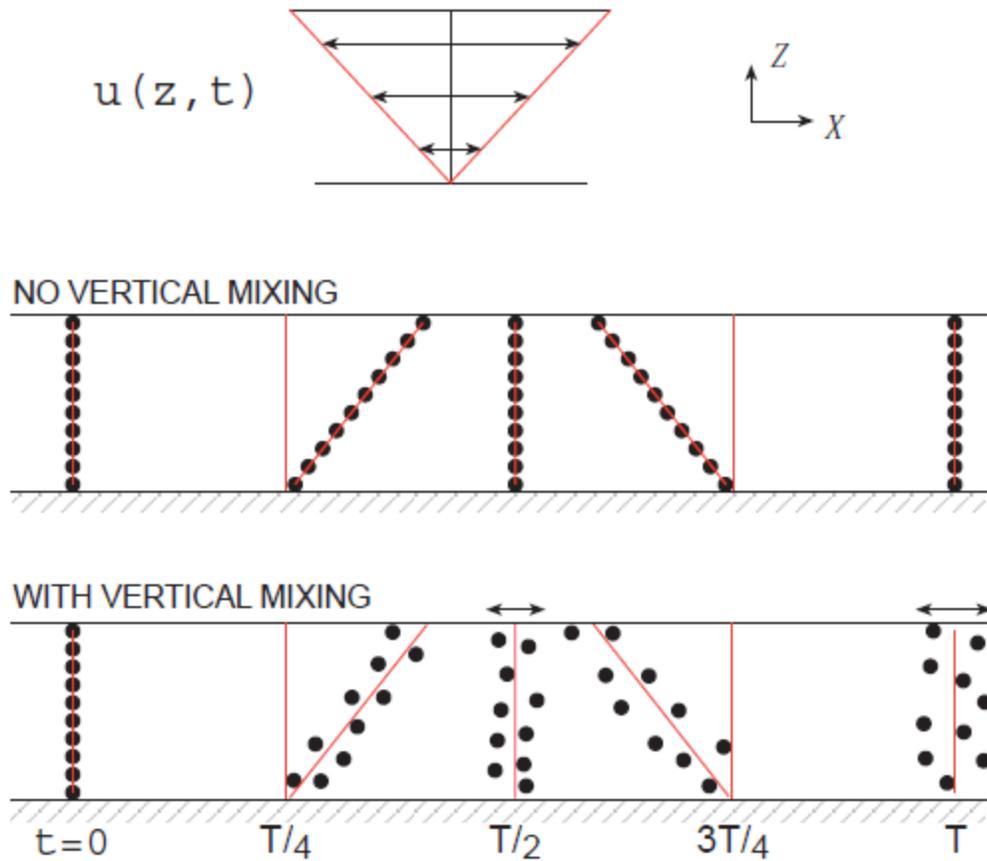
Figure 2. Cartoon demonstrating the importance of vertical mixing to horizontal dispersion in vertically sheared flows. Consider a purely periodic flow shown in the top panel. In the absence of vertical mixing (middle panel), periodic flow brings particles back to their original starting positions. In the presence of vertical mixing, particles are displaced vertically from the titled line resulting in horizontal dispersion during each particle tilting. The case shown (a tilt in each direction during a tidal period) assumes peak currents at t = 0 (u = cosωt). (Courtesy of Drozdowski et al., 2004).

The modified Rouse profile is defined by the equation

$$C(z) = C_a (a/z)^P \qquad\qquad\qquad (1)$$

where C(z) is the time averaged sediment concentration at a height z above the bed, Ca is the reference concentration at the reference height z = a, above the seabed and P is the Rouse number, which is equal to the settling velocity of a size class of particles, W_s, divided by k = 0.4, which is von Karman's constant, multiplied by u*, which is the friction velocity. The modified Rouse profile is valid in the range of z/h << 1 and z/a >> 1, where h represents the water depth.

In this version 7.0 of BBLT, a 2-layer formulation is used for the concentration profile.   A combined wave-current boundary layer is forced with a combined wave-current shear velocity u^*_{wc} with current shear velocity layer, u^*_c, above it. The 2-layer Rouse profile couples the 2 individual modified Rouse profiles.

Another feature of BBLT is the use of "packets" or pseudo-particles. The mass of material to be modelled, M, is divided into N packets each with a mass, m = M/N and each packet has a position in X, Y, and Z. The packets are mathematical constructs with different vertical movement properties with the net effect of their movement intended to represent shear dispersion. The movement of the packets is divided into 2 parts, the vertical distribution and the horizontal transport. Given a time dependent velocity field the packets are advected horizontally over an advection time step. Vertical motions are not modelled explicitly but rather they are parameterized in terms of the modified Rouse profile. Vertical distribution occurs through the expansion and contraction of the

profile (i.e. change in stress) and through vertical mixing. The vertical mixing is also not modelled explicitly but is parametrized in terms of a shuffling of packets, which occurs after each advection time step and extracts the net effect of the shear dispersion process without having to model the motions of individual packets.

Inputs to the model are a time series of depth-dependent currents, the bottom stress either from currents or combined wave and current stresses, and settling velocity of the particles and/or sediment of interest along with critical stress for each particle size class. Basic output from BBLT numerical model consists of drift, diffusivity, and concentration. (For a complete description of BBLT, see Hannah et al., 1995 and Drozdowski et al., 2004)

2.2   Study Location

Jordan Bay is located on the Atlantic coast of Nova Scotia and is exposed to wind waves and longer period swell from the southerly direction. The Jordan Bay aquaculture site is located in the outer part of the Bay (43 42.0 N, 65 11.7 W) and is close to Blue Island (Fig 3). The average water depth at the site is approximately 18 m, and the average tidal range is 1.5 meters (Law et al., 2018). The aquaculture site occupies an area that is about 500 m in length by about 200 m in width. It is made up of twenty circular pens with in two parallel rows of 10 (Fig. 3).   The seabed at the site is primarily fine sand with median, d50, values of approximately 150 μm, has a small <4 μm fraction, of < 2 % and is considered non-cohesive (Law et al., 2018).
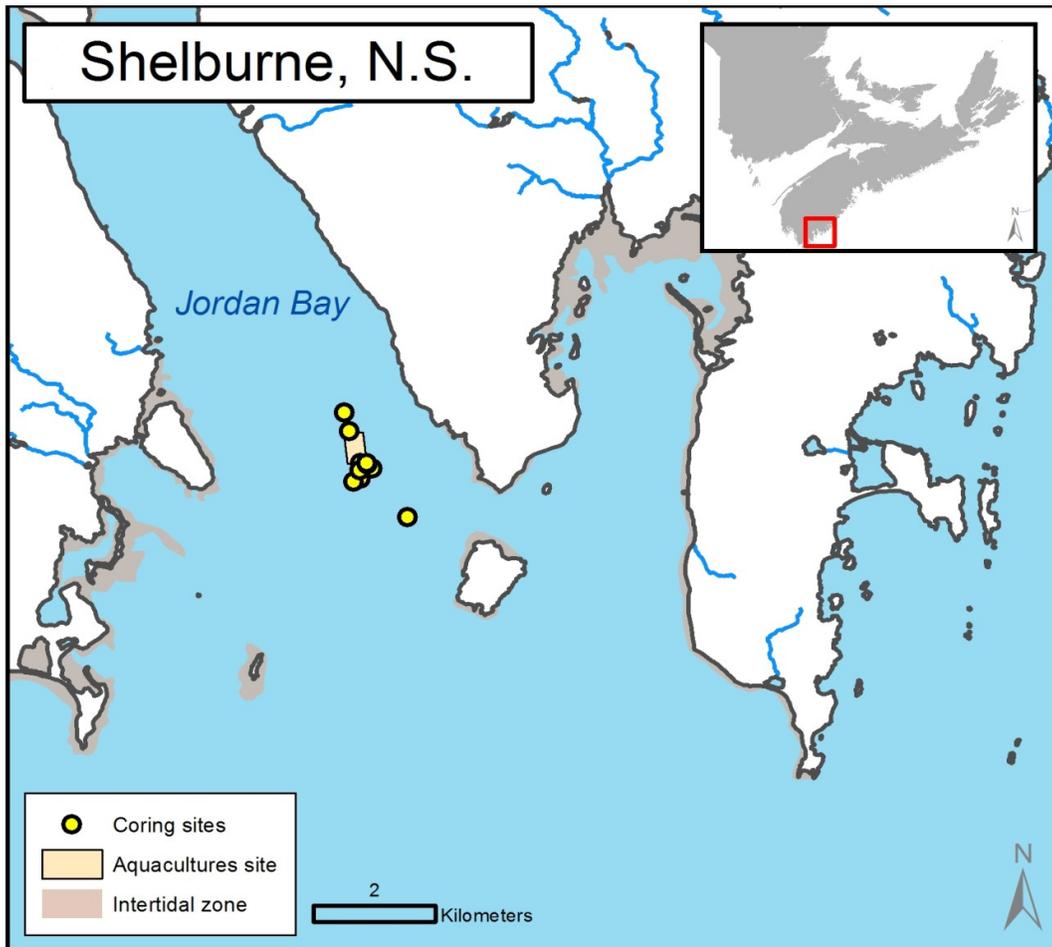
Figure 3. Map of the study area in Jordan Bay, Nova Scotia. The salmon aquaculture site is defined by the beige rectangle and the coring sites to the south of the aquaculture site are where the ADCP instrumentation was placed.

2.3 Data Collection

A downward-looking Acoustic Doppler Current Profiler, ADCP (2 MHz, Nortek Aquadopp) was deployed for 46 days, starting on September 23rd, 2014 from a tripod using an extendable arm that was 1.5 m from the frame and was positioned approximately 1 m above the seabed. Data were collected in burst mode at 8 Hz and 4800 samples. The frequency of sampling allowed data collection for 10 minutes every two hours and gave the ability to obtain both current velocities and the orbital velocities due to waves. A wave-current interaction model developed by Grant and Madsen was used to determine the combined wave-current shear velocities at the seabed and also the wave-boundary layer height for the deployment time period (Grant and Madsen 1986; Madsen 1994).

A 600 KHz RDI ADCP (67_1) with an installed waves package was deployed starting on September 24th, 2014, for 70 days, in an upward looking position adjacent to the Nortek Aquadopp. The RDI current data was a 5-minute average collected every 20 minutes at 1Hz, while wave sampling was a 10-minute average every hour. The RDI instrument was used to measure current velocities at every meter from roughly 4 m above the bottom to the surface and measures wave heights at the surface through echo ranging and bottom pressure from the pressure transducer in the instrument. Combined wave-current shear velocities also were calculated based on the RDI data using the model SEDTRANS96 (Li and Amos, 2001) which required surface wave heights, period, direction and currents near the seabed extrapolated from the lowest,

resolvable bin of the RDI which was approximately 5 m off the bottom based on beam correlations.

A second RDI 1200 KHz ADCP (66_1) was deployed in a downward-looking direction and measured currents from approximately 5 m off the seabed to the seabed itself. This ADCP was deployed for only a few days to compare current velocities of the longer sampling RDI ADCP and the aquadopp and to extrapolate current velocities between the 2 longer measuring instruments.

2.4 BBLT Simulation Set-up

BBLT was forced with the profiles of currents and the corresponding bottom stress.   Four different size classes were considered. The four size classes were, background fines, flocs, fish fecal waste, and uneaten feed pellets (Table 1). BBLT assumes a single settling velocity and critical stress for each sediment class. Each class modelled was represented by an average particle diameter and corresponding settling velocity and critical stress based on Law et al. (2014; 2016). In BBLT, when the bottom stress was below the critical stress, all the sediment packets resided in bottom bin where they experienced no horizontal motion. When the critical shear stress for erosion was exceeded, all sediment packets from the bottom bin were put into suspension and therefore is considered a depth limited suspension in sediment transport models.

Bottom roughness height was set to 1.0 mm. This roughness height is the default parameter based on previous simulations on relatively sandy seabeds (Hannah et al., 1995). An additional modelling consideration involves the

Table 1. Waste Class Parameters used in simulations.

Sediment Waste Class	Fines (1)	Flocs (2)	Fecal (3)	Pellets (4)
Settling velocity (mm/s)	0.1	1	40	100
Critical Stress (m/s); i.e. friction velocity)	0.0015	0.003	0.009	0.015
Average Diameter (mm)	0.04	0.20	0.5	10
Reference Height (href; mm)	1	1	1.25	5
Input Mass (M_0; g)	20000	20000	20000	20000
Input Period (T; days)	1	1	1	1
Maximum Initial Concentration (C_{max}; g/m^3)	102	102	102	102

reference height (href) which is the bottom of the Rouse profile in BBLT. This height should be greater than or equal to the roughness height. This is important for large grains such as large fish pellets, whose average diameter is 10 mm, which leaves them exposed to stronger currents (Table 1). For fines and flocs, the diameter is negligible and the reference height equals the roughness height (Table 1). BBLT limits the vertical extent of the resuspension with the parameter hmax. This was set to 18 m, the depth of the water at the ADCP instrument locations (Table 2).

For each simulation, a mass of waste equaling M_0 grams was introduced instantaneously into the fish cage each day for the entire simulation. This mass gives a maximum daily concentration of C_{max} which would only occur if all the material dumped on the first day settled in the bottom 10 cm directly under the fish cage with D (= 50 meter) diameter (a volume of Vo= 0.1 π $D^2/4$ = 196.3 m^3 here) . The 10-cm level was the default parameter used in original BBLT studies (Hannah et al., 1995). Most concentrations presented in this report are normalized by C_{max} and hence can be generalized to any introduction rate and cage size simply by multiplying by C_{max} = M_0 /Vo. The actual descent of sediment to the bottom is not modeled by BBLT. All sediment input is redistributed vertically based on the Rouse profile once a set threshold for tau critical, τc is exceeded. Because sediment with smaller settling velocities is mixed more in the horizontal by shear dispersion and because it has lower τc,

Table 2 BBLT Simulation Parameters

Start Time	Day 0 (=00:00Z 25-Sep-2014)
Duration	46 days
Number of Packets	10000 added every 24h Total =480 000
Advection time step	0.03 hours
Bottom Roughness	1.0 mm
Maximum Vertical Extent (hmax)	18 m

Table 3. Statistical summary of all current meter data from both RDI ADCP's and the Aquadopp. All velocities are in cms^{-1}.

	ADCP 67_1			ADCP 66_1		Aquadopp	
Bin # (mab)	**1 (5)**	**7 (11)**	**14(18)**	**3(0.3)**	**25(2.5)**	**1(1.06)**	**7(0.1)**
Mean u	0.31	0.92	0.02	-0.17	0.35	-0.74	-0.09
Mean v	-0.6	2.5	0.59	-0.36	-1.26	0.64	0.23
Max. speed	28.53	31.06	30.51	11.29	18.12	12.38	3.87
Min. speed	0.14	0.11	0.14	0.4	0.09	0.02	0.01
RMS speed	11.1	9.3	8.5	5.3	7.2	3.9	1.05
Tide as % of Tot. Var.	24.7	42.1	38.8	---	---	22.1	---
M2 as % of Tot. Tide	81	83.8	78.8	---	---	69.5	---
Sample Count	5125	5125	5125	302	302	606	606

these classes rarely achieve concentrations of C_{max}. Sediment with larger

settling velocities is mixed less in the horizontal and has higher τc, so these

classes are more likely to accumulate near the release point of sediment.

Accumulation can lead to normalized concentrations greater than 1. The original

BBLT released all sediment packets at the origin of the model grid. To represent

releases from a fish cage more realistically, a modification was made to the code

to release sediment packets over the circular area of the cage. The distribution

of release points for the packets was random. The simulations ran for 46 days,

which covered the period when data from both the aquadopp and the RDI

ADCP's were available. For the purpose of the simulation, all input data time

series were interpolated to a common time step of 18 minutes.

3.0 RESULTS

Three ADCP's, two RDI current meters and 1 Nortek aquadopp measured

current velocities from very near bottom to near surface (Table 3). Maximum

velocities were approximately 30 cm s^{-1} and occurred higher in the water column

(Table 3). The root-mean-square velocities decreased near the bottom, reaching

1.0 cm s^{-1} at 0.1 meters above bottom (Table 3). The M2 tide was the dominant

component of tidal flow and accounted for 70-80 % of the total tidal energy

(Table 3). The principal axis of the tide was in the north-south direction along the

axis of Jordan Bay (Fig 3). Significant wave heights measured with RDI ADCP,

67_1 reached a maximum of almost 3 meters, while the period of waves ranged

from approximately 5 to 15 seconds. Directions were from the south. (Fig 4).
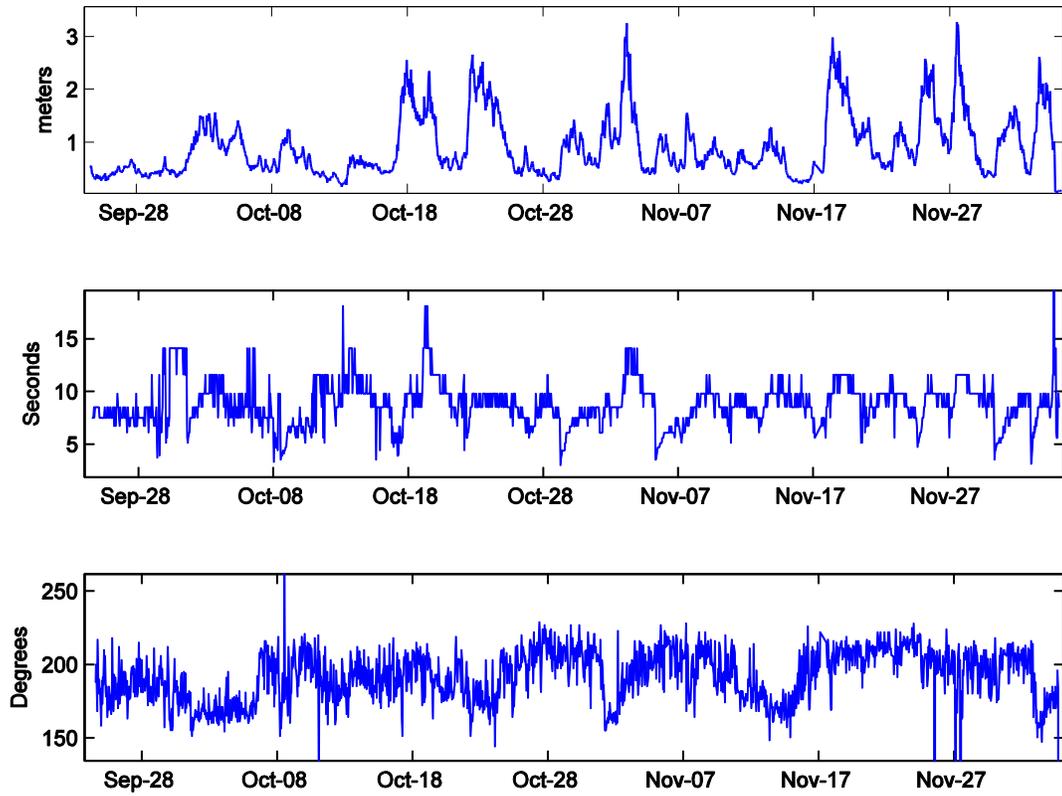
Figure 4. Significant wave height (top), period (middle) and direction (bottom) from which waves are travelling (Deg. True) as recorded by RDI ADCP 67_1.
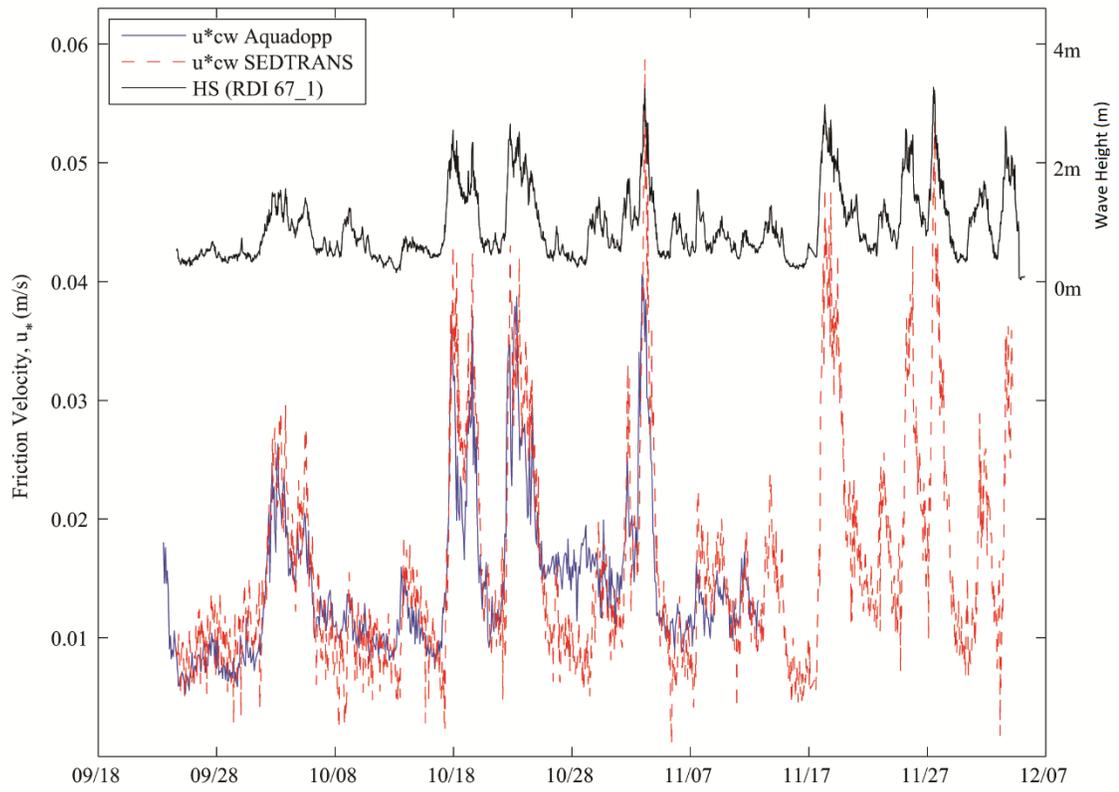
Figure 5. Time series of friction velocity and wave height in Jordan Bay.
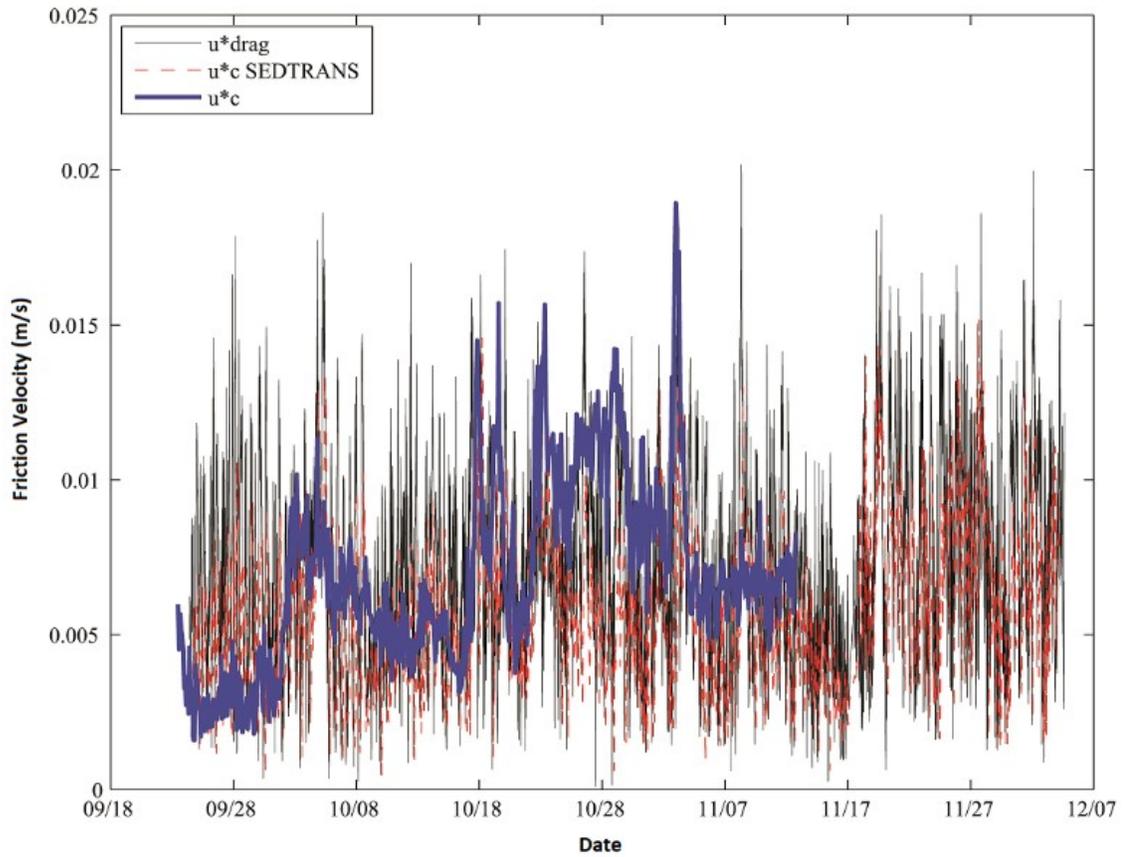
Figure 6. Times series of Jordan Bay currents stress for different methods. Current stress is calculated based on an estimated drag of 0.005, SEDTRANS96 derived and from aquadopp data.
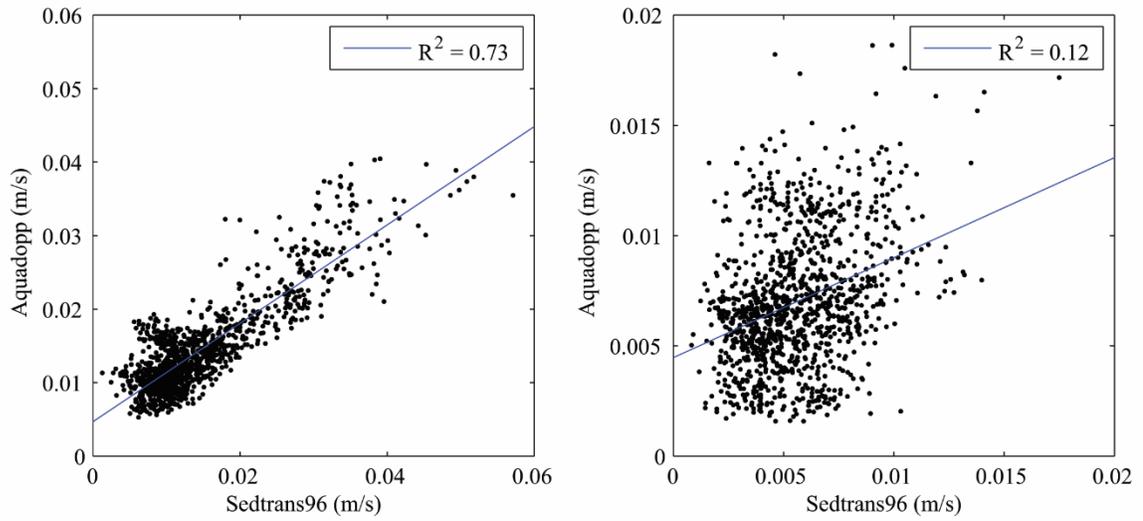
Figure 7. Comparison of values for shear stress estimated with two methods. Wave-current shear velocities are compared on the left, and currents-only shear velocities are compared on the right. Blue lines shows linear regression fit.

Combined wave-current shear velocities, u_{*wc}, were calculated from data

collected from the aquadopp using a wave-current interaction model developed

by Grant and Madsen (1986; 1994)(Fig. 5). Shear velocities also were calculated

with SEDTRANS96 model using the significant wave height, period and direction,

in addition to the current velocities at 5m above bottom from RDI ADCP 67_1

(Fig. 5). Values of shear velocity usually exceeded 0.01 m s^{-1} and reached as

high as 0.05 m s^{-1} (Fig.5). Large increases in combined wave-current shear

velocity corresponded to the major wave events during the deployment. (Fig. 5).

Currents-only friction velocities were calculated to run BBLT in a "current-only"

mode. This mode facilitated comparison with other aquaculture transport models

such as DEPOMOD that use currents only to simulate the transport of

aquaculture waste products. Current friction velocities were calculated using the

aquadopp current data, SEDTRANS96 model and a quadratic drag law with drag

coefficient of 0.005 at 1 meter above bottom (Drozdowksi et al., 2004). Current

friction velocities ranged from just above 0.001 m s-1 to 0.02 m s-1 (Fig. 6). The

wave-current stresses calculated from the aquadopp data and the Grant and

Madsen wave current interaction model were linearly correlated with stresses

calculated with the RDI 67_1 current meter data and SEDTRANS96 model

output (R^2 of 0.73, p < 0.001) (Fig. 7). The correlation between the aquadopp

current shear velocity and SEDTRANS96-calculated shear velocity for currents

only, in contrast, was poor (R^2 = 0.12, p < 0.002). The disagreement between

SEDTRANS96 and aquadopp-calculated shear velocities likely arose from the

fact that the aquadopp measured the currents at roughly 1m above bottom and that SEDTRANS96 used an extrapolation method to calculate bottom currents at 1 meter above bottom based on observed velocities at 5 meters above the bottom.

Time series of bottom concentration, the average of the concentration in the bottom 10 cm below the cage, is variable for the four different size classes (Fig. 8). The fines and flocs disperse rapidly leaving low concentrations most of the time. Fecal waste began to accumulate over days 0 to 7 peaking at day 8 which means all the sediment dumped over the 8 days accumulated near bottom inside the perimeter of the cage. The arrival of wave event 1 cleared the accumulated fecal waste, and no further buildup occurred. For the feed pellets the trend was different. The early buildup occurred and cleared as it did for fecal waste, but accumulation occurred again for days 11-22 and for days 40-45. The accumulation of feed pellets was cleared by the fourth wave event towards the end of the simulation (Fig 8). The time series of the concentration of the four settling classes at 1 meter above bottom was similar to that found in the bottom 10 cm (Fig. 9). Fines and floc time series are almost identical to that in the bottom 10 cm while fecal and pellet waste is zero aside from a small spike on day 39 which corresponded to the fourth wave event and dispersed larger material higher into the water column.

The spatial distributions of the four particle classes after the 46-day simulation differed (Fig 10). Background fines (0.1 mm s^{-1}) dispersed widely. The fines had a nearly uniform distribution of material at very low concentrations

(3-6 x 10^{-6}) in the proximity of the cage with slightly higher values inside the

perimeter of the cage. In the far field plot the e-folding distance, which is the

distance for concentration to drop to 1/e of its peak value in the cage perimeter,

extended about 1.5 km North/South and 0.4 km East/West (Fig 10). This elliptical

pattern is consistent with the M2 tidal ellipse. Tidal excursion (calculated by

taking the half the M2 major axis amplitude in m s-1 over half the tidal period, in

s) gives about 800 m. Hence the elliptical pattern is attributed to the back and

forth motion of the tides.

Flocs (1 mm s^{-1}) also dispersed, leaving a residual mean concentration of

6 x 10^{-4} inside the cage (Fig 10). The e-folding length reached just outside the

cage, indicating this class spent more time near the bottom and did not move as

freely with the tide as the fines. Mean fecal (40 mm s^{-1}) and pellet (100 mm s^{-1})

waste concentrations were 1.2 and 2.7 under the cage, and they were small

outside the cage perimeter (Fig 10). Fecal waste extended ~80 m northwest of

the cage. Waste fecal matter and pellets did not extend outside of an ellipse

1000 m North/South and 0.5 km East/West (i.e. white indicates zero particle

count) during the simulation period (Fig 10).

4.0 Discussion

4.1 Rouse Parameter

Suspended sediment mass is distributed in the a boundary layer as a

function of the Rouse parameter (Fig. 11). The distribution of sediment mass

changes dramatically at Rouse numbers around 1, which represents the
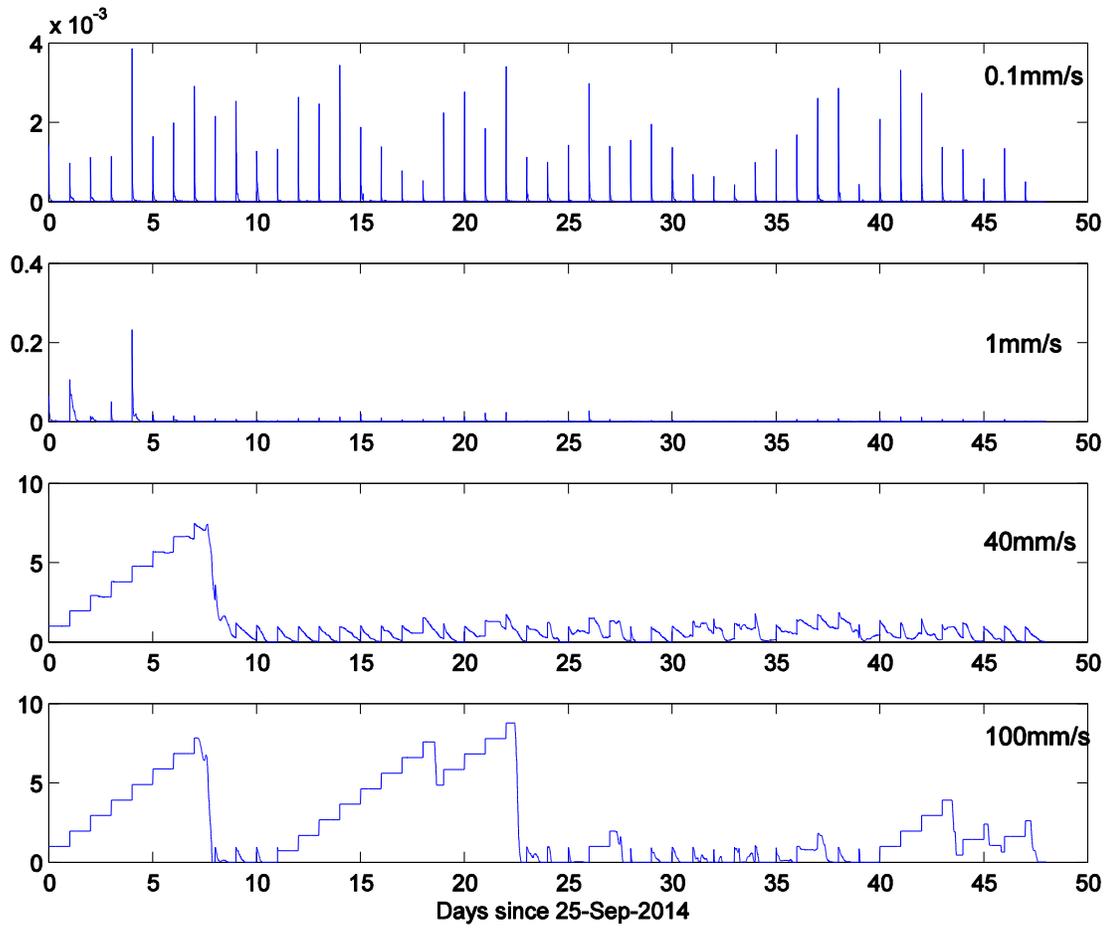
Figure 8. Normalized bottom concentration under fish cage for the 4 sediment classes forced with the Full forcing scenario.
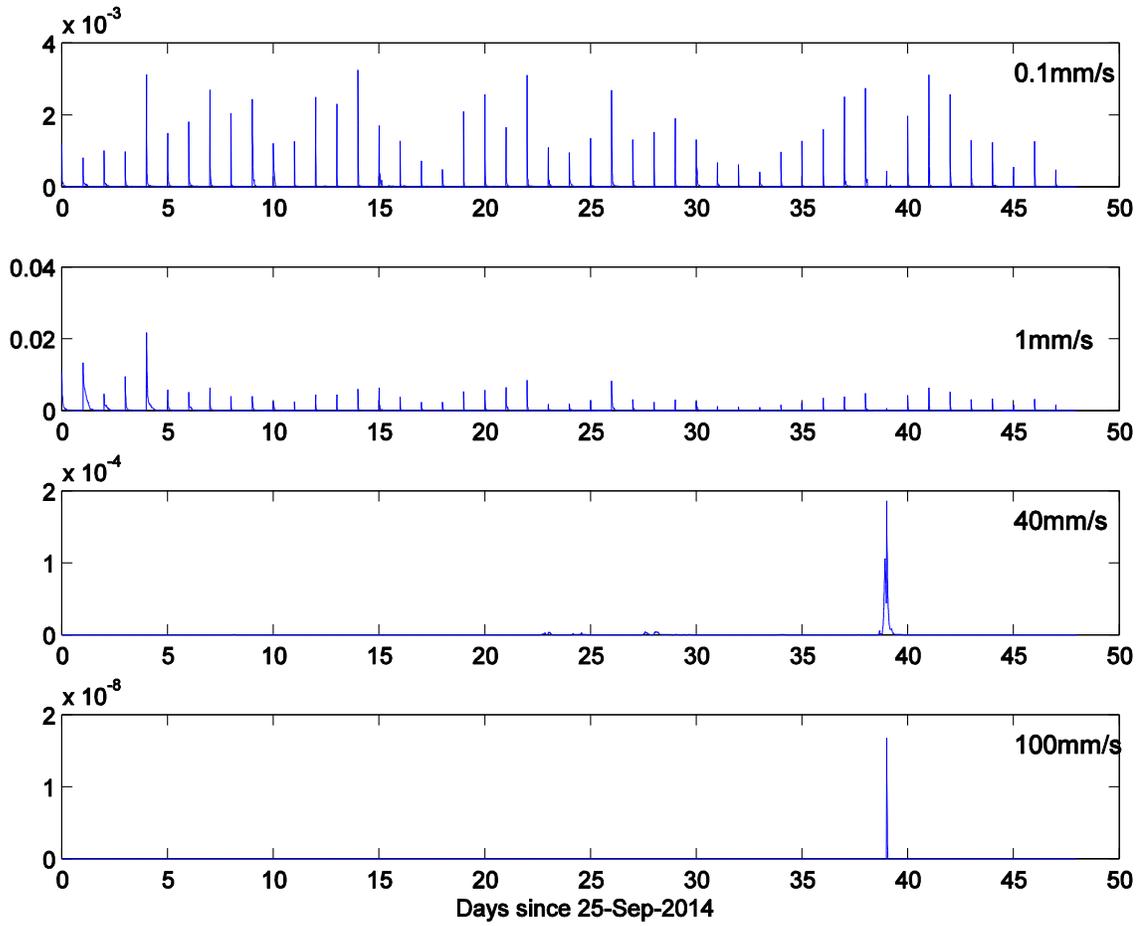
Figure 9. Normalized concentration 1 meter above bottom under fish cage for the 4 sediment classes forced with the Full forcing scenario.
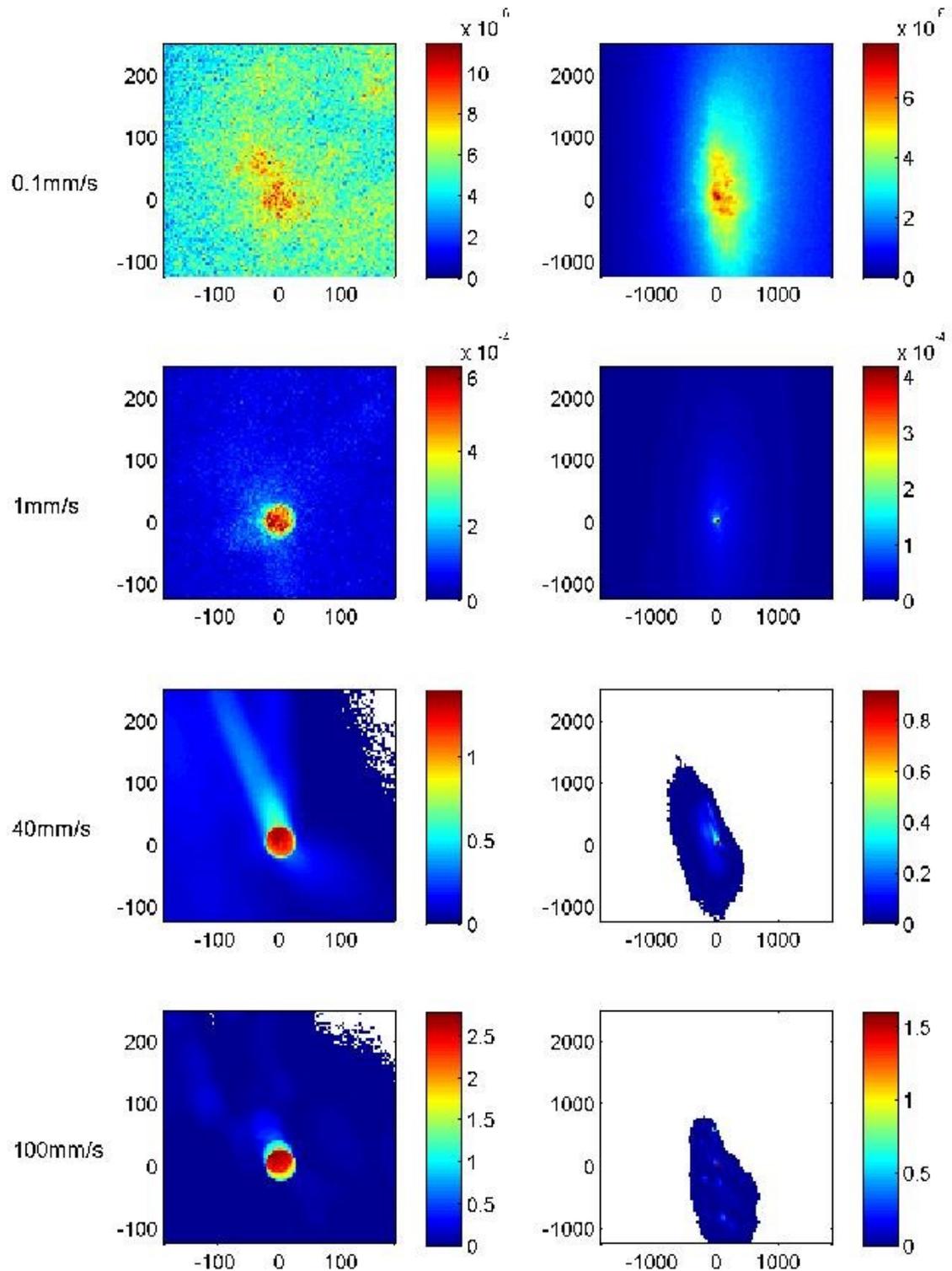
Figure 10. Near field (left) and far field (right) normalized mean bottom concentration for 4 waste class scenarios for the Full forcing simulation. Horizontal units are meters in all spatial distribution plots.
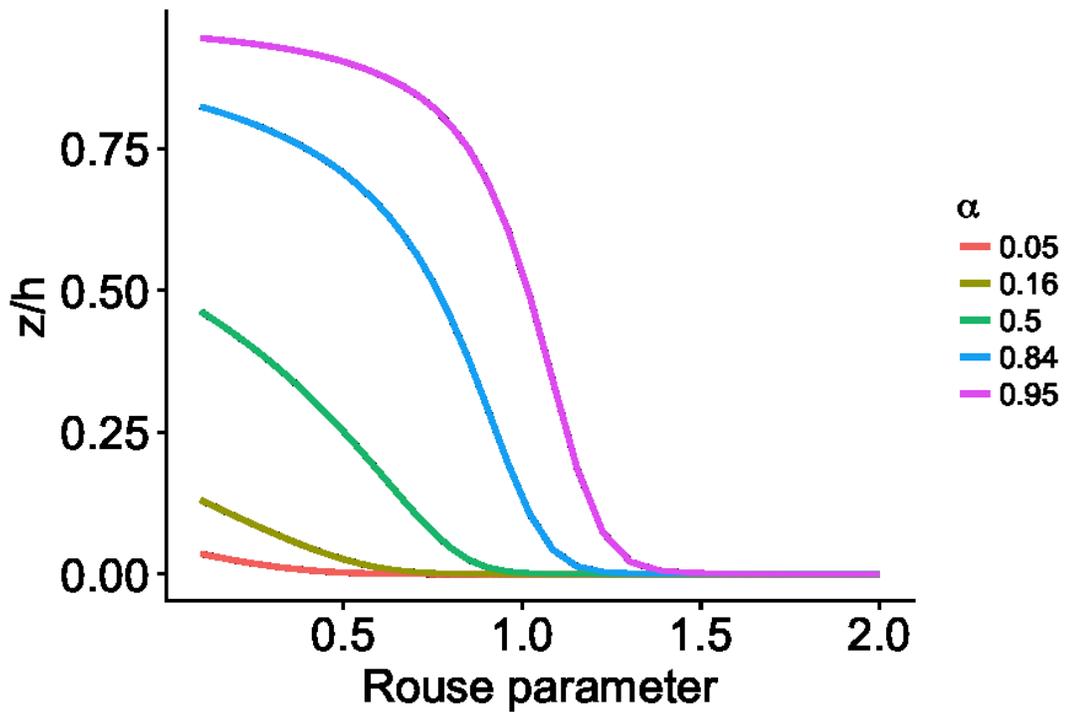
Figure 11. Relative height below which (α*100)% of the suspended sediment resides as a function of the Rouse parameter for a simplified, currents-only flow. When Rouse numbers are less than 1, suspended sediment is mixed by turbulence throughout the boundary layer, so it is exposed to larger horizontal currents speeds and greater shear dispersion. At Rouse numbers greater than 1, sediment is restricted to the nearbed region, where currents are slower and shear dispersion is reduced. A Rouse number of unity therefore is an approximate boundary for determining whether a waste particle class will be dispersed widely or not.

Table 4. Summary of Results. Normalized concentrations and e-folding periods are equal (See Eq. 2 and Section 2.5) hence are listed in same column. Values proceeded by >, indicate that steady state was not reached. Heights are the Mean/Maximum of the center of mass of all sediment.

Settling Velocity (mm/s)	C_0 / C_{max} (normalized) or $\propto/T$	C_0 (g/m³)	Mean/Maximum Height Above Bottom (meters)	Mean/Maximum Rouse Number	Percentage of time at rest
Full forcing scenario					
0.1	3 e-5	0.003	8.9 / 9.0	1.5e-2 / 3.5 e-2	0
1	8 e-4	0.082	7.2 / 8.5	0.15 / 0.35	0
40	1.2	122.4	1.8e-3 / 6.5e-3	5.9 / 14	15
100	2.3	234.6	5.3e-3 / 7.0e-3	14.8 / 34.9	62

boundary between what is typically considered susupended load and bedload (Fig 11). Four size classes of particles were considered in our study and include fines, flocs, fecal material and feed pellets each with their own distinct settling velocity and critical erosion shear velocity. The fines and floc pools in this study have values of the Rouse parmater that are less than 1 (Table 4). As a result, the fines and flocs are suspended throughout much of the boundary layer, which exposes them to higher current speeds and more shear dispersion (Fig 10). The fecal material and feed pellet pools never have Rouse numbers less than one, so they are always remain near the bottom, where currents are slower and shear dispersion is reduced (Table 4). As a result, feed and feces are normally transported in the near field area of aquaculture operations, which extends less than 1 km away (Fig 10).

4.2 Concentration

The maximum initial concentration, Cmax, in the bottom 10 cm directly below the cage was 102 g m^{-3}. The equilibrium concentration of each size class varied by about 5 orders of magnitude with the larger settling velocity and less erodible fecal material and feed pellets building up in the bottom boundary layer near and inside the cage footprint (Table 4, Fig. 8). The fines and floc concentrations extended farther up into the water column and were dispersed over longer distances (Table 4, Figs. 8; 9; 10).

In Jordan Bay and at several other salmon aquaculture sites in Southwest New Brunswick, feeding at salmon aquaculture sites still occurs from a boat that manually pumps feed onto the water surface. For a 50 m diameter cage and at

near peak production, when the fish are feeding at a maximum rate, approximately 50 bags of feed pellets, each with a nominal weight of 20 Kg are used per day.   The input mass used in this study was 20000 g or 20Kg, roughly equivalent to 1 bag of feed pellets and evenly distributed into the 10,000 packets used every day. Based on a feed loss rate of 2%, the amount of pellets that would go uneaten, roughly 1 bag of feed pellets would be lost to the seabed per day based on maximum feeding rates. In addition, feed conversion rates (Reid et al., 2009) could be easily calculated on the numbers used in this study and concentrations for any number of cage sizes and feeding rates by multiplying C_{max} by the input mass divided by the cage volume. For simplicity 20 Kg of mass was also used as the added input of the packets for fines, flocs and fecal material.

4.3 Model Parameters and Uncertainty

The modelling undertaken in this study used currents and waves from one area to map the resuspension and transport of aquaculture derived material, made up of fines, floc, fecal material and feed pellets. This approach is similar to that of DEPOMOD (Cromey et al., 2002a), which uses depth-dependent currents from one location, but unlike DEPOMOD, BBLT used combined wave-current stress to simulate resuspension and transport and limits the total material in suspension. In addition, this study used 4 individual size classes each with their own settling velocity and critical stress for erosion based on previous work (Law et al., 2014, Law et al., 2016), whereas DEPOMOD uses a single value of current velocity to simulate all resuspension.

Broch et al. (2017) recently used the dispersal model DREAM coupled to the hydrodynamic model SINMOD and used 3D spatially explicit currents and waves at three salmon aquaculture farms in Norway to investigate the dispersal and deposition of fish farm wastes and how it related to the Norwegian environmental monitoring program. A coupled 3D sediment particle-hydrodynamic model is better adapted to simulate and resolve current fields in nearshore areas that are affected by changing bathymetry and shorelines, but this approach is computationally demanding. The DREAM model used a number of particle size classes and densities with different settling velocities and like the results here showed that particles smaller than 2 mm with similar settling velocities to that of flocs were transported to distances greater than 2 km in the far field. Bannister et al. (2016) modelled fecal material from salmon aquaculture as a variety of individual size classes each with their own settling velocity based on lab experimentation. Their study used a variety of size classes and validated sediment trap data and increasing organic matter deposition to the far field and attributed it to the far field dispersal of fecal material of different sizes over distances greater than 1km and up to a few km. This study used a value of settling of fecal material of 40 mm s^{-1} which was similar to a median value from the of the study of Bannister et al. and may help explain why fecal material in this study was mostly contained to within 1km of our study area.

Other factors that were not included in this study were processes such as feed pellet disintegration, feed consumption by other species, compaction and dewatering of flocs at the sediment-water interface and subsequent

consolidation, and the erosion differences due to different bottom substrates.

Stewart and Grant (2004) showed that under different flow regimes feed pellets

break down and disintegrate and are usually undetectable within 30 days of

being deposited on the seabed. Models such as DEPOMOD and other sediment

transport models (i.e. sediment module in Regional Ocean Modelling System

(ROMS), Community Sediment Transport Modelling System (CSTMS) allow

settled material to consolidate and become part of the seabed matrix on order of

days if there is no further resuspension. Law et al. (2016) investigated the

effects of bottom type on the resuspension of aquaculture waste and determined

that up to an order of magnitude difference in mass eroded could occur because

of different bottom substrates.

The results from this study have not been validated with field observations

to understand the transport of all the size classes used, although in comparison

to other studies such as that of Broch et al. (2017) and Bannister et al. (2016),

the simplistic approach is promising. First, the fines and flocs used in this study

were transported to similar distances as the flocs used in the study of Broch et al

(2017) using similar settling velocities and densities. Second, the fecal material

and pellets used in our study were confined to the area near the aquaculture site,

suggesting that these are the are the source of increased organic matter in

sediments in the near field zone of influence around the site. This result

contrasts with several DEPOMOD simulations in which the resuspension module

led to transport of pellets and fecal material beyond the near field (Chamerlain

and Stucchi, 2006; Chang et al., 2011; Keeley et al., 2013; Law et al., 2018).

This low dispersal for fast-sinking particles occurs in this study because of the Rouse parametrization of vertical distribution of sediment limits large, fast sinking particles to the near-bed region where currents are lower.

4.4 Implications for Aquaculture Waste Transport and Future Work

In this study combined wave-current stresses were responsible for the resuspension and transport of the larger settling velocity and higher critical erosion stress fecal material and feed pellets in comparison to fines and flocs. It is mainly the fecal material and pellets that are responsible for the depositional footprint of organic matter near and around salmon aquaculture operations. Models that map the depositional footprint from salmon aquaculture operations are increasingly accurate at mapping the depositional footprint but fail to map or predict the transport of material out of the lease domain and into the far field. In lower energy environments, primarily with muddy seabeds, the effects of waves on the bottom are generally negligible, however, in higher energy environments such as the one in this study, with a sandy seabed, the modelling of waves or the combined wave-current stress is required to predict accurately the transport of material (Fig. 8; Fig. 10) such as larger fecal material and feed pellets.

Results of this study suggest that fines and flocs can be transported to the far-field (i.e. km from the site) at low seabed stresses as they are resuspended off the seabed at lower stresses and mixed higher into the water column where they are subject to larger currents. Fines as defined in this study are similar to the single grain sediment population detailed by Law et al., (2014), which includes small pieces of broken down feed or fecal material that have lower

settling velocities and critical stress for erosion. The concentration of fines and flocs are shown to decrease with distance from aquaculture operations but may also provide a mechanism for organics, contaminants such as trace metals from things such as antifouling paints, and other chemicals (e.g. pesticides) that are particle reactive to be transported to the far field.

The findings of this modelling study require validation with field observations. Nonetheless, the BBLT model offers a relatively simple method to increase predictive capacity of waste dispersal around aquaculture operations. More specifically techniques to differentiate waste products from aquaculture operations and to track their movement in the marine environment are needed. One idea may be the use of magnetic particles with distinct sizes and densities representative of different settling velocities and critical stress for erosion. These particles could then be collected on magnetic plates both in the near and far field to validate transport pathways. These findings could lead to better developed monitoring programs and finally to a better answer for the question "If aquaculture derived wastes are moving to the far field and at specific distance-dependent concentrations, what are the possible effects?". These results would help with the sustainability of salmon aquaculture and public awareness and perception.

5.0 Conclusions

The BBLT model was adapted to examine its suitability for use to predict the dispersal of salmon aquaculture waste products to the near and far field. The Rouse parameter governs the distribution of suspended sediment size classes in

the boundary layer and values greater than or less than 1 determine if material will be transported near the bed where current speeds are low or more evenly distributed throughout the water column where current speeds are higher. Although simplistic in approach, using 4 size classes with differing settling velocities and critical erosion shear stresses, the results in terms of spatial distribution of waste products are similar to more sophisticated coupled 3D hydrodynamic dispersal models. The modelling approach in this study clearly shows the importance of parameterizing wave energy for resuspension and transport especially for the larger size classes of fecal material and feed pellets. The refinement of models in future work will help with salmon aquaculture sustainability efforts.

Chapter 6 - Conclusions

The salmon aquaculture industry in Canada has been around since the 1970s and for the last 30 years scientists have been studying environmental impacts in both the near and, to a lesser extent, the far field. With the entrance of industrial activities into an environment, the questions of, 1) how concentrated, 2) how widespread, and 3) how deleterious are any introduced materials need to be addressed to obtain both social license and sustainability. Early research established that fast settling feed and intact fecal material falls almost immediately under and adjacent to salmon farms, and these materials are responsible for the observed organic enrichment that affects the seabed within several hundred meters around operations. Larger uncertainty surrounds subsequent reworking and transport of wastes to the far field, due to inadequate understanding of the particle packaging of degraded wastes and of the variables that affect resuspension, as well as overly simplistic models of sediment resuspension and transport. The goal of this thesis was to improve understanding of far-field transport of aquaculture wastes with investigations of the in-situ packaging of particulate material in the vicinity of farming operations and of how substrate and organic matter loading affect erodibility of wastes on the seafloor. With knowledge from these field and laboratory studies, a proof-of-concept modelling study was used to address the primary shortcomings of DEPOMOD, a commonly used model of aquaculture waste transport.

A review of the biophysical properties of salmonid feces and implications for waste dispersal models by Reid et al. (2009) stated that information in the

literature was limited on particle size, density, and the settling velocity of material at aquaculture cage environments. From the Chapter 2 study (Law et al. 2014), at an active salmon aquaculture site, flocs (> 133 μm) dominated the volume distribution of particles. Average floc settling velocities were approximately 1 mm s^{-1}. The estimated floc fractal dimension, which describes the packaging of material in suspension, was higher in this study than observed in previous studies in the marine environment (Mikkelsen et al. 2006; 2007, Curran et al. 2007; Hill et al. 2011; Hill et al. 2013). In addition, the density of the component particles in the flocs was lower in this study compared to other floc populations measured in a variety of marine environments (Mikkelsen et al. 2006; 2007, Curran et al. 2007; Hill et al. 2011; Hill et al. 2013). Interestingly, they were similar to densities of aquaculture waste material described previously in laboratory studies (Ogunkoya et al 2006; Moccia et al. 2006). These observations provided indirect support to the hypothesis that particles associated with finfish aquaculture activities are incorporated into easily transported flocs. Based on these findings, flocs should be considered as a possible transport vector in models of dispersion of aquaculture wastes.

Cromey et al. (2002a,b) introduced resuspension into the DEPOMOD model of dispersal of finfish aquaculture wastes. The model was simplistic, because it applied only one critical erosion shear stress, regardless of the characteristics of waste particles or the underlying substrate. It also did not consider the effect of waves on resuspension. DEPOMOD with resuspension included had mixed success in terms of being able to match waste accumulation

and associated altered geochemistry in the seabed near farm sites (Cromey et al., 2002; Chamberlain and Stucchi, 2007; Chang et al., 2011), suggesting that its particle and seabed parameterizations are too simple. For example, aquaculture in Canada first was situated in fjords in British Columbia and over soft muddy bottoms in south-west New Brunswick. With the expansion of finfish aquaculture into parts of Newfoundland and Nova Scotia over hard bottoms (i.e. rock) and sandy bottoms respectively, the single values of critical erosion shear stress and the erosion parameter in DEPOMOD may be inadequate for quantifying resuspension on the different bottom substrates .

Results in Chapter 3 showed that bottom sediment substrate plays a large role in the erodibility of aquaculture waste material. Comparison of 5 different bottom substrates indicated that more wastes were eroded from muddy substrates than from sandy and gravel substrates. An order of magnitude difference existed in the cumulative mass eroded of waste fecal material, implying that the erosion parameter, M, is different over a mud versus a cobble seabed. A seabed composed of sand was characterized by cumulative mass erosion between that of cobble and mud. The critical erosion shear stress, τc , was determined to be between 0.01 and 0.02 Pa in this study, which was similar to the value used by Cromey et al. (2002b) in DEPOMOD. The erosion experiments in our study, however, also showed that little to no erosion of waste solids or bottom substrate occurred above 0.32 Pa, which was evidenced by low turbidity and therefore unlike DEPOMOD, the erodibility parameter, M, changed with time. In all but the erosion experiments conducted on a muddy seabed,

there was evidence that some of the waste solids remained stored in the substrate even after completion of the erosion experiments. On average > 97 % of salmon waste material added to the mud substrate was eroded, but less than 25% of the material added to the cobble substrate was removed. The substrates composed of sand averaged about 65% removal from the bed. In addition, erodibility studies carried out using different sized feed pellets showed large differences in τ_c. Results also indicated that higher critical erosion shear stress values than the single value used by DEPOMOD are required to model the transport of feed pellets . In summary, waste fecal material and feed pellets need to be treated as separate entities in aquaculture waste transport models and substrate type needs to be considered in the choice of model parameters.

Chapter 4 described in-situ investigations into resuspension differences between different bottom types (mud vs sand), and it explored how the accumulation of particulate waste products in the sediment around farms changed resuspension dynamics. This study, based on observations of mass eroded at aquaculture sites from cohesive (mud) and non-cohesive (sand) farm sites, showed several important factors that should be considered in aquaculture waste transport modelling. First, the organic content of bed sediments affects erosion. Second, organic content of bed sediments near aquaculture operations increases when fish are present. This accumulation of organic matter leads to lower erosion rates, which creates a positive feedback. The perturbation caused by the addition of fish, leads to increased organic matter concentration in the bed sediment, which leads to decreased erosion of bed material, which leads to a

greater increase in organic matter until a maximum is reached or the organic supply is turned off. Third, the effect of increasing organic matter in bed sediments is diminished but does not vanish in non-cohesive sediments. Finally, waves at more exposed sites such as Jordan Bay can supply the erosive force to resuspend waste materials that are subsequently transported by currents.

Chapter 5 examined the potential of BBLT as an alternative modelling framework to DEPOMOD. Like DEPOMOD, BBLT takes time series data from a single point to simulate dispersal, so it is not expensive to either build or run a simulation. Unlike DEPOMOD, BBLT can use combined wave-current stress to simulate resuspension and transport, and it can alter the critical stresses for erosion and the erosion parameter. Most importantly, however, unlike DEPOMOD, BBLT simulates the different vertical distributions of different particles classes in the boundary layer which leads to greater dispersal of smaller, slower sinking particles and limited dispersal of larger, faster sinking particles.

The BBLT model produced dispersal patterns of different size classes that were consistent with previous work. First, the fines and flocs, each with their own transport parameters, were transported to the far field around the farm site. Second, the large, fast settling material such as the pellets (100 mm s^{-1}) and fecal material (40 mm s^{-1}) were confined to the area near the farm site and were not consistently transported away as has occurred in several DEPOMOD simulations (Chang et al., 2011; Keeley et al., 2013). This result is attributable to the settling-velocity dependent vertical distribution of particles simulated by

BBLT. Large, fast sinking particles are limited to the near-bed region where currents are lower and therefore most of the transport is reduced.

Use of BBLT as a predictive tool for waste dispersal will require validation of simulations with in situ studies of dispersal of waste particles of different sizes. Techniques to differentiate waste products from aquaculture operations and to track their movement in the marine environment are needed.   One idea is use of magnetic particles with distinct sizes and densities representative of different settling velocities and critical stress for erosion. These particles could be released at a site and collected on magnetic plates both in the near and far field to examine transport distances and distributions.

The goal at the outset of this project was to investigate and quantify the transport of aquaculture waste products to the far field around farm sites. The work has demonstrated that the likeliest mode of transport to the far field is by incorporation of wastes into particles that have settling velocities of order 1 mm s^{-1} or less. These particles sink slowly enough to be transported high in the water column as suspended load, leading directly to enhanced shear dispersion. The work also has demonstrated that the properties of the substrate affect the escape of fines from a site. Coarse-grained sediments have potential to retain wastes in interstial pore spaces, and accumulation of organic matter in sediments can cause decreases in erodibility. Finally, as aquaculture operations move to sites that are more exposed to wave energy, it is essential that wave resuspension be incorporated into models that predict dispersion.

Quantifying far field effects clearly requires more research into the concentration and potentially deleterious effects of aquaculture wastes. This research has shown how to transport material to the far field, but it sheds no light on potential risks of this transport. Continued expansion of open net pen aquaculture demands widespread acceptance by coastal communities, and that acceptance will only come if risks are realistically addressed.

References

Aquaculture Canada. 2007. The aquaculture association of Canada.
www.aquacultureassociation.ca

Agrawal, Y.C., Pottsmith, H.C., 2000. Instruments for particle size and settling
velocity observations in sediment transport. Marine Geology 168 (1-4), 89-
114.

AMEC E&E Division, 2007. Physical oceanography input to the effluent modelling
study for the long harbour commercial processing plant environment
assessment. Oceanographic component: Effluent solid waste dispersion
modelling, short and long term fate. Report prepared for Voisey Bay Nickel
Ltd.

AMEC E&E Division, 2011. Labrador – Island Transmission Link. Strait of Belle
Isle: Oceanographic Environment and Sediment Modelling. Report
prepared for Nalcor Energy Ltd.

Amos, C.L., VanWagoner, N.A., Daborn, G.R., 1988. The influence of subaerial
exposure on the bulk properties of fine-grained intertidal sediment from
Minas Basin, Bay of Fundy. Estuarine and Costal Shelf Science, 27, 1-13.

Amos, C.L., Daborn, G.R., Christian, H.A., Atkinson, A., Robertson, A., 1992. In-
situ erosion measurements on fine grained sediments from the Bay of
Fundy. MarineGeology. 108, 175-196.

Amos, C.L., Feeney, F., Sutherland, T.F., Luternauer, J.L., 1997. The stability of
fine-grained sediments from the Fraser River Delta. Estuarine, Coastal,
and Shelf Science. 45, 507-524.

Bannister, R.J, Johnsen, I.A., Hansen, P.K., Kutti, T., Asplin, l., 2016. Near and
far-field dispersal modelling of organic waste from Atlantic salmon
aquaculture in fjord systems. ICES Journal of marine Science, 73 (9),
2408-2419.

Black, K.S., Tolhurst, T.J., Paterson, D.M., Hagerthy, S.E., 2002. Working with
natural cohesive sediments. Journal of Hydraulic Engineering 128, 2-8.

Boss, E., Slade, W.H., Hill, P.S., 2009a. Acceptance angle effects on the beam
attenuation in the ocean. Optics Express, 17 (3), 1535-1550, doi:
10.1364/OE.17.001535.

Boss, E., Slade, W., Hill, P., 2009b. Effect of particulate aggregation in aquatic
environments on the beam attenuation and its utility as a proxy for
particulate mass. Optics Express, 17(11), 9408-9420, doi:
10.1363/OE.17.009408.

Bothner, M.H., M. Buchholtz ten Brink, and F.T. Manheim, 1998. Marine Environmental Research, 45:127-155.

Broch, O.J., Daae, R.L., Ellingsen, I.H., Nepstad, R., Bendiksen, E.A., Reed, J.L., Senneset, G., 2017. Spatiotemporal dispersal and deposition of fish farm wastes: A model study from central Norway. Marine Fisheries, Aquaculture and Living Resources, Frontiers in Marine Science, 4:199, 1-15, doi:10.3389/fmars.2017.00199.

Chamberlin, J., Stucchi, D., 2007. Simulating the effects of parameter uncertainty on waste model predictions of marine finfish aquaculture. Aquaculture, 272: 296-311.

Chang, B.D., Page, F.H., Losier, R.J., Mccurdy, E.P., MacKeigan, K.G. 2011. Characterization of the spatial pattern of benthic sulfide concentrations at six salmon farms in south-western New Brunswick, Bay of Fundy. Canadian Technical Report of Fisheries and Aquatic Sciences, 2915, 1-30.

Chen, Y.S., Beveridge, M.C.M., Telfer, T.C., 1999. Settling rate characteristics and nutrient content of the faeces of Atlantic salmon, Salmo salar, L. and the implications for modelling of solid waste dispersion. Aquaculture Research, 30, 395-398.

Chen, C., Packman, A.I., Zhang, D., Gaillard, J.F., 2010. A multiscale investigation of interfacial transport, pore fluid flow and fine particle deposition in a sediment bed. Water Resources Research, 46, 413-427.

Cranford, P. J., Gordon, Jr., D. C., Hannah, C. G., Loder, J. W., Milligan, T. G., Muschenheim, D. K., Shen, Y., 2003. Modelling potential effects of petroleum exploration drilling on northeastern Georges Bank scallop stocks. Ecological Modelling 166,19 - 39.

Cranford, P.J., Armsworthy, S.L., Mikkelsen, O.A, Milligan, T.G., 2005. Food acquisition responses of the suspension-feeding bivalve Plactopecten magallanicus to the flocculation and settlement of a phytoplankton bloom. Journal of Experimental Marine Biology and Ecology, 326:128-143

Cranford, P.J., Brager, L., Wong, D., 2017. A dual indicator approach for monitoring benthic impacts from organic enrichment with test application near Atlantic salmon farms. Marine Pollution Bulletin, DOI:10.1016/j.marpolbul.2017.07.049.

Cromey, C.J., Thomas, T.D.,Black, K.D., 2002a. DEPOMOD-Modeling the deposition and biological effects of waste solids from marine cage farms. Aquaculture, 214: 211-239.

Cromey, C.J., T.D. Nickell, K.D. Black, P.G. Provost, Griffiths, C.R., 2002b. Validation of a fish farm waste resuspension model by use of a particulate tracer discharged from a point source in a coastal environment. Estuaries, 25: 916 – 929.

Curran, K.J., Hill, P.S., Milligan, T.G., Mikkelsen, O.A., Law, B.A., Durrieu de Madron, X., Bourrin, F., 2007. Settling velocity, effective density, and mass composition of suspended sediment in a coastal bottom boundary layer, Gulf of Lions, France. Continental Shelf Research, 26 (17-18), 2299-2318, doi: 10.1016/j.csr.2006.07.018

Dean, R.J., Shimmield, T.M., Black, K.D., 2007. Copper, zinc and cadmium in marine cage fish farm sediments: an extensive survey. Environmental Pollution, 145, 84-95.

deGelleke, L., Hill, P.S., Kineast, M., Piper, D.J.W, 2013. Sediment dynamics during Heinrich event H1 inferred from grain size. Marine Geology, 336, 160-169.

Dickhudt, P.J., Friedrichs, C.T., Sanford, L.P., 2010. Mud matrix solids fraction and bed erodibility in the York River estuary, USA and other muddy environments. Continental Shelf research, 31, Supplement, S3-S13.

Droppo, I., Jaskot, C., Nelson, T., Milne, J., Charlton, M., 2007. Aquaculture Waste Sediment Stability: Implications for Waste Migration. Water, Air and Soil Pollution, 183, 59-69.

Drozdowski, A., Hannah, C., Tedford., T., 2004. BBLT Version 7.0 user's manual. Can. Tech. Rep. Hydrogr. Ocean Sci. 240: vi + 69 pp. Available from www.mar.dfompo.gc.ca/science/ocean/coastal_hydrodynamics/WEBBBLTgui/BBLTgui.html

Drozdowski, A. 2009. BBLT3D, the 3D Generalized Bottom Boundary Layer Transport Model: Formulation and Preliminary Applications. Can. Tech. Rep. Hydrogr. Ocean Sci. 263: vi + 32 pp.

Dupont, Frédéric, Charles G. Hannah and David Greenberg. 2005. Modelling the Sea Level in the Upper Bay of Fundy. Atmos.-Ocean. 43(1), 33-47.

Eisma, D., 1986. Flocculation and de-flocculation of suspended matter in estuaries. Netherlands Journal of Sea Research, 20, 183-199.

Einstein, H.A., 1950. The bed-load function for sediment transportation in open channel flows. United States department of Agriculture, Technical Bulletin, No. 1026.

FAO. 2007. Food and Agriculture Organization. www.fao.org.

FAO. 2012. Food and Agriculture Organization. www.fao.org.

FAO. 2016. Food and Agriculture Organization. www.fao.org.

Findlay, R.H., Watling, L., 1994. Toward a process level model to predict the effects of salmon net-pen aquaculture on the benthos. In: Modelling Benthic Impacts of Organic Enrichment from Marine Aquaculture. Canadian Technical Report of Fisheries and Aquatic Sciences, no. 1949, pp. 47-77.

Fox, J.M., Hill, P.S., Milligan, T.G., Boldrin, A., 2004. Flocculation and sedimentation on the Po River Delta. Marine Geology, 203, 95-107.

Fugate, D.C., Friedrichs, C.T., 2003. Controls on suspended aggregate size in partially mixed estuaries. Estuarine Coastal and Shelf Science 58 (2), 389–404.

Grant, J., Gust, G., 1987. Prediction of coastal sediment stability from photopigment Content of mats of purple sulphur bacteria. Nature, 330, 244-246.

Grant, J, Emerson, C.W., Hargrave, B.T., Shortle, J.L., 1991. Benthic oxygen consumption on continental shelves off Eastern Canada. Continental helf Research, 11, 1083, 1097.

Grant, W. D., Madsen, O. S., 1986. The continental shelf bottom boundary layer. Annual Review of Fluid Mechanics 18, 265-305.

Graydon, C.M., Robinson, S.M.C., Scheibling, R.E., Cooper, A.J., 2012. Canthaxanthin as a potiential tracer of salmon feed in mussels (Mytilus spp.) and sea urchins (Strongylocentrotus droebachiensis). Aquaculture, 367, 90-97.

Gust, G., Muller, V., 1997. Interfacial hydrodynamics and entrainment functions of currently used erosion devices. In Burt, N. Parker, R. Watts, J. (Eds.), Cohesive Sediments. Wiley, Chichester, UK, pp. 149-174.

Hannah, C. G., Shen, Y., Loder, J. W., Muschenheim, D. K., 1995. BBLT: Formulation and exploratory applications of a benthic boundary layer transport model. Can. Tech. Rep. Hydrogr. Ocean Sci. 166: vi + 52 pp.

Hannah, C. G., Drozdowski, A., 2005. Characterization of drift and dispersion of drilling mud on three offshore banks. Marine Pollution Bulletin 50, 1433-1443.

Hargrave, B.T., Duplisea, D.E., Pfeiffer, E., Wildsih, D.J, 1993. Seasonal-changes in benthic fluxes of dissolved oxygen and ammonium associated with marine cultured Atlantic salmon. Marine Ecology Progress Series, 96, 3, 249-257.

Harris, J.R., Gorley, R.N., Bartlett, C.A., 1993. ECoS Version 2 – A user manual. Plymouth Marine Laboratory, U.K.

Heuttel, M, Ziebis, W., Forster, S., 1996. Flow-induced uptake of particulate matter in permeable sediments. Limnology and Oceanography, 41, 309-322.

Hill, P.S., 1996. Sectional and discrete representation of floc breakage in agitated suspensions. Deep Sea Research Part 1: Oceanographic Research Papers, 43 (5), 679-702.

Hill, P. S., Voulgaris, G., Trowbridge, J.H. 2001. Controls on floc size in a continental shelf bottom boundary layer. Journal of Geophysical Research 106, 9543-9549.

Hill, P.S., Syvitski, J.P., Cowan, E.P., Powell, R.D., 1998. In situ observations of floc settling velocities in Glacier Bay, Alaska. Marine Geology, 145 (1-2), 85-94.

Hill, P.S., Boss, E., Newgard, J.P., Law, B.A., Milligan, T.G., 2011. Observations of the sensitivity of beam attenuation to particle size in a coastal bottom boundary layer. Journal of Geophysical Research 116, C02023. http://dx.doi.org/10.1029/ 2010JC006539.

Hill, P.S., Newgard, J.P., Law, B.A. , Milligan, T.G., 2013. Flocculation on a muddy intertidal flat in Willapa Bay, Washington, Part II: Observations of suspended particle size in a secondary channel and adjacent flat, *Continental Shelf Research,* doi: 10.1016/j.csr.2012.06.006.

Jago, C.F., Jones, S.E., Sykes, P., Rippeth, T., 2006. Temporal variation of suspended particulate matter and turbulence in a high energy, tide-stirred, coastal sea: relative contributions of resuspension and disaggregation. Continental Shelf Research, 26, 2019-2028.

Kach, D.J., Ward, J.E., 2008. The role of marine aggregates in the ingestion of picoplanktonsize particles by suspension-feeding molluscs. *Marine Biology,*153, 797-805.

Keeley, N.B., Cromey, C.J., Goodwin, E.O., Gibbs, M.T., MacLeod, C.M., 2013. Predictive depositional modelling (DEPOMOD) of the interactive effect of current flow and resuspension on ecological impacts beneath salmon farms. Aquaculture Environment Interactions, 3, 275-291. doi: 10.3354/aei00068.

Khelifa, A., Hill, P.S., 2006. Models for effective density and settling velocity of flocs. Journal of Hydraulic Research, 44, 390-401.

Kranck, K. 1973. Flocculation of suspended Sediment in the Sea. Nature, 246, 348-350.

Kranck, K., Milligan, T.G., 1979. The use of Coulter Counters in studies of particle size distributions in aquatic environments. Report Series/ BI-R-79-7/November, p. ii+48.

Kranck, K., Milligan, T.G. 1985. Origin of Grain Size Spectra of Suspension Deposited Sediment. Geo-Marine Letters, 5, 61-66.

Kristensen, E., 1990. Characterization of biogenic organic matter by stepwise thermongravity (STG). Biogeochemistry, 9, 135-159.

Krumbein, W.E., Paterson, D.M., Stal, L.J, editors. 1994. Biostabilization of Sediments. Oldenburg, Germany, Verlag.

Law, B.A., Hill, P.S., Milligan, T.G., Curran, K.J., Wiberg, P.L., Wheatcroft, R.A., 2008. Size sorting of fine-grained sediments during erosion: results from the western Gulf of Lions. Continental Shelf Research (In Press). dx. Doi.org/ 10.1016/j.csr.

Law, B.A, Hill, P.S., Maier, I., Milligan, T.G., Page, F, 2014. Size, settling velocity and density of small suspended particles at an active salmon aquaculture site. Aquaculture Environment Interactions, 6, 29-42, doi: 10.3354/aei00116.

Law, B.A., Hill, P.S., Milligan, T.G., Zions, V.S., 2016. Erodibility of aquaculture waste from different bottom substrates. Aquaculture Environment Interactions, 8, 575-584. doi:10.3354/aei00199.

Law, B.A., Hill, P.S., 2018. Spatial and temporal erodibility at areas of active salmon aquaculture: Details from a sandy and a muddy seabed site. Submitted to Aquaculture Environment Interactions.

Li, M. Z., Amos, C. L., 2001. SEDTRANS96: The upgraded and better calibrated sediment-transport model for continental shelves. Comput. Geosci. 27, 619-645.

Li, Z.K., Lee, K., King, T., Niu, H.B., Boufadel, M.C., Venosa, A.D., 2011. Application of entropy analysis of in-situ droplet size spectra in evaluation of oil chemical dispersion efficacy. Marine Pollution Bulletin, 62 (10), 2129-2136.

Maa, J.P.Y., Sanford, L.P., Halka, J.P., 1998. Sediment resuspension characteristics in Baltimore Harbour, Maryland. Mar. Geol. 146, 137-145.

Madsen, O.S., 1994. Spectral wave–current bottom boundary layer flows. In: Coastal Engineering 1994. Proceedings of the 24th International Conference on Coastal Engineering Research Council, Kobe, Japan, pp. 384–398.

McCave, I.N. 1984. Size spectra and aggregation of suspended particles in the deep ocean. Deep-Sea Research, 31 (4), 329-352.

Mikkelsen, O.A., Milligan, T.G., Hill, P.S., Moffatt, D., 2004. INSSECT - an instrumented platform for investigating floc properties close to the seabed. Limnology and Oceanography-Methods 2, 226-236.

Mikkelsen, O.A., Hill, P.S., Milligan, T.G., Chant, R.J., 2005. In situ particle size distributions and volume concentrations from a LISST-100 laser particle sizer and a digital floc camera. Continental Shelf Research 25 (16), 1959-1978.

Mikkelsen, O.A., Hill, P.S., Milligan, T.G., 2006. Single-grain, microfloc, and macrofloc volumn observations observed with a LISST-100 and digital floc camera. Journal of sea research, 55, 87-102.

Mikkelsen, O.A., Curran, K.J., Hill, P.S., Milligan, T.G., 2007. Entropy analysis of in-situ particle size. Estuarine and Coastal shelf Science, 72(4), 615-625.

Milligan, T.G., Kranck, K., 1991. Electroresistance particle size analyzers. In: Syvitski,   J.P.M. (Ed.), Principles, Methods, and Application of Particle Size Analysis. Cambridge University Press, New York, pp. 109 -118.

Milligan, T.G., Kranck, K., 1992. Characteristics of suspended particles at an 11 hour anchor station in San Francisco Bay, California. Journal of Geophysical Research, 97 (C7), 11373 – 11382.

Milligan, T.G. and D.H. Loring, 1997. The effect of flocculation on the size distributions of bottom sediment in coastal inlets: implications for contaminant transport. Water Air Soil Pollution 99, 33-42.

Milligan, T.G., Kineke, G.C., Blake, A.C., Alexander, C.R., Hill, P.S., 2001. Flocculation and sedimentation in the ACE basin, South Carolina. Estuaries 24 (5), 734–744.

Milligan, T.G. and B.A. Law. 2005. The effect of marine aquaculture on fine sediment dynamics in coastal inlets. The Handbook of Environmental Chemistry, 5, 239-251. Springer, Berlin.

Milligan, T.G., Hill, P.S., Law, B.A., 2007. Flocculation and the loss of sediment from river plumes. Continental Shelf Research, 27, 309-321.

Milligan, T.G., Law, B.A., 2013. Contaminants at the sediment-water interface: Implications for Environmental Impact Assessment and Effects Monitoring. Journal of Environmental Science and Technology, 47(11), 5828-5834. doi: 10.1021/es3031352.

Moccia, R.D., Bevan, D.J., Reid, G.K., 2007. Composition of feed and fecal waste from commercial trout farms in Ontario: physical characterization and relationship to dispersion and depositon modeling. Technical Report for Environment Canada. Ontario Sustainable Aquaculture Working Group. University of Guelph, pp. 21.

Niu, H., Drozdowski, A., Lee, K., Veitch, B., Reed, M., Rye, H., 2014. Modeling the transport of drilling muds: comparison of BBLT and ParTrack models. Oceans - St. John's, 2014. IEEE. DOI: 10.1109/OCEANS.2014.7003015

Ogunkoya, A.E., Page, G.I., Adewolu, M.A., Bureau, D.P., 2006. Dietary incorporation of soybean mael and exo-genous enzyme cocktail can affect physical characteristics of faecal material egested by rainbow trout (Oncorhynchus mykiss). Aquaculture, 254, 466-475.

Otsu, N. (1979), A threshold selection method from gray‐level histograms, IEEE Trans. Syst. Man Cybern., 9(1), 62–66, doi:10.1109/TSMC.1979.4310076.

Panchang, V., Cheng, G., Newell, C., 1997. Modeling hydrodynamics and aquaculture waste transport in coastal Maine. Estuaries 20: 14-41.

Parthenadies, E., 1962. A study of erosion and deposition of cohesive soils in salt water. University of California, Berkely, Ph.D., Thesis, pp. 182.

Petrie, B., Bugden, G., Tedford, T., Geshelin, Y., Hannah, C., 2004. Review of the physical oceanography of Sydney Harbour. Can. Tech. Rep. Hydrogr. Ocean Sci. 215: vii + 43 pp.

Reid, G.K., Liutkus, M., Robinson, S.M.C., Chopin, T.R., Blair, T., Lander, T. Mullen, J., Page, F., Moccia, R.D. 2009. A review of the biophysical properties of salmonid faeces: implications for aquaculture waster dispersal models and integrated multi-trophic aquaculture. Aquaculture Research, 40, 257-273.

Rouse, H., 1937. Modern concepts of the mechanics of turbulence. Trans. Am. Soc. Civ. Eng. 102, 463-543.

Rye, H., Reed, M., Frost, T. K., Utvik, T. I. R., 1998. Comparison of the ParTrack mud/cuttings release model with field data based on use of synthetic-based drilling fluids. Environmental Modelling & Software 21, 190-203.

Sanford, L.P., Panageotou, W., Halka, J.P., 1991. Tidal resuspension of sediments in northern Chesapeake Bay. Marine Geology, 97, 87-103.

Sanford, L.P., Maa, J.P.Y., 2001. A unified erosion formulation for fine sediments. Marine Geology, 179, 9-23.

Sanford, L.P., 2008. Modeling a dynamically varying mixed sediment bed with erosion, deposition, bioturbation, consolidation, and armoring. Computers and Geosciences, 34, 1263-1283.

Sara, G., Scilipoti, D., Milazzo, M., Modica, A. 2006. Effects of fish farming wastes on sedimentary and particulate organic matter origin in a Southern Mediterranean area (Gulf of Castellammare, Sicily): A multiple stable isotope study. Aquaculture 234, 199-213.

Schaaf, E., Grenz, C., Pinazo, C., 2006. Field and laboratory measurements of sediment erodibility. Journal of Sea Research, 55, 30-42.

Schendel, K.E., Nordstrom, S.E., Lavkulich, L.M. 2004. Floc and sediment properties and their environmental distribution from a marine fish farm. Aquaculture Research, 35, 483-493.

Sheldon, R. W., A. Prakash, and W. H. Sutcliffe, Jr. 1972. The size distribution of particles in the ocean. Limnology and Oceanography 17, 327-339.

Shields, A., 1936. Application of the theory of similarity and turbulence research to bedload movement. Mitt. Preuss. Verssuchsanst Wasserbau Schiffbau 26, 5-24.

Smith, J.N., Yeats, P.A., Milligan, T.G. 2005. Geochronologies for fish farm contaminants in sediments from Limekiln Bay in the Bay of Fundy. The Handbook of Environmental Chemistry, 5, 221-238. Springer, Berlin.

Soulsby, R.L., 1983. The bottom boundary layer of shelf seas. In: Johns, B. (Ed.), physical Oceanography of coastal and Shelf Seas. Elsevier, New York, USA, pp. 189-266.

Soulsby, R., 1997. Dynamics of marine sands. A Manual for Practical Applications. Thomas Telford Publishing, London.

Sternberg, R.W., Berhane, I., Ogston, A.S., 1999. Measurement of size and settling velocity of suspended aggregates on the Northern California continental shelf. Marine Geology 154, 43-54.

Stevens, A.W., Wheatcroft, R.A., Wiberg, P.L., 2007. Sediment erodibility along the western Adriatic margin, Italy. Continental Shelf Research 27, 400-416.

Stewart, A.R.J., Grant, J., 2002. Disaggregation rates of extruded salmon feed pellets: influence of physical and biological variables. Aquaculture Research, 33, 799-810.

Strain, P.M., Hargrave, B.T., 2005. Salmon Aquaculture, Nurtient Fluxes and Ecosystem Processes in Southwestern New Brunswick. The Handbook of Environmental Chemistry, 5, 239-251. Springer, Berlin.

Sutherland, T.F., C.L. Amos, C. Ridley, I.G. Droppo, and S.A. Petersen. 2006. The settling behaviour and benthic transport of fish feed pellets under steady flows. Estuaries and Coasts, 29 (5): 810 – 819.

Syvitski, J.P. M., Asprey, K.W., Leblanc, K.W.G., 1995. In-situ characteristics of particles settling within a deep-water estuary. Deep Sea Research, Part II, 42 (1), 223-256.

Tedford, T., Hannah, C. G., Milligan, T. G., Loder, J. W., Muschenheim, D., 2002. Flocculation and the fate of drill mud discharges. In: Spaulding, M. L. (Ed.), Estuarine and Coastal Modelling: Proceedings of the 7th International Conference. ASCE, pp. 294-309.

Tedford, T., Drozdowski, A., Hannah, C. G., 2003. Suspended sediment drift and dispersion at Hibernia. Can. Tech. Rep. Hydrogr. Ocean Sci. 227: vi + 57 pp.

Tolhurst, T.J., Black, K.S., Shayler, S.A., Mather, S., Black, I., Baker, K., Paterson, D.M., 1999. Measuring the in-situ erosion shear stress of intertidal sedimentswith the cohesive strength meter (CSM). Estuarine and Coastal Shelf Science,49, 281-294.

Tolhurst, T.J., Black, K.S., Paterson, D.M., Mitchener, H.J., Termatt, G.R., Shayler, S.A., 2000. A comparison and measurement standardization of four in situ devices for measuring the erosion shear stress of intertidal sediments. Continental Shelf Research 20 (10-11), 1397-1418.

Thomsen, L., Gust, G., 2000. Sediment erosion thresholds and characteristics of resuspended aggregates on the western European continental margin. Deep-Sea Research, Part I 47, 1881-1897.

Traykovski, P., Latter, R.J., Irish, J.D., 1999. A laboratory evaluation of the laser in situ scattering and transmissometery instrument using natural sediments. Marine Geology 159 (1-4), 355-367.

van Ledden, M., van Kesteren, W.G.M., Winterwerp, J.C., 2004. A conceptual framework for the erosion behaviour of sand-mud mixtures. Continental Shelf Research 24, 1-11.

Voulgaris, G., Meyers, S.T., 2004. Temporal variability of hydrodynamics, sediment concentration and sediment settling velocity in a tidal creek. Continental Shelf Research 24 (15), 1659–1683.

Ward, J.E.; Newell, R.I.E.; Thompson, R.J; MacDonald, B.A., 2008. In vivo Studies of Suspension-Feeding Processes in the Eastern Oyster, *Crassostrea virginica* (Gmelin). *Biology Bulletin,* 186, 221-240.

Wiberg, P.L., Smith, D.J., 1987. Calculations of the critical shear stress for motion of uniform and heterogeneous sediments. Water Resources Research 23, 1471-1478.

Wiberg, P.L., Drake, D.E., Cacchione, D.A., 1994. Sediment resuspension and bedArmoring during high bottom stress events on the northern California inner Continental shelf: measurements and predictions. Continental Shelf Research 14 (10-11), 1191-1219.

Wiberg, P. L., Law, B.A., Wheatcroft, R.A., Milligan, T.G., Hill, P.S., 2013. Seasonal variations in erodibility and sediment transport potential in a mesotidal channel-flat complex, Willapa Bay, WA, *Continental Shelf Research.* doi: 10.1016/j.csr.2012.07.021

Wildish, D.J. and G.W. Pohle. 2005. Environmental Effects of Finfish Aquaculture. The Handbook of Environmental Chemistry, 5, 275-304. Springer, Berlin.

Winterwerp, J.C., 1989. Flow induced erosion of cohesive beds. A literature survey. In cohesive sediments (Rep. 25). Delft. WI/Delft Hydraulics and Rijwaterstaat.

Winterwerp, J. C. (1998). A simple model for turbulence induced flocculation of cohesive sediment. Journal of Hydraulic Research, 36(3), 309-326.

Weise, A.M., Cromey, C.J., Callier, M.D., Archambault, P., Chamberlain, J., McKindsey, C.W. 2009. Shellfish-DEPOMOD: Modelling the biodeposition from suspended shellfish aquaculture and assessing benthic effects. Aquaculture, 288, 239-253.

Wu, Y., Hannah, C., Thupaki, Ruping, M., Law, B., 2017. Effects of rainfall on oil droplet size and the dispersion of spilled oil with application to Douglas Channel, British Columbia, Canada. Marine Pollution Bulletin, *doi:10.1016/j.marpolbul,2016.08.067*